Electronic Thesis and Dissertation Repository

5-19-2017 12:00 AM

Investigating Adenovirus E1A as an RNA Polymerase II C-Terminal Domain Mimic and its Role in Transcription Activation

Kristianne JC Galpin, *The University of Western Ontario*

Follow this and additional works at: https://ir.lib.uwo.ca/etd

Part of the Virology Commons

Abstract

Viruses rely on host cell machinery, often mimicking cellular components, in order to circumvent host cell defenses and hijack cellular processes. DNA viruses, such as human Adenovirus (hAdV), rely on host RNA Polymerase II (RNAPII) to transcribe viral genes. RNAPII has a C-terminal domain (CTD), made up of highly conserved heptad repeats of tyrosine-serine-proline-threonine-serine-proline-serine (YSPTSPS). Post-translational modifications of residues within the CTD, including phosphorylation, coordinates the transcription cycle. Several viruses, including Human Immunodeficiency Virus (HIV), Human Cytomegalovirus (hCMV), Epstein-Bar Virus (EBV) and Herpes Simplex Virus (HSV), modify the phosphorylation state of the RNAPII CTD by hijacking cellular cyclin dependent kinases (CDKs) to enhance viral transcription. The hAdV E1A protein, specifically the conserved region 3 (CR3), is a potent transcriptional activator. This region contains a sequence (YSPVSEP), highly conserved across hAdV subtypes, that has considerate sequence similarity to the heptad repeat of the RNAPII CTD. Two serine residues in E1A (S185 and S188) are phosphorylated, mimicking the phosphorylation of serine at positions 2 and 5 of the RNAPII CTD. **We believe that given the sequence similarity, and the phosphorylation at conserved serine residues, that E1A CR3 acts as a mimic of the CTD to promote transcriptional elongation of viral genes.** This study has demonstrated the role of the putative CTD mimic, and the specific phosphorylation of serine residues in this region, for maximal transcription activation. This study examined how this region may structurally and functionally mimic the RNAPII CTD. To assess functional mimicry, the E1A putative CTD mimic was investigated for it's ability to interact with CDK9, a protein known to interact with the RNAPII CTD. Although this interaction is not specific to the phosphorylation of S185 and S188, it may still rely on the putative CTD mimic region within E1A CR3. Finally, I constructed a novel hAdV point mutant (JM17-E1A S185/188A) and characterized the kinetics of viral gene expression so that it can be used as a tool to examine the role of the putative CTD mimic in transcription of viral genes. Cells infected with JM17-E1A S185/188A showed decreased amounts of E1A production, but not other viral genes,

when compared to wild type (WT) virus. This study investigated a novel example of viral mimicry, and the mechanism by which it enhances viral transcription.

Keywords

Co-Authorship Statement

Figure 1.3 was created by Dr. J.S. Mymryk, and is used in this thesis with permission.

Acknowledgments

Thank you, Dr. Joe Mymryk for taking me on as an MSc student. I am lucky to have had the chance to learn from your incredible work ethic and from the knowledgeable students in your lab.

Thank you to my committee members, Dr. Joe Torchia and Dr. Jim Koropatnick, for your time and your helpful insights over the past three years.

Thanks to all the Mymryk lab members for their input over the years. Specifically, I would like to thank Dr. Greg Fonseca for initiating the original experiments that inspired this project. Thanks to Dr. Mike Cohen for getting me started and teaching me everything I needed to know. Thanks to Dr. Matt Miller's perfectly detailed lab note books for teaching me about Adenovirus construction. Thanks to Ali Zhang and Jessica Hill for always being there to talk through and trouble shoot IPs. Thanks to Martin Prusinkiewicz for your help with qPCR. And last but not least, many, many thanks to Gloria Thomson for all her hard work keeping the lab running smoothly.

Thank you Stephanie, for making every day the very best day since I met you. Thank you for always patiently listening to me as I tell you about experiments that work or as I vent my frustrations about experiments that don't.

Thank you to my family for always supporting me and for being my biggest cheerleader. I wouldn't be here without you.

Finally, here's to all my friends and family who no longer have to ask, "Are your cells dead?" Whatever will we talk about now?

Table of Contents

List of Tables

List of Figures

List of Abbreviations

A549	Adenocarcinomic human alveolar basal epithelial cell
aa	Amino Acid
ADP	Adenovirus death protein
AKAPs	A-Kinase anchoring proteins
ATF	Activating Transcription Factors
BSA	Bovine Serum Albumin
bZIP	basic/leucine DBD
CAR	Coxsakievirus and adenovirus receptor
CBP	CREB binding protein
CDK	Cyclin Dependent Kinase
ChIP	Chromatic Immunoprecipitation
CPE	Cytopathic effect
CR	Conserved Region
CtBP	C-Terminal Binding Protein
CTD	C-Terminal Domain
DBD	DNA binding domain
DBP	DNA Binding Protein
dl/Δ	Delta/Deletion mutant
DRB	6-dichloro-1-b-D-ribofuranosylbenzimidazole
DSIF	DRB sensitivity-inducing factor
DYRK1	dual-specificity tyrosine-regulated kinase 1A
E1A	Early Region 1A
E1B	Early region 1B
E2E	Early region 2 early
E2L	Early region 2 late
E2F	E2 Binding Factor
E3	Early region 3
E4	Early region 4
EBV	Epstein-Barr virus
ELMs	Eukaryotic Linear Motifs

FOXK1/FOXK2	Forkhead transcription factors	
GFP	Green Fluorescent Protein	
HA	Hemagluttinn	
hAdV	Human Adenovirus	
hBre1	human BREfeldin A sensitivity	
hCMV	Human Cytomegalovirus	
HEK 293	Human Embryonic Kidney 293	
HIV	Human Immunodeficiency Virus	
hpi	Hours post infection	
HPV	Human Papilloma Virus	
hr5	Host range mutant 5	
HRP	Horseradish peroxidase	
HSV	Herpes Simplex Virus	
HT 1080	Human fibrosarcoma cell line	
HTLV	Human T-lymphotropic virus type 1	
IB	Immunoblot	
IDT	Integrated DNA Technologies	
IFNγ	Interferon Gamma	
IP	Immunoprecipitation	
ITR	Inverted Terminal Repeat	
kbp	Kilobase Pair	
kDa	Kilodalton	
KSHV	Kaposi Sarcoma Associated Herpes Virus	
LIG	Ligand sites	
LMs	Linear motifs	
LMP1	Latent Membrane Protein 1	
MAPK	Mitogen activated protein kinase	
MOI	Multiplicity of infection	
MRN	Mre11-Rad50-Nbs1 Complex	
NELF	Negative elongation factor	
NF-κβ	Nuclear factor of kappa light polypeptide gene enhancer in B-	

	cells
NLS	Nuclear Localization Signal
orf	Open Reading Frame
PBS	Phosphate Buffered Saline
pCAF	P300/CBP-associated factor
PFU	Plaque Forming Units
PKA	Protein Kinase A
pRb	Retinoblastoma Protein
P-TEFb	Positive transcription elongation factor b
R	Residues
RGD Motif	Arg-Gly-Asp Motif
RIDαβ	Receptor internalization and degradation αβ
RLUs	Relative Light Units
RNAPII	RNA Polymerase II
RNAPIIa	Hypophosphorylated/Unphosphorylated RNAPII
RNAPIIo	Hyperphosphorylated RNAPII
RNAPIIi	RNAPII intermediate
RT	Room Temperature
RT-qPCR	Real Time Quantitative PCR
S2	Serine 2 of the CTD
S5	Serine 5 of the CTD
S185	Serine 185 of E1A
S188	Serine 188 of E1A
SD	Standard deviation
SLiMs	short linear interaction motifs
SV40	Simian Virus 40
T	Truncation
TAF	TBP Associated Factor
TAR	Transactivation response
TBP	TATA Binding Protein
TBS	Tris Buffered Saline

TNF	Tumor necrosis factor
TP	Terminal Protein
TRAAP	Transformation/transcription domain-associated protein
TRAIL	TNF-related apoptosis-inducing ligand
UI	Uninfected/ Mock infected
VA RNA	Virally Associated RNA
WT	Wildtype hAdV

Chapter 1 : Introduction

1   Introduction

1.1   Adenovirus

Human Adenovirus (hAdV) was first isolated in 1953 from adenoid tissue and was later implicated as a causative agent for acute respiratory disorder in 1954 (Huebner et al., 1954; Rowe et al., 1953). As the first human virus discovered to cause cancer in rodents and transform human cells, Adenovirus, like other small DNA tumour viruses, has taught researchers much about cell cycle control and has played a large role in identifying cellular proteins implicated in cancer (Berk, 2005; Howley and Livingston, 2009; Trentin et al., 1962). The viral protein encoded by Early Region 1A (E1A) has been particularity insightful into understanding aspects of both cellular and viral biology, including immune modulation, control of transcription, nuclear localization, and viral mimicry, as it acts as a molecular hub interacting with a protein-protein interaction network that is potentially comprised of over 2100 proteins (Berk, 2005; Pelka et al., 2008). This thesis investigates E1A as a novel example of viral mimicry and its role in transcription activation.

1.1.1   Taxonomy of Adenoviruses

The Adenoviridae family, genus *Mastadenovirus*, are human pathogens that have been divided into seven species (A to G) based on phylogenetic distance and other shared characteristics (Table 1.1). Adenovirus types 1-51 were traditionally characterized by serological assays – combination tests of serum neutralization and hemagglutination (HA) inhibition. Newer adenovirus types, including 53-66, and as far as types 72, have been discovered by genome sequencing (Berk, 2007; King et al., 2012; Lion, 2014; Yoshitomi et al., 2016). Conventional naming has been modified to include identification of Penton Base, Hexon and Fibre genes, in order to accommodate for novel or recombinant/intratypic strains. The discovery of novel and recombinant or intratypic variants highlights the importance of screening populations to study adenovirus evolution and global spread (Aoki et al., 2011; Berk, 2007).

Table 1.1. Classification schemes for hAdV. Adenovirus types 1-51 were traditionally characterized by serological assays, while newer adenovirus types have been discovered by genome sequencing (Figure adapted from Berk, 2007; Kojaoghlanian et al., 2003; Lion, 2014).

Species	HA Group	CAR Receptor	Serotypes	Site of Infection	Tumors in Animals	Transformation in Tissue Culture	% G+ C in DNA
A	IV (little or no agglutination)	+	12,18,31, 61	GI Tract	High	+	48-49
B	I (Complete agglutination of monkey erythrocytes)	- (CD46)	3,7,11,14,16, 21,34,35,50,55,66, 72	Lung, Eye, Urinary Tract	Moderate	+	50-52
C	III (partial agglutination of rat erythrocytes)	+	1,2,5,6, 57	Upper Respiratory Tract	Low/None	+	57-59
D	II (complete agglutination of rat erythrocytes)	+	8,9,10,13,15, 17,19,20,22-30 32,33,36-39 42-49,51, 53, 54, 56, 58-60, 63-67	Eye, GI Tract	Low/None	+	57-61
E	III	+	4	Respiratory Tract	Low/None	+	57-59
F	III	+	40,41	Gastrointestinal Tract	Unknown	Unknown	50-51
G	Unknown	+	52	Gastrointestinal Tract	Unknown	N/A	55

1.1.2   Adenovirus Infection and Persistence

Adenovirus infection had been linked to acute illness, severe illness in immunocompromised individuals and among certain populations, and in some cases persistent infection is linked to rarer manifestations of disease. In immunocompetent adults and children, acute infections consist of respiratory illness, gastroenteritis and keratoconjunctivitis/conjunctivitis (Table 1.1). Species B and C are most often associated with respiratory illness, including pneumonia and febrile respiratory illness. Adenovirus types 40 and 41 from species F, the newly discovered species G (hAdV52), and some types from species A and D are associated with gastroenteritis (Jones et al., 2007; King et al., 2012; Kojaoghlanian et al., 2003). Types from species B and D cause adenoidal–pharyngeal conjunctivitis (hAdV3, 4, 7, 14) and keratoconjunctivitis (hAdV8, 19, 37, 53, 54). hAdV37, 8 and 19 are sometimes associated with sexually transmitted urethritis and can present concurrently with conjunctivitis (Bradshaw et al., 2002; Liddle et al., 2015). Incidences of viral co-infection have been observed with adenoviral species B, C and E (Vora et al., 2006; Wang et al., 2013). In immunosuppressed patients, such as those following organ transplant or those with Human Immunodeficiency Virus (HIV), infections can disseminate and become fatal (Lion, 2014). Adenovirus infection, by types 4 and 7 and to a lesser extent types 21 and 14, is particularly high among military recruits due to the close quarters and high stress environment experienced during basic training. A new oral vaccine strategy against hAdV4 and 7 was implemented in 2011 that has a 99% efficacy (Lion, 2014; Russell et al., 2006)

A recent study demonstrated the first model of Adenovirus persistence whereby interferon gamma (IFNγ) suppresses virus replication to evade the immune system and establish a persistent infection in normal, non-transformed cells (King et al., 2016a; Zheng et al., 2016). Persistent hAdV infections are associated with an inflammatory response relevant to Chronic Obstructive Pulmonary Disease and asthma risk (Hogg, 2001). Adenoviridae are also among a number of different viruses that cause acute and chronic forms of heart disease. DNA has been detected in the myocardium of 3-23% patients with myocarditis (Bowles et al., 2003; Pankuweit and Klingel, 2013). From

patient biopsy data, persistent infection has been associated with the development of dilated cardiomyopathy and progressive cardiac dysfunction (Kühl et al., 2005; Tátrai et al., 2011). In the first mouse model of its kind, researchers demonstrated that acute adenovirus infection leads to expression of IFNγ and myocyte necrosis, while a persistent infection is associated with an increased heart mass and cardiac hypertrophy (McCarthy et al., 2015; Weinberg et al., 2005). hAdV (types 36, 37, and 5) is one of five infectious agents linked to obesity in both animals and humans (Mitra and Clarke, 2010). In humans, hAdV36 seropositivity in adipose tissues is associated with risk of obesity and weight gain (Ponterio and Gnessi, 2015; Tambo et al., 2016). Adenovirus infection has also been shown in a number of different animal studies (rodent and non-human primate models) to induce adiposity (weight gain and increased body fat), to modify the serum lipid composition, and shows an increase in insulin sensitivity (Dhurandhar et al., 2002; Kapila et al., 2004; Pasarica et al., 2006).

1.1.3   Transformation and Apoptosis

In 1962, when researchers demonstrated that hAdV12 induced tumours in hamsters, Adenovirus joined the growing group of animal viruses with the ability to cause cancer and became the first human oncovirus (Trentin et al., 1962). Future studies showed species A viruses (12, 18, 31) were highly oncogenic in rodents, while species B (3), species C (2) and species D (9) were more weakly oncogenic (Berk, 2007; Brusca et al., 1984; Freeman et al., 1967a, 1967b; Huebner et al., 1962). While Adenovirus can transform human cells in culture models, it is not associated with cancer in humans. It appears only to cause tumours in rats and hamsters. Transfection by the hAdV genes E1A and E1B alone proves sufficient for transformation of human and rodent cells. Indeed, Human Embryonic Kidney (HEK 293) cells were immortalized by stable transfection of the left end of the hAdV genome, which includes E1A and E1B (Graham et al., 1977; Whittaker et al., 1984). E1A functions to promote cell cycle progression from G1 to S phase, primarily though the interaction with the Retinoblastoma Protein (pRb) (Felsani et al., 2006). Thus, the E1A oncoprotein became a powerful and insightful tool in identifying cellular proteins and host pathways involved in cancer (Berk, 2005; Howley and Livingston, 2009; Pelka et al., 2008). Other viral proteins involved in tumorigenesis

include the anti-apoptotic factors, E1B-55K and E1B-19K (Chiou et al., 1994; Dobner et al., 1996; Nevels et al., 1999). The viral proteins E4orf3 and E4orf6 further play a role in tumorigenesis and can substitute for E1B (Täuber and Dobner, 2001). The E1B and E4 genes are described in greater detail in Section 1.1.4. In human cells, disrupting cell cycle regulation, as described above, leads to a permissive environment for Adenovirus replication. However, in rodents this same dysregulation leads to tumorigenesis (Berk, 2007). Paradoxically, E1A expressed at high levels in already transformed cell lines, suppresses the oncogenic phenotypes and acts to promote apoptosis and mesenchymal to epithelial transition (Douglas and Quinlan, 1995; Frisch and Mymryk, 2002; Schaeper et al., 1995). Genetically modified Adenoviral vectors are also used in oncolytic virotherapy as experimental cancer treatments (Yamamoto et al., 2017).

1.1.4   Physical Properties of Adenovirus

The hAdV species C type 5 and type 2 are the most commonly studied types. Most of what we know about Adenovirus biology is based on these two virus types because they are easy to grow in the laboratory. In the Mymryk lab, we commonly study hAdV5, which will be the focus of this thesis as well. The virus capsid has icosahedral symmetry (Figure 1.1 A, B), meaning it has 20 facets, that are made up of 240 hexon trimers. Each of the 12 vertices is comprised of a pentameric penton base and a trimeric fibre protein. Structural proteins IIIa, VI, VII, and IX are considered minor components of the capsid, which are involved in stability and assembly. Proteins V, VII, U, IVa2 and the TP are structural components that are associated with the dsDNA genome as part of the viral core. Finally, the p23 viral cysteine protease is a structural protein that is necessary for assembly and maturation of the virion by cleaving precursors of viral proteins (Berk, 2007; Russell, 2009).
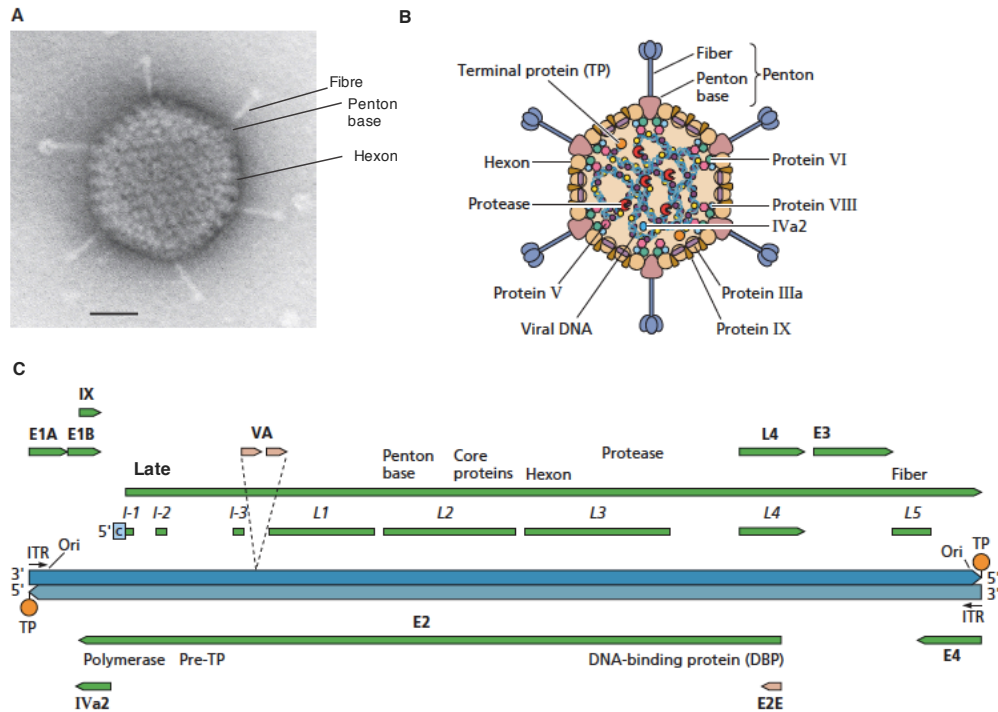
Figure 1.1. Physical Properties of Human Adenovirus Type 5.

A) Virion Structure. Electron micrograph of a negatively stained hAdV5 particle. Bar=50nm. **B) Diagrammatic representation of Adenovirus structure.** Major and minor structural proteins are depicted, as well as the DNA/Protein core. **C) Genome Organization**. The 36 kbp genome is represented in blue with the red TP at the 5' end of each strand. Green and Tan arrows represent RNAPII and RNPIII transcription products, respectively, and are labeled in bold type. Hatched lines show splicing of the Late transcript. ITR = Inverted terminal repeat. TP = terminal protein. Ori = Origin of Replication. (Modified from Flint et al., 2015)

The hAdV5 dsDNA genome is approximately 36 000 kilobase pairs (kbp) in length and encodes for around 40 proteins (Berk, 2007). It contains a perfect inverted terminal repeat (ITR) that is 100 nucleotides long and has a 55 kilodalton (kDa) terminal protein (TP) covalently bound to the 5' ends of each strand. The TP is thought to act as a protein primer during genome replication (Rekosh et al., 1977). Genes are expressed on both strands of the genome. The genome is expressed temporally with Early (E1A, E1B, E2E, E3 and E4), Intermediate (IX and IaV2, E2L) and Late Genes (L1-L5) (Figure 1.1 C) (Berk, 2007).

1.1.5   The Genes and Life Cycle of Adenovirus

Adenovirus gains entry into the host cell via receptor mediated endocytosis. Attachment by species A and species C-G occurs when the viral fibre protein binds coxsackie and adenovirus receptor (CAR), whereas species B viruses bind to CD46 (Berk, 2007; Roelvink et al., 1998; Seya et al., 1998). Subsequently the penton base binds to integrin via an RGD (Arg-Gly-Asp) peptide motif to stimulate internalization of the virus. The fibre proteins detach and the viral capsid is endocytosed via clathrin coated vesicles (Cuzange et al., 1994; Varga et al., 1991; Wickham et al., 1993). Ad40 and 41 do not use integrins for infection and instead use an alternative mechanism for internalization (Albinsson and Kidd, 1999; Berk, 2007). Acidification within the endosome causes the virions to disassemble, promoting release of the virion core containing the viral genome. The core traffics via microtubules to the nuclear pore where the final stages of core disassembly occurs. The genome is released into the nucleus via the nuclear pore for DNA replication and transcription of viral genes necessary for production of progeny virions (Dales and Chardonnet, 1973; Greber and Way, 2006; Leopold et al., 2000; Lonberg-Holm and Philipson, 1969; Philipson and Lonberg-Holm, 1969).

E1A is the first protein expressed during viral infection and it's many functions will be described in Section 1.2. It plays two main roles during initiation of the viral replication cycle: 1) Promotes cell cycle progression from G1 to S phase to make the cell permissive to viral replication and 2) turns on all early viral gene transcription (Berk, 2007).

The Early Region 1 is composed of E1A and E1B. E1B proteins are named after their molecular weight and function primarily to block apoptosis induced by E1A (Berk, 2007). E1B-55K binds and inhibits p53 to repress transcription of p53 responsive genes and, in conjunction with E4orf6, targets p53 for polyubiquitination and its subsequent degradation (Querido et al., 2001; Yew and Berk, 1992; Yew et al., 1994). E1B-55K also regulates the Mre11-Rad50-Nbs1 (MRN) complex in conjunction with E4orf6 to inhibit this DNA damage response, that otherwise triggers the concatenation of viral genomes into unpackageable multimers (Karen et al., 2009; Stracker et al., 2002). E1B-19K acts as a homologue of the cellular BCL-2 protein to bind and inhibit apoptotic BAX and BAK (Chiou et al., 1994; Sundararajan et al., 2001; White et al., 1992).

The E2 transcription unit encodes the DNA-dependent-DNA Polymerase, the TP, and the DNA Binding Protein (DBP) that function to replicate the genome. Viral replication is primed by the 5' TP and proceeds in a 5' to 3' direction by the DNA polymerase. DBP binds and stabilizes single stranded DNA, aiding in initiation and elongation of viral replication, by binding of TP to complete second strand synthesis of progeny genomes (Challberg and Kelly, 1979; Dekker et al., 1997; Hoeben and Uil, 2013; Mul and van der Vliet, 1993).

The E3 region encodes six proteins: where the receptor internalization and degradation (RIDαβ) complex, gp19K, E3 14.7K, and E3 6.7K function to evade the host immune system for cell survival, and the adenovirus death portion (ADP) functions in cell lysis for release of progeny virions (Reviewed in Lichtenstein et al., 2004). While ADP is pro-apoptotic (Tollefson et al., 1996), RIDαβ, E3 14.7K, and 6.7K function as anti-apoptotic factors by blocking cell death signaling pathways triggered by Tumour Necrosis Factor (TNF), Fas ligand, nuclear factor kappa-light-chain-enhancer of activated B cells (NF-kB), and TNF-related apoptosis-inducing ligand (TRAIL). RIDαβ and E3 6.7K are transmembrane proteins that function by downregulating cellular "death" receptors as well as antagonizing signalling pathways (Benedict et al., 2001; Elsing and Burgert, 1998; Friedman and Horwitz, 2002; Lichtenstein et al., 2004; Moise et al., 2002; Tollefson et al., 2001). E3 14.7K is a soluble protein and functions by binding and inhibiting factors such as TNF and NF-kB (Gooding et al., 1990; Lichtenstein et al.,

2004). gp19K is a transmembrane protein in the endoplasmic reticulum that downregulates MHCI expression on the cell surface and evades the CTL-mediated killing of adenovirus infected cells (Andersson et al., 1985; Burgert and Kvist, 1985). As of yet, E3 12.5K has no known function and it's deletion does not affect viral growth (Hawkins and Wold, 1992).

The E4 region produces 7 differentially spliced protein products named after the open reading frame (orfs) and they have a diverse set of functions including viral replication, cell cycle control and regulating the switch from early to late stages of infection (Halbert et al., 1985; Tigges and Raskas, 1984; Weitzman, 2005; Yoder and Berget, 1986). E4orf1 functions only in Group D Adenovirus to promote transformation of rodent cells (Javier, 1994; Weiss et al., 1997). E4orf2 and E4orf3/4 do not have any known functions and their deletion has no effect on viral growth (Dix and Leppard, 1995). E4orf3 inhibits the MRN complex by interacting with promyelocytic leukemia nuclear bodies and altering their structure. E4orf3 may function to inhibit the DNA damage response and play a role in viral replication (Carvalho et al., 1995; Stracker et al., 2002). E4orf4 binds to protein phosphatase 2A, thus inhibiting it and downregulating transactivation (Kleinberger and Shenk, 1993). E4orf4 is also capable of inducing p53-independent apoptosis (Marcellus et al., 1998). As mentioned previously, E4orf6 can function in conjunction with E1B to inhibit p53 and the MRN complex (Dobner et al., 1996; Karen et al., 2009; Querido et al., 2001). E4orf6/7 works in conjunction with E1A to stimulate the transcription at the E2 promoter by binding directly to the E2 Binding Factor (E2F), which promotes stable DNA binding at the promoter (Neill et al., 1990).

The early gene products function to make the host cell environment permissive to virus replication and assembly of progeny virions. Early genes induce cell cycle progression, inhibit the cellular antiviral response, activate transcription of cellular and viral genes, and disrupt protein-protein regulatory networks (Berk, 2007). Adenovirus also encodes two non-coding virally associated (VA) RNAs that help to subvert the immune system and promote transcription of late viral genes. VA RNAI and VA RNAII are transcribed by RNAP III, they are approximately 150-200 nucleotides long, and are expressed at high levels in infected cells. VA RNAI is the most predominant from and is required for

efficient viral replication. It inhibits the anti-viral response by the double-stranded RNA-activated protein kinase (Ma and Mathews, 1996; Mathews and Shenk, 1991). VA RNAs interfere with host cell RNA interference system by interacting with the nuclear Exportin 5. This inhibits cellular miRNA's and the Dicer complex from being exported into the cytoplasm. In the cytoplasm, VA RNA also directly inhibits Dicer from processing cellular miRNA's (Lu and Cullen, 2004; Vachon and Conn, 2016; Xu et al., 2007). The structural and non-structural late proteins (expressed by L1-L5 transcription units) function to package the viral genome and assemble progeny virions. The host cell is then lysed and progeny virions are released (Berk, 2007).

1.2 Adenovirus E1A

1.2.1 Adenovirus E1A Gene and Transcripts

The hAdV E1A protein is the first protein expressed in viral infection and is required for productive viral replication through transactivation of viral genes and in reprogramming the host cell for productive infection. The hAdV E1A gene produces 5 mRNA products (Figure 1.2 A) 13S, 12S, 11S, 10S and 9S that are translated into 289, 243, 217, 171, and 55 residues (R) proteins respectively (Perricaudet et al., 1979; Stephens and Harlow, 1987; Ulfendahl et al., 1987; Virtanen and Pettersson, 1983). The 13S (289R) and 12S (243R) forms are the most predominant forms expressed during infection. The 243 form differs in the 46 amino acid transactivating portion. 13S and 12S are capable of transformation, but only 13S is capable of transactivation of both cellular and viral genes (Berk and Sharp, 1978; Ferguson et al., 1985; Roberts et al., 1985). Produced later in infection, 10S (217R) and 11S (171R) mRNA are translated in the same reading frame as 12S and 13S mRNAs but differ in that they lack 72 amino acids (aa 27 to 98) present in the larger isoforms. Viruses expressing only 10S and 11S E1A products are limited in virus growth, transcription activation and fail to transform rodent cells. These observations highlighted the importance of the region from aa 27 to 98 for transformation (Stephens and Harlow, 1987; Ulfendahl et al., 1987). The majority of current research focuses on the function of 13S and 12S E1A isoforms and little is known about the functions of 10S and 11S isoforms. However, a recent study in our lab examined the function of 9S (55R) E1A. 9S E1A is expressed at late times in infection and consists of

the first 26 amino acids in the N-terminus of E1A which is shared with other E1A isoforms, as well as a unique C-terminus caused by a frame shift in the exon 2 reading frame. Through the N-terminal portion (shared with other E1A) isoforms, 55R E1A was shown to interact with S8, a regulatory component of the 26S proteasome, and that this interaction is required for viral replication. Additionally, there may be novel binding partners that target the unique frame shifted C-terminal region of 9S E1A (Miller et al., 2012; Virtanen and Pettersson, 1983).

1.2.2   E1A as a Molecular Hub

E1A is a structurally disordered protein, meaning that it lacks a tertiary structure, and it has no known crystal structure to date (Ferreon et al., 2013; Wright and Dyson, 2015). Bioinformatics analysis of the protein suggests the protein exists in a native unfolded conformation with the exception of the structured zinc finger in CR3 and an alpha helix region in the N-terminus (Pelka et al., 2008). Sequence alignment from a number of adenoviral serotypes has revealed regions of highly conserved sequences: CR1, CR2, CR3 and CR4 (Figure 1.2 B) (Avvakumov et al., 2002, 2004). Structurally disordered proteins act in a dynamic fashion as their interaction is not limited to a single fold or globular domain, and instead can interact with a number of different proteins through short linear sequences in a number of different conformations (Davey et al., 2011). Such proteins act as molecular hubs, which functionally interact with a number of different pathways. E1A is thus considered a molecular hub (Figure 1.3), where regions within CR1, CR2, CR3, and CR4 interact directly or indirectly with a potential network of over 2100 different proteins to alter many different aspects of the host cell to make it permissive to viral replication (Pelka et al., 2008). The multi-functional hAdV E1A has led to many discoveries and a greater understanding of transcription and cell cycle (Berk, 2005).

A)

E1A

13S (289R) ——— ■■■■■■ ■■■■ —AAA

12S (243R) ——— ■■■■ ■■■■ —AAA

11S (217R) ——— ■■ ■■■ ■■■■ —AAA

10S (171R) ——— ■■ ■■ ■■■■ —AAA

9S (55R) ——— ■■ ▬▬▬ —AAA

B)

289R		CR1		CR2	CR3		CR4
243R		CR1		CR2			CR4
217R				CR2	CR3		CR4
171R				CR2			CR4
55R					▬▬▬▬		
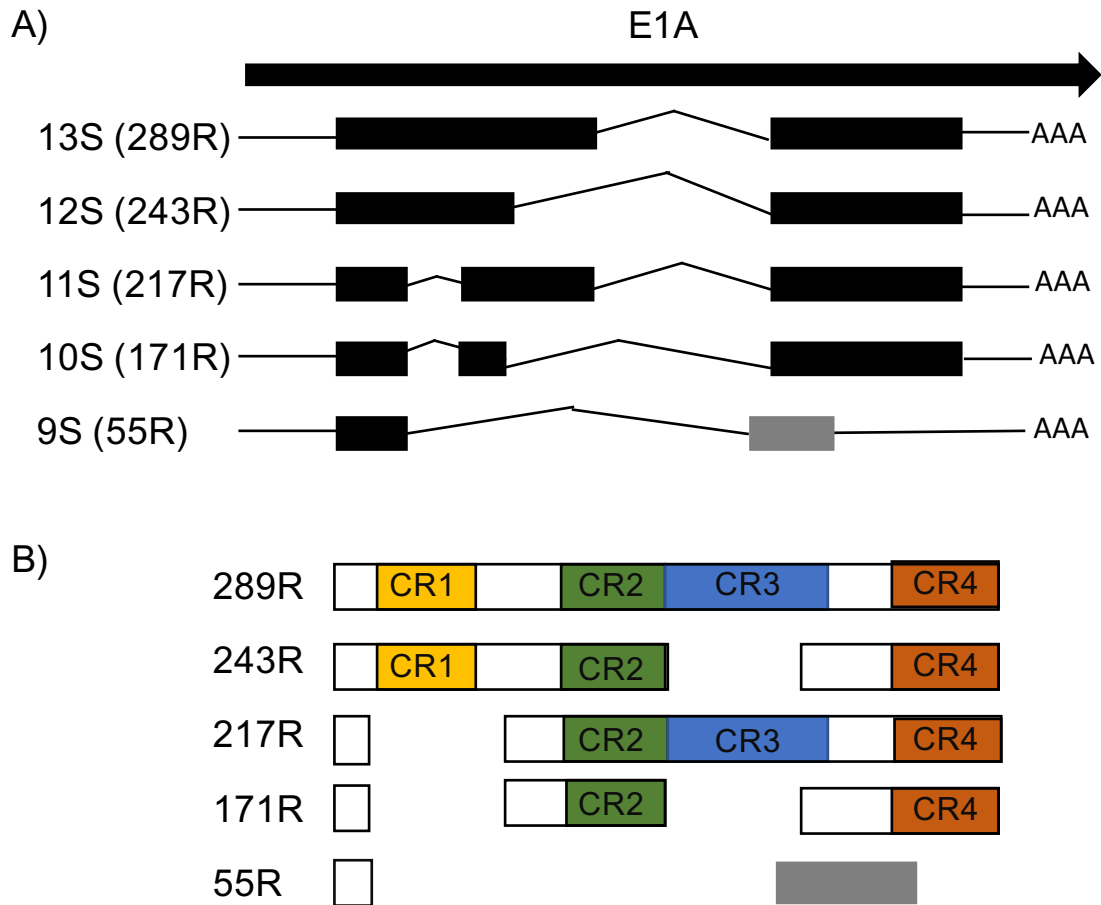
Figure 1.2. hAdV5 E1A Splice Products.

A) The primary RNA transcript from the hAdV5 E1A gene is differentially spiced into 5 mRNA products ranging in size from 13S to 9S. Blocks represent the exons, while lines represent introns. All splice events maintain the translational reading frame except in 9S mRNA transcript and is represented by a grey block. B) A representation of the E1A protein products encoded by the 5 mRNA products. Conserved Regions (CR) 1 - 4 are labeled and denoted by yellow, green, blue and orange blocks respectively. The novel sequence in the 55R protein produced by the 9S mRNA is denoted by a grey block.

The N-terminus/CR1 region is involved in transformation, cell cycle progression, cell signalling and transactivation. The N-terminus of E1A comprises the first 41 amino acids and CR1 covers the region from aa 42-72 (Pelka et al., 2008). The N-terminus interacts with: proteasomal subunits including S8 and S4 of the 19S regulatory proteasome subunit (Rasti et al., 2005), cellular kinases including Nek9 (Pelka et al., 2007) and Protein Kinase A (PKA) (King et al., 2016b), and factors that coordinate transactivation including p300/CBP associated factor (pCAF) (Pelka et al., 2009a), p300/CBP (Rasti et al., 2005), GCN5 (Ablack et al., 2012) and TATA Binding Protein (TBP) (Rasti et al., 2005). The N-terminus of E1A also binds the p400 complex and coordinates with CR1 for binding of p300/CBP and Transformation/Transcription domain associated factor (TRAAP) all of which are necessary for the transforming activity of E1A (Fuchs et al., 2001).

The interaction of E1A with pRb is coordinated by CR2 and CR1, and is necessary for transformation of primary rodent cells (Subramanian et al., 1991). CR2 spans residues 115-137 and functions in cell cycle regulation and transformation. pRb interacts with CR2 of E1A though the pocket binding domain. This high affinity binding provides an accumulation of stable pRb-E2F/CR2 complexes that allows CR1 to bind pRb and forces E2F dissociation. CR1 directly competes with E2F from pRb and helps drive complete dissociation of E2F and the binding of CR2 to pRb. E2F dissociation is also related to E2F activated transcription, which drives cell cycle progression from G1 to S phase which makes the cells permissive to adenovirus replication (Dyson et al., 1992; Felsani et al., 2006; Morris and Dyson, 2001). CR2 also has an area of high density overlapping protein motifs that are involved in the binding to cellular proteins such as BS69, UBC9 and the newly discovered interaction with STING (Ansieau and Leutz, 2002; Lau et al., 2015; Yousef et al., 2010).

The function of CR3 is largely attributed to transactivation. CR3 transactivation is the main focus of this thesis and is covered in greater detail in the following sections (Section 1.2.3-1.2.5).
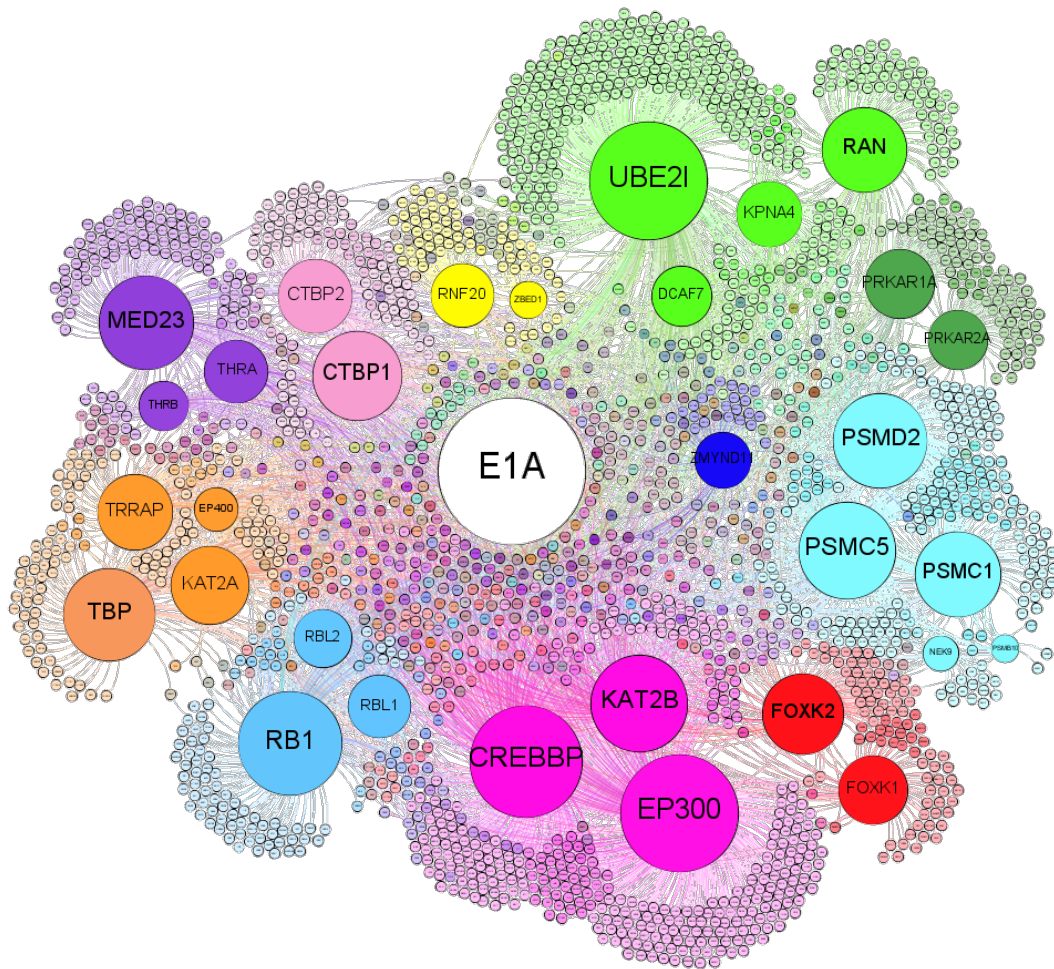
Figure 1.3. E1A as a Molecular Hub

E1A interacts with at least 31 primary interactors and a potential network of 2125 secondary interactors. Primary interactors were chosen from the literature, with at least two citations in PubMed. Secondary interactors were then determined via the BioGRID database. Gephi was then used to visualize the protein interaction network of E1A. (Figure provided by J.S. Mymryk).

CR4 spans residues 240 to 288 and plays a role in E1A induced oncogenesis. It is required for transformation with E1B, but paradoxically can also induce mesenchymal-to-epithelial transition and act as a tumour suppressor (Chinnadurai, 2002; Douglas and Quinlan, 1995; Schaeper et al., 1995; Subramanian et al., 1991). CR4 interacts with C-terminal Binding Protein (CtBP), dual-specificity tyrosine-regulated kinase 1A (DYRK1), HANII and Forkhead transcription factors (FOXK1 and FOXK2) (Chinnadurai, 2002; Komorek et al., 2010; Zhang et al., 2001). The CtBP and DYRK1A interaction with CR4 are required for E1B-55K mediated transformation. Recent data suggests that CtBP is not involved in Ras mediated suppression of transformation but that DYRK1 with HANII and FOXK1/FOXK2 may carry out this function (Cohen et al., 2013). The C-terminal portion of E1A CR4 also contains a well characterized Nuclear Localization Signal (NLS), aa 285-289 (KRPRP), that interacts with importin alpha3 for nuclear import (Köhler et al., 2001; Lyons et al., 1987).

1.2.3   CR3 Model for Transactivation

CR3, which spans aa 139 to 204 in hAdV5, is a potent transcriptional activator. CR3 alone is sufficient to activate transcription when tethered to a promotor via fusion with a heterologous DNA Binding Domain (DBD) (Lillie and Green, 1989). Models of CR3 activation were primarily studied in the hAdV5 background, but this region is highly conserved across species of Adenovirus (Avvakumov et al., 2002, 2004). Not surprisingly, CR3 can act as a transcriptional activator in all six species tested (species A-F), although there are differences in the activation potential between species. All species require binding to factors such as MED23 for activation of transcription (Ablack et al., 2010).

Like many viral and cellular proteins that activate transcription, E1A has a consensus zinc finger motif that binds a zinc ion through four conserved cysteine residues (C154, C157, C171, and C174). Bioinformatics analysis of this region suggests that this region is structured. Mutating the zinc coordinating cysteine residues or a number of other residues within this region leads to loss of function, likely due to loss of structure and the ability to

bind the zinc ion (Culp et al., 1988; Geisberg et al., 1994; Pelka et al., 2008; Webster and Ricciardi, 1991). E1A binds to TBP and MED23 through the zinc finger region of CR3. The interaction of E1A CR3 with TBP and MED23 require separate residues within CR3, but both require the coordination of the zinc ion for binding (Figure 1.4). Binding of TBP and MED23 leads to transcriptional activation through the rapid formation of the pre-initiation complex, which includes RNAPII and TBP-Associated Factors (TAFs) (Berk, 2005; Boyer et al., 1999; Geisberg et al., 1994; Stevens et al., 2002).

Since E1A has no DNA binding capabilities, E1A must first be targeted to the promoter. This is primarily thought to occur via the recruitment by sequence specific transcrption factors such as YY1, USF, ATF-2, SP1, S8 of the 19S proteosome and $TAF_{II}110$ and $TAF_{II}250$ (See Section 1.2.4. and Table 1.2). These factors interact with E1A through the portion of CR3 from aa 180-188, named the promotor targeting region of CR3 (Liu and Green, 1994; Webster and Ricciardi, 1991). The current model for CR3 function is that E1A is recruited to promotors of viral genes via the promotor targeting region, after which the zinc finger region recruits TBP and MED23 in order to nucleate the pre-initiation complex and activate transcription (Figure 1.4).

E1A CR3 has more recently been shown to interact with additional factors that elegantly fine tune coordination of transcription activation. For example, E1A CR3 serves as a second independent interaction site for the histone acetyltransferases pCAF and p300/CBP, which also bind E1A via the N-terminus. These chromatin modifying enzymes act as co-activators of transcription (Pelka et al., 2009a, 2009b). The E1A interaction with CtBP has a second binding site in CR3 in addition to the binding site in CR4. This interaction acts to relieve repression by CtBP at viral promotors (Bruton et al., 2008). The 26 Proteasome is made up of the 20S proteolytic subunit and the 19S regulatory subunit. The 20S subunit activates transcription independently of the 19S subunit though interaction with E1A aa 161-177. Presumably, proteosome-mediated degradation of E1A, or E1A regulatory proteins, regulates the capacity for E1A transactivation (Rasti et al., 2006).
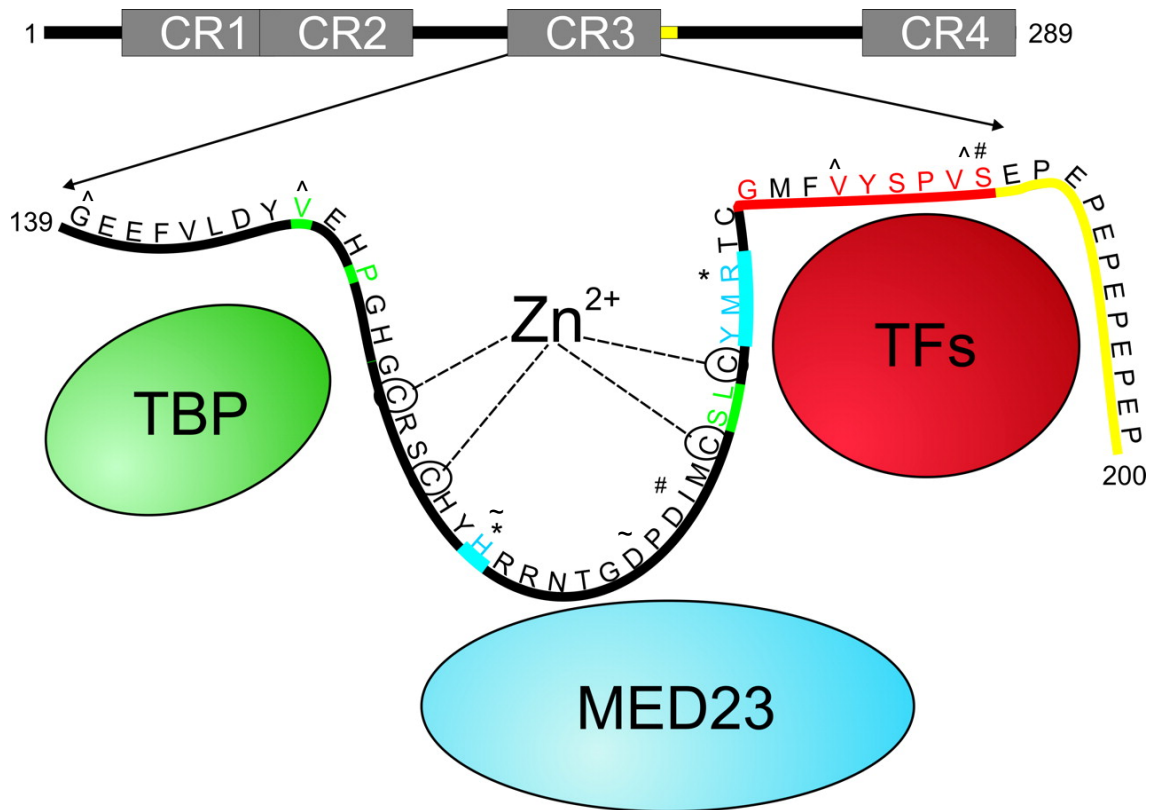
Figure 1.4. The current model of E1A CR3-dependent activation of transcription

Top: A linear representation of 289R E1A. CRs are labeled, and AR1 is denoted in yellow.

Bottom: Residues of E1A CR3 from aa 139 to 200 are indicated using a one-letter code. The coordinating cysteines are circled, and the key targets of CR3 are shown in green (TBP), blue (MED23), and red (Transcription Factors (TFs)), respectively. The key residues interacting with each target are indicated by the corresponding colors. The boundaries of the residues of CR3 known to be required for interaction with APIS (residues 169 to 188) and the 20S proteasome (residues 161 to 177), pCAF (residues 139-147 and 180-188) and CtBP (residues 161-167) are marked by # and *, ^, and ~ respectively. p300/CBP interacts with residues within 137-204 E1A CR3. (Figure modified from Pelka et al., 2008.)

A third region of CR3 is important for the efficient transactivation ability of E1A hAdV5. It is required for transcription activation of all early viral promotors as well as the cellular HSP70 gene. Named Auxiliary Region 1 (AR1), it consists of six glutamic acid-proline (EP) repeats, spanning amino acid residues 189 to 200 in the 289R E1A gene. It was shown that the number of EP repeats is critical for function; reducing the number of repeats to four or increasing the number of repeats to eight or ten, significantly reduces the transactivation capabilities of E1A. When the glutamic acid residues of AR1 were mutated to aspartic acid, E1A retained its transactivation capabilities. However, when mutating this residue to a positively charged amino acid, it impaired transactivation abilities by E1A. Mutating the proline residues did not reduce the transactivation abilities. Therefore, the activation function appears to be due to the acidic nature of this region and the number of repeats present (Ström et al., 1998).

1.2.4   Promoter Targeting by CR3

While E1A has no specific DNA binding activity, it can interact with a number of other proteins or transcription factors (Table 1.2), which directly interact with DNA and directs E1A to the promoter regions of viral genes (Pelka et al., 2008). Activating Transcription Factors (ATFs) are a family of proteins that have basic/leucine (bZIP) DBDs. ATF binding sites are found within E1A targeted promotors of viral early genes. In particular, the ATF binding site within the E4 promoter region is required for E1A mediated transactivation. This led researchers to the discovery of the first cellular transcription factor that E1A uses for promotor targeting purposes. E1A binds ATF-2, and through it's sequence specific DBD, is recruited to promoters containing ATF sites to mediate transcription activation by E1A (Gilardi and Perricaudet, 1986; Liu and Green, 1990). Researchers later discovered that E1A can interact with other members of the ATF family (ATF-1 and ATF-3) as well as other cellular transcription factors that contain different DNA binding domains, such as c-JUN (bZIP DBD), SP1 (zinc finger DNA DBD) and USF (basic/helix-loop-helix bHLH DBD). These interactions were able to mediate E1A activated transcription (Liu and Green, 1994).

Table 1.2. List of Proteins to Interact with the Promotor Targeting Region of CR3

Protein	Interaction Residues	Function	Reference
YY1	140-188	Cellular transcription factor	(Lewis et al., 1995)
TAF$_{II}$110 TAF$_{II}$250	180-188	TBP - Associated Factor	(Geisberg et al., 1995)
ATF-2	179-193	Activating Transcription Factor	(Liu and Green, 1990)
c-Jun	179-193	Transcription Factor AP-1	(Liu and Green, 1994)
USF	179-193	Upstream Stimulatory Factor	(Liu and Green, 1994)
Sp1	179-193	Specificity Protein 1	(Liu and Green, 1994)
S8	169 -188	26S Protease Subunit/Transcription Factor	(Rasti et al., 2006)
pCAF	180-188	p300/CBP Associated Factor	(Pelka et al., 2009a)
GCN5	178-188	Cellular Lysine Acetyltransferase	(Ablack et al., 2012)

Additionally, E1A CR3 interacts via the promotor targeting region with several additional components of the transcription apparatus. Activation of transcription by TBP with E1A CR3 is dependent on several TBP associated factors (TAFs), including $TAF_{II}110$ and $TAF_{II}250$ (Geisberg et al., 1995). YY1 is a zinc finger protein and a cellular transcription factor that represses transcription when bound upstream of heterologous basal promoters. E1A proteins binds YY1 though both the N terminus (aa 15-35) and CR3 (aa 140-188) and relives the repression by YY1, thus activating transcription (Lewis et al., 1995). E1A also binds the S8 subunit of the 19S regulatory proteasome component that binds E1A via aa 169-188, which includes the promotor targeting region. This interaction activates transcription initiation independently of the 20S proteolytic component (Rasti et al., 2006).

1.2.5   E1A and Elongation

There is increasing evidence that E1A is involved in regulating transcription past the formation of the pre-initiation complex. This makes studies of the effects of E1A on transcriptional elongation an important area of research in future studies. E1A binds hBre1 (human BREfeldin A sensitivity) through the N-terminus and recruits the hPaf1 complex to early viral genes. The hPaf1 complex is known for its ability to promote RNAPII mediated elongation which may account for E1A/hPaf1 activation of early viral genes and increased viral replication (Fonseca et al., 2014). E1A, S8 and the 20S proteasome are found at various gene elements throughout the E1B gene, in addition to at enhancer and promotor regions. This indicates that these components transit with the elongating polymerase from the transcription start site and may also be involved in elongation. Although proteasome-mediated degradation of E1A is required for efficient E1A-CR3 mediated transcription initiation, other proteasome components may function to regulate elongation, given that S8 functions independently of the 20S proteasome. SUG1, the yeast homolog of S8, is required for both transcription activation and elongation, which suggests S8 may play a conserved role in cellular and viral genes (Rasti et al., 2006). All E1A isoforms, including the 9S (55R) isoform, interacts with S8 via aa

4-25 which suggests a role for the N-terminus in addition to CR3 in elongation and initiation (Miller et al., 2012; Rasti et al., 2005).

E1A CR3 also interacts with CDK9 as well as other components of the super elongation complex, including CDK9, cyclin T1/T2, AFF4, ELL, and EAF. CDK9 is critical for activating transcription in vitro, for hAdV replication and in activating transcription of early viral genes such as E2 and E4. CDK9 may play a role in elongation of viral genes through interaction with E1A CR3 and possibly MED23 (Vijayalingam and Chinnadurai, 2013). Elucidating the mechanism by which CDK9 in involved with regulating elongation of viral genes is an exciting avenue for future research and may link Adenovirus E1A to other viral models of elongation regulation (See Section 1.4).

In addition to activation and promoting efficient elongation, E1A may negatively regulate elongation. GCN5 is a cellular lysine acetyl transferase and a chromatin modifying factor that facilitates elongation by acetylation of histones. E1A binds and recruits GCN5 to viral promotors through both the N-terminus of E1A and aa 178-188 of CR3 (Table 1.2). E1A recruited GCN5 acetylates histone H3 at the viral E4 promotor and is a negative regulator on elongation. E1A recruited GCN5 may also potentially acetylate CDK9 which represses it's ability to phosphorylate RNAPII and activate elongation (Ablack et al., 2012).

1.3 Mimicry

1.3.1 Introduction to Linear Motifs

For many years, viral mimicry and the study of protein-protein interactions was thought only to pertain to folded globular domains. However, the role of linear motifs or non-globular motifs, particularly in viral mimicry, is an expanding field of study. The following sections introduce the importance of linear motifs, particularly the importance of these motifs in understanding how hAdV5 E1A functions. Linear motifs (LMs), also called short linear interaction motifs (SLiMs), MiniMotifs or Eukaryotic Linear Motifs

(ELMs), are three to ten aa in length and function independently of a tertiary structure. In viral proteins, these ELMs are involved in hijacking a number of different cellular processes such as viral entry and cellular transport, transcriptional regulation, cell cycle regulation, subverting host cell protein- protein interaction networks, and modulating the host cell immune response. The limited length of these ELMs allows viral proteins to encode a large number of these motifs in a single protein. The use of ELMs is advantageous, as they are resistant to mutation, are permissive for functional redundancy, and are conducive to convergent evolution (Chemes et al., 2015; Davey et al., 2011; Dyer et al., 2008). To date the ELM database contains over 170 linear motif classes, 111 of these are ligand sites (LIG) or interaction motifs that mediate protein binding (Davey et al., 2012; Dinkel et al., 2012).

1.3.2   Mimicry in Viral Pathogenesis

Viruses rely heavily on host cell machinery, repurposing it for their own use, in order to control cell cycle and transcription, immune responses and nuclear import. In order to circumvent host cell defenses and hijack cellular processes, viruses will often mimic the host cell (Dyer et al., 2008). Viruses such as HIV, EBV, Kaposi's sarcoma-associated herpesvirus (KSHV), Respiratory Syncytial Virus, and hCMV, encode globular domains in viral proteins that mimic cellular cytokines and chemokines. Other viruses encode proteins that mimic cytokine and chemokine receptors (Alcami, 2003). However, viral proteins are often significantly shorter than host proteins given genome size limitations, and therefore numerous viruses such as EBV, HIV, Adenovirus, Influenza and HPV will use ELMs rather than globular domains to usurp host cell processes (Reviewed in Davey et al., 2011). As some selected examples, HIV Nef1 mimics the SH3 binding PxxP motif of cSrc and activates members of the Src family tyrosine kinases Hck, Lyn and and cSrc itself (Moarefi et al., 1997; Saksela et al., 1995; Trible et al., 2006). Some studies suggest the Nef PxxP motif plays a role in AIDS progression and HIV pathogenesis and this has led to screens of large libraries of small molecule inhibitors in order to discover new therapeutics to target these interactions (Moroco et al., 2015; Trible et al., 2006; Wales et al., 2015). Influenza PB2 (a component of the influenza virus polymerase) and Simian

Virus 40 (SV40) T-Antigen mimic bipartite and monopartite nuclear localization signals (NLSs) respectively, and these motifs mediate binding to importin alpha. By mimicking mammalian NLSs viruses can make use of host cell transport machinery to traffic viral proteins to the nucleus (Fontes et al., 2003; Mukaigawa and Nayak, 1991; Tarendeau et al., 2007).

Motif rich viral proteins also play an important role in oncogenesis and these proteins have led to many discoveries about cell cycle progression (Davey et al., 2011). The density of motif mimicry within EBV latent membrane protein (LMP1) leads to dysregulation of multiple cellular pathways by a single protein and results in cancer progression. LMP1 mimics cellular CD40, a member of the TNF receptor family, in order to hijack cellular signalling pathways for immortalization of B cells by disrupting cellular proliferation and apoptosis. The EBV LMP1 protein interacts with JAK through the proline rich PxxPxP motif which leads to phosphorylation of JAK and the activation of the JAK/STAT pathway (Gires et al., 1999). LMP1 also binds TNFR-associated factor (TRAF) through the PxQxT motif which leads to activation of the NF-kB pathway (Mitchell and Sugden, 1995; Ye et al., 1999).

In summary, the examples above are by no means an exhaustive list, but they highlight the importance of viruses mimicking host proteins at all stages of the viral replication cycle.

1.3.3 Mimicry and Evolution

Adenoviral E1A, Human Papilloma Virus (HPV) E7, SV40 T-antigen, JC virus T antigen, and BK virus T-antigen, all interact with pRb via an LxCxE motif, suggesting that similar functions though SLiMs evolved via different pathways in various families of DNA tumour viruses (Felsani et al., 2006). ELMs do indeed tend to be the product of convergent evolution, which is defined as: "Multiple independent appearances of a given motif that can occur both in unrelated proteins and in separate branches of a protein phylogeny" (Chemes et al., 2015; Hagai et al., 2014). Globular domains evolve slowly, restricted in that they must maintain correct folding, but these linear sequences easily

appear and readily undergo positive selection in a population (Chemes et al., 2015; Davey et al., 2011). Researchers took a data set of over 2208 non-redundant viruses and scanned the disordered domains of all viral proteins that match with a database of ELMs (Dinkel et al., 2012; Hagai et al., 2014). They discovered ELMs tended to be shorter and less complex, and that the number of ELMs correlated to the length of the disordered regions in viral proteins. Additionally, certain pairs of ELMs exist in viral proteins, which suggests highly regulated interaction networks (Hagai et al., 2014). Computational biology is an invaluable tool for studying large datasets of viral proteins to identify new instances of ELMs, as well as novel ELMs, leading to the discovery of novel protein-protein interactions. Such approaches have become a vital tool in studying evolution in pathogenesis. Furthermore, the rapid evolution of viral ELMs leads to rapidly changing host-virus interaction networks, which may have an important long term impact on the evolutionary course of host cells (Bhowmick et al., 2015; Dinkel et al., 2012; Edwards and Palopoli, 2015; Elde and Malik, 2009; Hagai et al., 2014).

1.3.4   Mimicry by Adenovirus

Adenovirus has a genome of approximately 36 kbp and employs multiple examples of structural, functional and motif mimicry in order to get around the limited coding capacity of the genome and hijack the host cell for permissive viral replication. The adenoviral penton base expresses an RGD-containing loop, that mimics the integrin binding motif present on extracellular matrix proteins such as fibronectin, and is critical for adenoviral binding to integrins for internalization of the virus (Bai et al., 1993; Chiu et al., 1999; Cuzange et al., 1994; Nemerow and Stewart, 2016). The adenoviral genome is packaged in a way that resembles chromatin, where the nucleoprotein VII (PVII) condenses adenoviral DNA akin to cellular nucleosomes. During infection, PVII is also found associated with cellular nucleosomes in host DNA, where it can protect DNA from degradation. Thus, the PVII protein not only acts as a functional histone mimic in viral chromatin like structures, but also acts within the host cell chromatin to bind cellular factors and block host immune responses (Avgousti et al., 2016; Johnson et al., 2004; King et al., 2016c; Vayda et al., 1983). The adenoviral E1B-19K protein functions like

the cellular oncogene BCL-2 to inhibit apoptosis and is required for transformation of rodent cells (Chiou et al., 1994; Radke et al., 2014).

1.3.5   Mimicry by hAdV E1A

Although E1A is only 289 amino acids long, it alone interacts directly with over 30 proteins and potentially targets a protein-protein network of over 2100 cellular proteins (Figure 1.3). To accomplish this task, E1A itself must also therefore rely on numerous examples of structural, functional and motif mimicry. The N-terminal region of E1A, aa 14-28, functionally and structurally mimics cellular A-kinase anchoring proteins (AKAPs) in order to bind PKA and relocate it to the nucleus to increase transcription of viral genes and increase virus replication (King et al., 2016b). E1A interacts with the OCT4 transcription factor via the N-terminus and CR3 where E1A acts as a mimic of a cofactor required to activate OCT4 and regulates reprogramming of host cells to induce pleuripotent stem cells (Brehm et al., 1999; Marthaler et al., 2016; Schöler et al., 1991).

E1A CRs extensively mimics a number of ELMs that function in binding to cellular factors to hijack for the virus's own use (Reviewed in Davey et al., 2011). For example, E1A binds the transcriptional regulators CREB binding protein (CBP) and p300 via the conserved FxDxxxL motif (O'Connor et al., 1999). CtBP interacts with E1A through the PxDLS motif in CR4 of E1A and regulates oncogenic transformation (Chinnadurai, 2002; Schaeper et al., 1995, 1998). BS69 interacts with E1A through the PxLxP motif in CR2 and acts as a suppressor of E1A mediated transactivation (Ansieau and Leutz, 2002; Hateboer et al., 1995). E1A interacts with pRb via the LxxLY motif in CR1, and also binds to pRb pocket binding domain via the LxCxE motif in CR2 (Dyson et al., 1992; Felsani et al., 2006; Morris and Dyson, 2001). New data shows that the LxCxE motif is also critical for E1A interaction with STING, which may antagonize the DNA sensing cGAS pathway to prevent an antiviral response (Lau et al., 2015). pRb, BS69, STING as well as UBC9 all interact with both distinct and overlapping motifs in the CR2 region of E1A. This density of interactions highlights the importance of motif mimicry and making

use of functional motifs to use the minimum amount of coded protein for the maximum functional output (Davey et al., 2011; Pelka et al., 2008).

1.4 Viruses, the CTD, and Elongation

Of the three cellular RNA polymerases (RNAPI, II, and III), RNAPII is largely responsible for the production of mRNA. DNA viruses, such as hAdV, rely primarily on RNAPII to transcribe viral genes. RNAPII is made up of a ten subunit core with the Rpb4/7 subcomplex flexibly linked to the RNAPII core. The C-terminal domain (CTD) is linked to the largest subunit of RNAPII (Rpb1) by an 80 residue flexible linker, and itself consists of a consensus sequence tyrosine-serine-proline-threonine-serine-proline-serine (YSPTSPS). The functional unit is defined as one full repeat and the next four residues (Cramer et al., 2008; Eick and Geyer, 2013). The CTD is largely unstructured, although it shows some evidence of B-turns formed by SPXX motifs (Meinhart et al., 2005; Suzuki, 1989) The length of the CTD and the overall structural disorder is critical for function (Liu et al., 2010). In humans, there are 52 heptad repeats, and a minimum of 22 are required to support transcription (Rosonina and Blencowe, 2004).

The functional motifs of the CTD are post translationally modified by phosphorylation, glycosylation, methylation and isomerization, which together creates a so-called CTD code. A single functional unit has over 10 000 potential combinations of post translational combinations. This, along with the disordered nature of the CTD, allows for multiple different and dynamic docking sites for a number factors involved in mRNA splicing and coordination of the transcription cycle (Eick and Geyer, 2013; Meinhart et al., 2005).

Two important modifications of the CTD are the phosphorylation of serines at positions 2 and 5 of the heptad repeat. Unphosphorylated RNAPII (also called hypophosphorylated or RNAPIIa) is recruited to the DNA template. CDK7 in complex with Cyclin H then preferentially phosphorylates serine 5 (S5) for transcription initiation. Positive transcription elongation factor b (P-TEFb), which consists of CDK9 in complex with Cyclin T, next preferentially phosphorylates serine 2 (S2) to stimulate transcription

elongation, resulting in the hyperphosphorylated form of RNAPII (RNAPIIo) (Eick and Geyer, 2013). A further regulation step consists of controlling the release of the stalled polymerase, paused proximally at the promoter. Negative elongation factor (NELF) acts with DRB sensitivity-inducing factor (DSIF) to pause the polymerase complex after it transcribes the initial 20 to 60 nucleotides. P-TEFb then phosphorylates NELF and DSIF to de-repress paused transcription, releasing the polymerase to continue transcriptional elongation (Gilchrist et al., 2008; Kwak and Lis, 2013).

A number of different viral proteins from viruses such as; HIV, EBV, hCMV, HSV, KSHV, and Human T-lymphotropic virus type 1 (HTLV), have been shown to interact with CDK9 to enhance viral transcription by relief of promotor pausing to promote elongation. Several of these viruses, including HIV, EBV, hCMV and HSV, will also modify the phosphorylation state of the RNAPII CTD through regulation and recruitment of CDK9 (Reviewed in Zaborowska et al., 2016). Adenovirus E1A has also been shown to interact with CDK9 and this may be a way by which it too promotes elongation of viral genes (Vijayalingam and Chinnadurai, 2013). Investigating this interaction is of great importance as it may place Adenovirus in a category with other viruses that hijack RNAPII for virally enhanced elongation.

1.4.1   HIV

HIV is likely the most well studied of these viruses and the mechanism by which it affects transcriptional elongation has been well characterized. Early on, researchers discovered that HIV Tat (a transcriptional activator) modifies the substrate specificity of CDK9 to phosphorylate S5 in addition to S2 of RNAPII CTD (Zhou et al., 2000). During elongation, Tat binds to the transactivation response (TAR) - RNA element, which is a stem loop structure that forms at the 5' end of nascent viral transcripts, and the P-TEFb complex is recruited to TAR. Tat directed CDK9 phosphorylation is critical for this interaction (Garber et al., 2000; Kim et al., 2002). The complex then phosphorylates the CTD, as well as NELF and DSIF, to release the stalled polymerase and stimulate efficient elongation (Ott et al., 2011; Zhou et al., 2000). Treating cells with the P-TEFb/CDK9

inhibitors such as DRB (6-dichloro-1-b-D-ribofuranosylbenzimidazole) or Flavopiridol reduced Tat induced CDK9 phosphorylation and blocks HIV transcription and replication (Chao et al., 2000; Zhou et al., 2000).

1.4.2   HTLV-1

HTLV-1 encodes a transcriptional activator Tax. P-TEFb is recruited to promotors in the presence of Tax, where Tax induces the phosphorylation and activation of CDK9. The use of a CDK9 inhibitor (Flavopiridol) and siRNA against CDK9 demonstrates that CDK9 is critical for Tax transactivation (Zhou et al., 2006). Further studies show the dual roles for Tax in regulating the P-TEFb complex. Tax displaces the inhibitory 7SK snRNP/HEXIM1 complex from P-TEFb to form the Tax/P-TEFb complex, which results in more efficient transcriptional activation at the HTLV-1 LTR. Normally Brd4 is present on the HTLV-LTR in an inactive form, but in the presence of Tax, Brd4 levels decrease while the levels of CDK9 increase. This suggests that the Tax/P-TEFb complex is recruited to the LTR to activate transcription (Cho et al., 2010; Zaborowska et al., 2016).

1.4.3   EBV

In a similar fashion to HIV-Tat, the EBNA-2 protein of EBV is involved in transcriptional activation, and specifically requires CDK9. EBNA-2 hijacks CDK9 to phosphorylate S5 of the CTD of RNAPII rather than S2. This may indicate CDK9 and EBNA-2 modify RNAPII in order to direct promotor clearance and elongation. DRB treatment also inhibits EBNA-2 activated transcription, which further highlights the importance of CDK9 in viral transcriptional activation and CTD phosphorylation. DRB and Flavopiridol were discussed as potential treatments for EBV infection (Bark-Jones et al., 2006).

1.4.4   hCMV

HCMV infection leads to the formation of transcriptomes, which are the site of intermediate early gene transcription and thus function as recruitment centres for cellular transcriptional regulators. HCMV infection alters the phosphorylation of RNAPII and the accumulation of CDK7 and CKD9 at these centres at different stages of infection. HCMV infection also results in higher kinase activity of CDK7 and CDK9. At early times in infection, S2 phosphorylated RNAPII, CDK9, and CDK7 colocalize with the intermediate early (IE1/IE2) proteins. At 48 hours post infection, CDK7 and unphosphorylated RNAPII are found at viral replication centres, while CDK9 and S2 phosphorylated RNAPII are observed in punctate around the nuclei, and S5 phosphorylated RNAPII is seen at the peripheries of the replication centres. Treating with the CDK inhibitor Roscovitine at early times of infection reduced phosphorylation of RNAPII and transcription of viral genes. These observations suggests that a viral protein functions to regulate the cellular CDKs and the alters phosphorylation of RNAPII to promote viral transcription (Tamrakar et al., 2005).

In fact there are three proteins expressed by hCMV that interact with P-TEFb: pUL69, pUL97 and IE2 86 (Graf et al., 2013; Kapasi et al., 2009; Rechter et al., 2009). pUL97 is considered a mimic of CDKs activity due to structural and functional similarities to its cellular counterpart. Deletion of pUL97 leads to decreased viral replication. pUL97 interacts with Cyclin-T1 but does not phosphorylate RNAPII *in vivo* (although it does *in vitro*) (Baek et al., 2004; Graf et al., 2013). pUL97 phosphorylates pUL69 which can modulate pUL69 function and nuclear localization during hCMV infection. pUL69 is a transcriptional activator and mRNA export factor, which is also phosphorylated by CDK9, providing another level of regulation (Graf et al., 2013; Rechter et al., 2009). IE2 86 is a 86-kDa is major immediate-early protein, and it contains a serine rich region that must be phosphorylated for efficient transcription of viral genes (Barrasa et al., 2005). Later studies showed that the viral protein IE2 86 is vital for the interaction between Cyclin T1 and CDK9, for CDK9 activity, and for the recruitment of CDK9 to viral replication centres (Kapasi and Spector, 2008; Kapasi et al., 2009). Thus, hCMV encodes a number of different factors that interact with the P-TEFb regulatory complex.

Collectively, these induce an infection specific subcellular localization of viral and cellular factors, induce hyperphosphorylation of RNAPII, and promote viral transcription and replication (Zaborowska et al., 2016).

Although the viral protein pUL79 does not bind to cellular CDKs and does not modify the phosphorylation of RNAPII, it does appear to act as a virally encoded factor that relieves a stalled polymerase and promote elongation of viral genes at late points of infection (Perng et al., 2014).

1.4.5   HSV

HSV infection has also been shown to modify the phosphorylation state of the CTD, producing an HSV specific from of RNAPII, an RNAPIIi or intermediate form that is solely phosphorylated on S5. ICP22 interacts with CDK9 and phosphorylates the RNAPII CTD on S5 in a fashion that is dependent on the viral U_S3 protein. Additionally, ICP22 with viral U_L13 triggers the loss of phosphorylated S2 in an alternate mechanism (Durand and Roizman, 2008; Durand et al., 2005; Rice et al., 1995). The regulatory protein ICP27 interacts with RNAPII and may play a role in relocalization of RNAPII to viral transcription sites, where S2 phosphorylated RNAPII undergoes proteasomal degradation, resulting in a global reduction in levels of phosphorylated S2 during infection (Dai-Ju et al., 2006; Fraser and Rice, 2005, 2007).

In addition, HSV modification of RNAPII by ICP22 is essential for transcription of viral genes. During HSV infection, CDK9 and RNAPII co-localize with ICP22, bringing researchers to believe that CDK9 may bring ICP22 into the RNAPII complex. ICP22 then functions to alter expression of viral genes though interactions with viral proteins such as U_L13 or VP16 (Bastian and Rice, 2009; Durand and Roizman, 2008; Guo et al., 2012; Rice et al., 1995). Inhibiting CDK9 with DRB, Flavopiridol, or Roscovitine impedes transcription of viral genes in HSV infection (Durand et al., 2005; Ou and Sandri-Goldin, 2013).

1.4.6   KSHV

As an interesting example of mimicry, the region from aa 633 to 652 in the KSHV transactivator protein K-RTA shows homology to a region in the NELF-B component of NELF. Within this region of homology, these two proteins in particular share conserved phosphorylated serine residues. These residues, serine-634 and serine-636, in K-RTA are phosphorylated by the recruitment of CDK9 *in vitro*. Replacing these residues with alanines in K-RTA impaired its ability to activate transcription, reduced CDK9 recruitment, and resulted in an overall decrease in KSHV replication. Treating infected cells with CDK9 inhibitors such as Flavopiridol, Roscovitine, or DRB, led to a reduction in transcription of K-RTA regulated genes. They concluded that this motif in K-RTA bears similarity to a functional domain in NELF-B and functions to recruit CDK9 to the viral genome for more efficient transcription, perhaps through bypassing promotor pausing of RNAPII (Tsai et al., 2012).

1.5 Thesis Overview

1.5.1   Rationale

The hAdV E1A protein is the first gene expressed upon adenovirus infection. E1A is a potent activator of transcription and is responsible for turning on all early viral genes. E1A CR3 is necessary and sufficient to activate transcription when fused to a heterologous DBD in mammalian cells (Ablack et al., 2010, 2012; Shuen et al., 2002). For full transcriptional activation, CR3 requires all three functional regions be intact: the zinc finger region, the C-terminal region, and the negatively charged AR1 (Glenn and Ricciardi, 1987; Pelka et al., 2008; Ström et al., 1998; Webster and Ricciardi, 1991).

Of these regions, the role of the C-terminal region of CR3 (aa 180-188) in transcriptional activation is probably the least well understood. The earliest studies demonstrating a function in this region were based on the characterization of random mutations created by treating hADv5 virions with nitrous acid. The host range 5 (*hr5)* mutant was sequenced

and found to have a single amino acid substitution at S185 for asparagine. The *hr5* mutant was unable to activate transcription at early viral genes E2, E3 and E4 (Berk et al., 1979; Glenn and Ricciardi, 1985). A pair of deletion mutants in this region, which include *dl1114 (Δ*178-184) and *dl1115* (Δ188-204), were also unable to activate transcription (Jelsma et al., 1988). Following these studies, Webster and Ricciardi mutated every single amino acid in E1A and examined the resulting peptides for their ability to activate transcription. Any substitutions in residues in this C-terminal region, or its deletion in its entirety, also abolished transactivation capabilities. Interestingly enough, mutating the C-terminal portion but leaving the zinc finger region of CR3 intact resulted in a trans-dominant phenotype. In this case, co-expression of the mutant E1A blocks transactivation by wild type (WT) E1A. Mechanistically, it was thought that while the above dominant negative mutants cannot bind a subset of associated cellular factors required for transactivation, it retains binding with the cellular transcription machinery that is recruited through the zinc finger and titrates such factors away from the early viral promotors (Glenn and Ricciardi, 1987; Webster and Ricciardi, 1991). These experiments established the C-terminal region as its own functional domain separate from the zinc finger domain (Glenn and Ricciardi, 1987; Webster and Ricciardi, 1991).

The C-terminal region appears unstructured and this likely contributes to its ability to interact with a number of different proteins. Studies have suggested that this C-terminal region binds to DNA binding transcription factors, such as members of the ATF family, USF, Sp1, TAFII250 and TAFII135 and S8 (Geisberg et al., 1995; Pelka et al., 2008; Rasti et al., 2006; Webster and Ricciardi, 1991). These discoveries established the C-terminal portion of CR3 as the promotor targeting region, and from here on in will be referred to as such. As E1A has no DNA binding capabilities, it is thought that the promotor targeting region of CR3 directs E1A to transcriptional templates for activation and formation of the pre-initiation complex (Ferguson et al., 1985; Liu and Green, 1994). However, how the promotor targeting region functions, in relation to the DNA binding proteins or other unknown factors, remains to be understood.

This promotor targeting region of E1A is arguably the most conserved region across adenovirus subtypes (Avvakumov et al., 2004). Therefore, it is an interesting observation

that in E1A CR3 we find a sequence (YSPVSEP) which has considerable sequence similarity to the consensus heptad repeat of the RNAPII CTD (YSPTSPS) (Figure 1.5). In addition, both the promotor targeting region of E1A CR3 and the RNAPII CTD are believed to be unstructured (Pelka et al., 2008; Srivastava and Ahn, 2015). Two serine residues in E1A CR3 (S185 and S188) are invariant and phosphorylated, which corresponds to the phosphorylation of S2 and S5 of the RNAPII CTD. S185 and S188 are shown to be hyperphosphorylated in vivo. Those researchers also show that S185 is found within a mitogen-activated protein kinase (MAPK) consensus phosphorylation site, and *in vitro* is phosphorylated by MAPK. However, S188 is not phosphorylated by MAPK, but appears to be phosphorylated by a kinase that is activated by MAPK, although the specific kinase is unknown. Phosphorylation of these residues, S185 and S188, were shown to be required for transactivation of the viral E4 gene by E1A (Whalen et al., 1997). Mutating these highly conserved serine residues impairs transactivation by E1A, particularly of the E4 gene, which highlights the importance of phosphorylation in transactivation regulation (Avvakumov et al., 2002, Glenn and Ricciardi, 1987; Whalen et al., 1997).

1.5.2 Hypothesis

We believe that given the sequence similarity, structural similarity, and the phosphorylation at conserved residues, that E1A CR3 acts as a mimic of the RNAPII CTD to promote transcription of viral genes.

E1A has been shown to interact with CDK9 and some evidence exists that E1A activates viral gene expression at both the initiation and elongation steps. Given the current models for HIV and EBV, that hijack CDK9 to relieve promotor pausing and allow for efficient elongation of viral genes, we further believe that E1A may function in a similar fashion.

1.5.3   Objectives

1) To determine the role of the putative CTD mimic in transcription activation.

2) To establish the extent of the structural/functional mimicry by E1A CR3 based on the sequence similarities between RNAPII CTD and E1A CR3.

3) To elucidate the mechanism by which the putative CTD mimic promotes transcription.

Figure 1.5. Sequence alignment of all hAdV Species (A-G) E1A CR3 with the RNAPII CTD consensus sequence.

Alignment demonstrates high conservation between adenovirus species in the promotor targeting region of E1A and demonstrates a high level of sequence similarity to the RNAPII CTD. Darker shading indicates highly conserved amino acids. + indicates conserved cysteine residues that coordinate a zinc ion to bind TBP and Mediator. * indicates conserved serine residues that are phosphorylated in both hAdV E1A and RNAPII.

Chapter 2 : Methods

2   Methods

2.1 Cells, Cell Culture, and Transfections

Human cell lines: A549 (alveolar basal epithelial cell line), HT1080 (fibrosarcoma cell line), and HEK293A (embryonal kidney cell line) were originally obtained from the American type culture collection (ATCC). All cells were maintained at 37°C and 5% CO_2 in Dulbecco Modified Eagle medium (Wisent) with 10% Performance Fetal Bovine Serum (Wisent) and 100 U/ml of penicillin-streptomycin (Wisent). HT1080 cells were transfected with the X-tremeGene HP DNA transfection reagent (Sigma) according to the manufacturer's directions in a ratio of 4μl to 1μg of DNA.

2.2 Viruses and Virus Construction

HAdV5, dl309 (expresses all E1A proteins), has been described previously (Jones and Shenk, 1979) and is used as wildtype (WT) in my experiments.

pXC1-Ad5 E1A S185/188A was created by cloning the E1A S185/188A coding sequence into the EcoRI and SalI restriction sites of pXC1 (a generous gift of F. Graham). CR3 S185/188A was amplified using the following primers, by a previous student (Greg Fonseca, 2013) in our lab, via two-step PCR:

CR3 5' F-CTACGCTCCTGTGGCTGAACCTGAGCC and

CR3 5' R- ACTGTCGACTTATGGCCTGGGACGTTTACAGCTC,

CR3 3' F-CGACGAATTCATGAGACATATTATCTGC and

CR3 3' R-GGTTCAGCCACAGGAGCGTAGACAAAC.
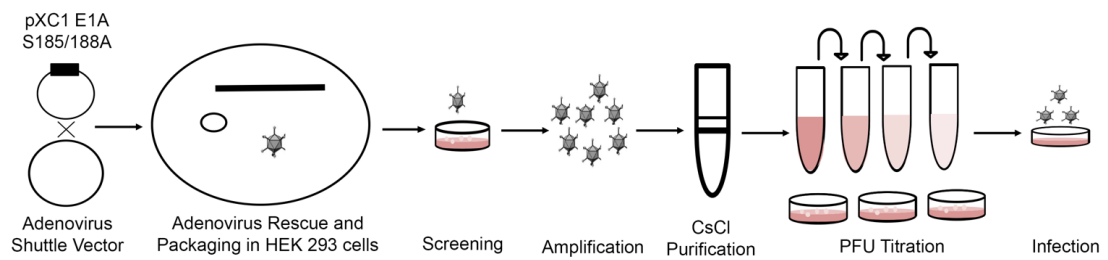
Figure 2.1. Steps involved in the rescue of the JM17 E1A S185/188A virus.

(Figure adapted from Vectorbiolabs.com, 2016)

HEK 293A cells were seeded in 10cm dishes 24 hours prior to transfection with the pXC1-E1A S185/188A plasmid and pJM17. HEK 293A cells constitutively express the E1 genes and are often used in order to create pure populations of mutant viruses. The cells complement defects in viruses containing mutations in the E1A and E1B genes by supplying the WT E1A and E1B in trans (Amalfitano et al., 1996; Graham et al., 1977; Ketner and Boyer, 2007; Krougliak and Graham, 1995). Recombinant virus was rescued by transfecting 5μg of pXC1- E1A S185/188A and 10μg of pJM17 into HEK 293A cells, using a 2:1 X-tremeGene HP DNA transfection reagent (Sigma) to DNA ratio (Figure 2.1). The pXC1 plasmid contains 16% of the left end of the hAdV5 genome, which includes the entire E1 region (McKinnon et al., 1982, 1985). For my experiments, WT E1A was replaced with the E1A S185/188A mutation. The pJM17 plasmid is an adenoviral shuttle vector containing the entire adenoviral genome without the packaging signal required for the encapsidation of the viral genome. This plasmid also contains an insert that makes the genome approximately 2 kbp larger than the maximum amount of DNA that can be packaged in adenoviral capsids. Infectious virus particles will only be produced when a recombination event takes place to excise the insert. pJM17 efficiently recombines with plasmids containing the left hand end of the adenoviral genome, such as the pXCI plasmid containing the desired E1A mutation (Ghosh-Choudhury et al., 1987; McGrory et al., 1988). Successful recombination results in a full length packagable genome and the production of infectious virus. Viral production and infection causes subsequent cell lysis. When 100% cytopathic effect (CPE) is observed in the transfected HEK293 cells, approximately 7 days post transfection, a crude viral stock is prepared harvesting cells and supernatant and repeatedly freeze/thawing the samples to release the virus particles.

Virus was serially diluted and titered by plaque assay. Single plaques were picked for propagation and sequencing of viral DNA (Purelink Viral RNA/DNA Mini Kit Invitrogen). Sequenced clones (BioBasic) demonstrated the successful rescue of the mutant JM17-E1A S185/188A virus. A single viral clone was amplified by infecting 6 x 15 cm plates of HEK 293 cells. Cells were harvested and the virus was purified by CsCl density gradient purification using standard methods. Briefly, cells were incubated with Tris Buffered Saline (TBS), 0.5% Deoxycholic acid, 0.02M $MgCl_2$, and 10mg/ml RNAse

prior to sonication. The density was adjusted to 1.34g/cc CsCl with TBS and transferred to a centrifuge tube. Sealed centrifuge tubes were spun overnight (~16 hours) at 33 000 rpm in a T65 rotor, Beckman Optima XL-100K Ultracentrifuge (Tollefson et al., 2007). Virus was then titered by plaque assay to determine plaque forming units (PFU/mL) in order to use the virus for future experiments with reliable and quantifiable results (n=2). Again, viral DNA from single plaques were sequenced to confirm the purified stock of virus contained a pure population of JM17-E1A S185/188A mutant virus.

Similar steps were taken to produce a virus replacing S185 and S188 of E1A with aspartic acid (S185/188D), thus creating a phospho-mimic of WT E1A. However, after the initial recombination step, the rescued virus was not infectious and could not be amplified and purified.

Virus infections were performed using A549 cells at the indicated multiplicity of infection (MOI) and cells were harvested at the indicated time points.

2.3 Plasmid Construction and Large Scale Preparations

All plasmids (Table 2.1) were transformed into DH5α competent cells (Bethesda Research Laboratories, 1986) and were grown in Luria Broth with appropriate antibiotics at 37 °C overnight. Small-scale preparations were made using PureLink Quick Plasmid Mini Kit (Invitrogen) and all large-scale preparations were made by PureLink HiPure Plasmid Filter Midiprep Kit (Invitrogen). All correct clones were verified by sequencing (Biobasic).

The GAL4-responsive luciferase reporter vector pGL2-(Gal4)$_6$-Luc and GAL4-DBD fusion for hAdV E1A CR3 has been described previously (Avvakumov et al., 2003; Shuen et al., 2002). E1A CR3 S185/188A CR3 S185/188D were cloned into EcoRI/SalI sites of pM (Clontech Labratories Inc.) or pGFP (expresses the green fluorescence protein driven by the cytomegalovirus promotor). E1A CR3 truncations (CR3 190T, 189T, 182T, 178T) were PCR amplified by a previous student in the lab (Jai Ablack, 2012) and were cloned into pM or pGFP via EcoRI/SalI restriction sites.

Table 2.1. A list of plasmids utilized in this study and their sources (JMB is <u>J</u>oe <u>M</u>ymryk <u>B</u>acteria Database)

Gene	Parent Vector	JMB	Source
Empty Vector	pM	301	Clonetech
CR3	pM	1493	Weimin Liu
CR3 S185/188A	pM	4429	Greg Fonseca
CR3 S185/188D	pM	4430	Greg Fonseca
CR3 190T	pM	3706	Jai Ablack
CR3 189T	pM	3705	Jai Ablack
CR3 182T	pM	3575	Jai Ablack
CR3 178T	pM	3876	Jai Ablack
CR3 183-200 WT	pM	4638	This study
CR3183-200 S185/188A	pM	4639	This study
CR3183-200 S185/188D	pM	4640	This study
CR3 183-190	pM	4643	This study
CR3 183-192	pM	4642	This study
CR3 183-196	pM	4641	This study
EP x6	pM	4644	This study
Human CTD Heptad	pM	4645	This study
Empty Vector	pGFP	925	Stephanie Derbyshire
CR3	pGFP	1756	Weimin Liu
CR3 S185/188A	pGFP	4440	Greg Fonseca
CR3 S185/188 D	pGFP	4441	Greg Fonseca
CR3 190T	pGFP	3708	Jai Ablack
CR3 182T	pGFP	3889	Jai Ablack
CR3 Δ180-188	pGFP	3168	Jai Ablack
CR3 183-200 WT	pGFP	4646	This study
CR3183-200 S185/188A	pGFP	4647	This study
CR3183-200 S185/188D	pGFP	4648	This study
CR3 183-190	pGFP	4651	This study
CR3 183-192	pGFP	4650	This study

CR3 183-196	pGFP	4649	This study
EP x6	pGFP	4652	This study
Human CTD Heptad	pGFP	4653	This study
13S E1A	pGFP	1449	Jennifer Curran
13S E1A S185/188A	pGFP	4654	This study
13S E1A S185/188D	pGFP	4655	This study
13S E1A	pXC1	152	F. Graham
13S E1A S185/188A	pXC1	4427	Greg Fonseca
13S E1A S185/188D	pXC1	4426	Greg Fonseca
CDK9	pCDNA4-HA		This study
hAdV5 Genome	JM17	184	Joe Mymryk

Table 2.2. List of self-annealing oligonucleotides used in this thesis.

	Forward Primer	Reverse Primer
CR3 183-200 WT	AATTCTTTGTCTACGATCCT GTGTCTGAACCTGAGCCTG AGCCCGAGCCAGAACCGG AGCCTTAAG	TCGACTTAAGGCTCCGGTT CTGGCTCGGGCTCAGGCT CAGGTTCAGCCACAGGAGC GTAGACAAAG
CR3 183-200 S185/188A	AATTCTTTGTCTACGCTCCT GTGGCTGAACCTGAGCCTG AGCCCGAGCCAGAACCGG AGCCTTAAG	TCGACTTAAGGCTCCGGTT CTGGCTCGGGCTCAGGCT CAGGTTCAGCCACAGGAGC GTAGACAAAG
CR3 183-200 S185/188D	AATTCTTTGTCTACGATCCT GTGGATGAACCTGAGCCTG AGCCCGAGCCAGAACCGG AGCCTTAAG	TCGACTTAAGGCTCCGGTT CTGGCTCGGGCTCAGGCT CAGGTTCATCCACAGGATC GTAGACAAAG
CR3 183-190	AATTCTTTGTCTACAGTCCT GTGTCTGAACCTTAAG	TCGACTTAAGGTTCAGACA CAGGACTGTAGACAAAG
CR3 183-192	AATTCTTTGTCTACAGTCCT GTGTCTGAACCTGAGCCTT AAG	TCGACTTAAGGCTCAGGTT CAGACACAGGACTGTAGAC AAAG
CR3 183-196	AATTCTTTGTCTACAGTCCT GTGTCTGAACCTGAGCCTG AGCCCGAGCCATAAG	TCGACTTATGGCTCGGGCT CAGGCTCAGGTTCAGACAC AGGACTGTAGACAAAG
EP x6	AATTCTTTGTCGAACCTGA GCCTGAGCCCGAGCCAGA ACCGGAGCCTTAAG	TCGACTTAAGGCTCCGGTT CTGGCTCGGGCTCAGGCT CAGGTTCGACAAAG
Human CTD Heptad	AATTCTTTGTCTATAGCCCG ACCAGCCCGAGCTAAG	TCGACTTAGCTCGGGCTGG TCGGGCTATAGACAAAG

Pairs of self-annealing oligonucleotides (Table 2.2), designed with EcoRI and SalI sticky ends, were purchased from Integrated DNA Technologies (IDT) and cloned into the EcoRI/SalI sites of either pM or pGFP. Correct clones were identified by restriction digest with XhoI/XbaI (pM clones) and XhoI/HpaI (pGFP clones).

WT 13S E1A fused to GFP has been described previously. 13S E1A S185/188A and 13S E1A S185/188D were cut from their respective pXC1 plasmids with EcoRI and SalI and cloned into EcoRI/SalI cut pGFP.

The CDK9 expression vector was generated using a custom gene synthesis service from IDT and was cloned into pCDNA4-HA with EcoRI/SalI.

2.4 Luciferase Reporter Assay

24 hours prior to transfection, HT1080 cells were seeded into six-well plates at a density of approximately of 2×10^5 cells/well.

The GAL4 fusion assay has been described previously (Ablack et al., 2010). The E1A CR3 activation assay was performed as follows: cells were first transfected in a 1:1 ratio of reporter vector [pGL2-(Gal4)$_6$-Luc] to activator (pM-CR3). Cells were then harvested 24 hours post transfection in 1x cell culture lysis buffer (Promega). Lysates were assayed for luciferase activity using Steady-Glo substrate (Promega) and the Lumat LB 9507 (Berthold) luminometer. Many thanks to the Drs. DiMattia and Shepard laboratory for the use of the machine. The number of relative light units (RLUs) were normalized to the protein concentration and plotted as the mean fold activation above that achieved with GAL4-DBD alone (pM) ± standard deviation (SD).

The competition assay has been described previously (Ablack et al., 2010). The competition assay was performed as follows: cells were first transfected in a 1:1:1 ratio of reporter [pGL2-(Gal4)$_6$-Luc]: activator (pM-CR3): squelcher (either pGFP or pGFP-CR3 fusion). Cells were harvested at 24 hours post transfection, as described above. The number of RLUs were normalized to the protein concentration and plotted as a percentage

of GAL4-Ad5 E1A CR3 WT (pM-CR3) activation with pGFP (empty vector) as the competitor ± SD.

2.5 Western Blotting and Co-Immunoprecipitation

Details for primary and secondary antibodies may be found in Table 2.3.

HT1080 cells were seeded 24 hours prior to transfection. Cells were then harvested 24 hours post transfection by scraping and washed once with 1X Phosphate Buffered Saline (PBS). In order to preserve phosphorylation of serine residues, cells lysates prepared for co-immunoprecipitation (Co-IP) were prepared in RIPA Buffer (50mM Tris, 150nM NaCl, 1% NP-40, 0.5% Na-Deoxycholate, 0.1% SDS, pH7.5) supplemented with 1X protease inhibitor cocktail (Sigma) and phosphatase inhibitors (0.5M NaF and 200mM Na-Orthovanadate and 225 mM Na-Pyrophospate). Co-IP protein samples were incubated overnight with rocking at 4°C with 100µl of 10% ProteinA-Sepharose beads (Sigma) and either 1µl of α-GFP or α-RNA Polymerase II antibodies. Typically, immunoprecipitates were washed five times with 1mL RIPA lysis buffer, resuspended in 25µl 1X NuPAGE LDS (lithium dodecyl sulfate) sample buffer with DTT, and boiled for 5 minutes. Cell lysates prepared for Western blotting (luciferase assay and virus infection time course) were prepared in NP-40 lysis buffer (150mM NaCl, 50 mM Tris-HCl pH 7.5, 0.1% NP-40) with 1X protease inhibitor cocktail (Sigma). Protein concentrations were determined with a BioRad protein assay reagent using BSA as a standard. Samples were prepared with equal amounts of protein by first calculating the amount of protein present in 26µl of the sample with the lowest concentration of protein. Diluted samples were boiled with 10µl 1X NUPAGE LDS sample buffer with 4µl DTT for 5 minutes. All samples were separated on precast NuPage 4-12% Bis-Tris gradient gels (Invitrogen) and transferred to PVDF membranes (Amersham) using the NuPage system. Membranes were blocked in TBS with 0.1% Tween-20, and 5% skim milk (BioShop) or 5% Bovine Serum Albumin (BSA) (Sigma). Western blot (IB) analysis was carried out with indicated primary overnight, followed by horseradish peroxidase (HRP)-conjugated secondary antibodies for one hour, and were then detected using an ECL Plus Western blotting detection

system (Amersham) and autoradiography with High performance chemiluminescence film (Amersham Hyperfilm ECL).

2.6 RNA isolation and RT- qPCR

Total RNA was prepared with PureLink RNA MiniKit (Invitrogen). A total of 1μg of RNA was reverse transcribed into cDNA with SuperScript Vilo MasterMix (Invitrogen) following the manufacturer's instructions. Quantification of cDNA was performed in triplicate using Power SYBR-Green PCR MasterMix (Applied Biosystems) for real time quantitative PCR (RT-qPCR) (Quant Studio 5, Applied Biosystems) with oligonucleotide sequences that specifically recognize Beta-actin (F- CTCGCCTTTGCCGATCC, R- GAATCCTTCTGACCCATGCC),E1A (F- AGTTTTGTCTACAGTCCTGTGTCTGAA, R- GATAGCAGGCGCCATTTTAGG) and E4 (F- GCCCCCATAGGAGGTATAAC, R- GGCTGCCGCTGTGGAAGCGC). Relative expression was calculated using the $\Delta\Delta C_T$ method, and results were normalized to Beta-actin and the uninfected sample (See User Bulletin #2, Applied Biosystems).

Table 2.3. List of antibodies used in this thesis. (Clone name indicated in brackets)

Antibody	Dilution	Description	Source (Catalog #)
HA (3F10)	100 ng/µl	Rat monoclonal	Roche (431001)
E1A (M73)	1:100	Mouse monoclonal	In house hybridoma (Harlow et al., 1985)
E1A (M58)	1:100	Mouse monoclonal	In house hybridoma (Harlow et al., 1985)
GFP	1:2000	Rabbit polyclonal	Clontech Living Colours (632592)
GFP	1:20 000	Mouse monoclonal	Clontech Living Colours (632375)
RNAPII (pSer2-pSer5)	1:1000	Rabbit polyclonal	Cell Signalling (4725)
GAL4 (DBD)	1:500	Mouse monoclonal	Santa Cruz (sc510)
DBP (E2A)	1:200	Mouse monoclonal	In house hybridoma
CDK9 (H-169)	1:1000	Rabbit polyclonal	SantaCruz (sc8338)
Ad5 - Capsid	1:10 000	Rabbit polyclonal	Cedar Lane (ab6982)
Actin	1:1000	Rabbit polyclonal	Sigma (A2066)
Tubulin	1:1000	Mouse monoclonal	Sigma (T6199)
Anti-Rat IgG	1:20 000	Goat, HRP	Pierce (31470)
Anti-Mouse IgG	1:5000	Goat, HRP	Jackson Immunoresearch
Anti-Rabbit IgG	1:5000	Goat, HRP	Jackson Immunoresearch

Chapter 3 : Results

3   Results

3.1   Transcriptional Activation by the Putative CTD Mimic

Transactivation by E1A CR3 has been studied predominantly in hAdV5 which makes it a well-established model for CR3 function. E1A CR3 is necessary and sufficient to activate transcription when fused to a heterologous DBD in mammalian cells (Jelsma et al., 1988; Shuen et al., 2002). Transactivation by this chimeric fusion is a model system that has been used for many years in our laboratory and is a simple way to examine the effect of mutations on activation of transcription (Ablack et al., 2010, 2012, Pelka et al., 2009a, 2009b). For maximum transcriptional activation, CR3 requires the three functional subregions be intact: the zinc finger region, the promoter targeting region, and AR1 (Figure 1.4) (Glenn and Ricciardi, 1987; Pelka et al., 2008; Ström et al., 1998; Webster and Ricciardi, 1991). However, the role of the promotor targeting region (aa 180-188) and how it contributes to the transactivation capability of E1A is the least well understood. We have proposed that this region acts as a RNAPII CTD mimic to promote transcription of viral genes (Figure 1.5). Therefore, transcription activation by this region (termed the putative CTD mimic for the purpose of this thesis) will be examined using a luciferase activation assay system, using specific substitution and truncation mutants to dissect the important residues of this region of interest.

3.1.1   Activation by CR3 of E1A

Consequently, for the purpose of these experiments, plasmids express the CR3 region from hAdV5 E1A (aa 139-204) in isolation from the rest of the protein. Wild type CR3 is known to be phosphorylated on serines at positions 185 and 188. These serines correspond to the phosphorylated serines at position 2 and 5 in the heptad repeat of the RNAPII CTD (Figure 1.5).
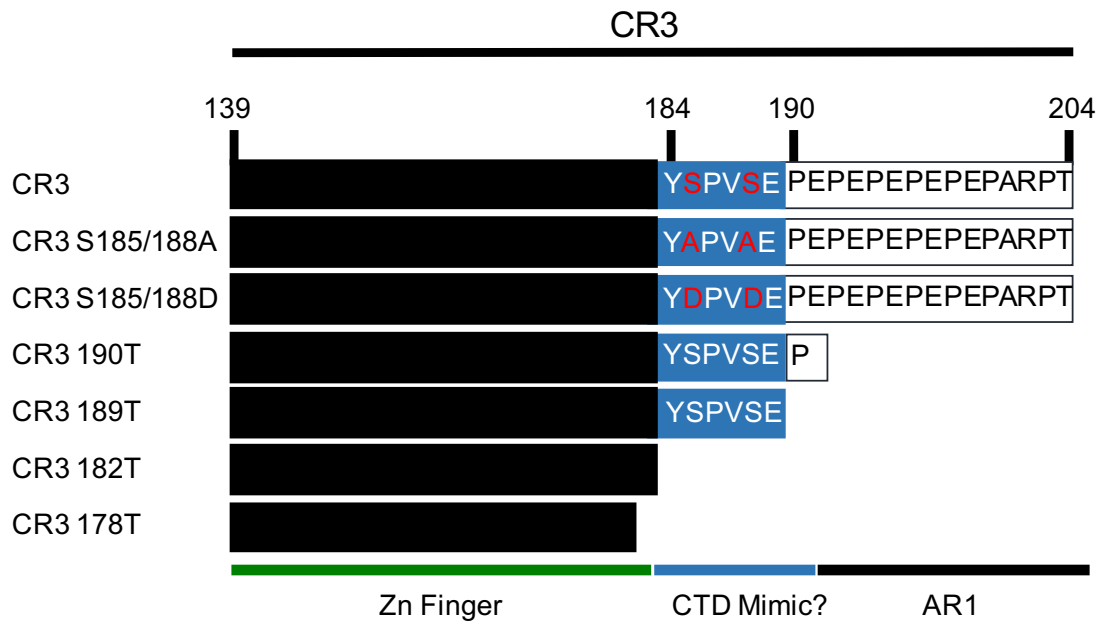
Figure 3.1. Map of CR3 constructs used in luciferase experiments.

Wild Type Conserved Region 3 (CR3). A non-phosphorylatable mutant with alanine substitutions at positions S185 and S188 (CR3 S185/188A) and a phospho-mimic with aspartic acid substitutions at positions 185 and 188 (CR3 S185/188D). CR3 truncated at amino acid 190 (CR3 190T), CR3 189T, CR3 182T, CR3 178T.

S185 and S188 were mutated to aspartic acid to create a phospho-mimetic (CR3 S185/188D) of WT CR3. The negatively charged aspartic acid residues are substituted for serine in similar studies to mimic the phosphorylation of serines (Smith et al., 2004; Tsai et al., 2012). Lastly, a non-phosphorylatable mutant was created with alanines at the positions S185 and S188 (CR3 S185/188A). In addition, truncation mutants were constructed that first truncates CR3 at aa 190 (CR3 190T) and 189 (CR3 189T), which deletes AR1 but leaves the zinc finger and the putative CTD mimic intact. Next, a truncation at amino acid 182 (CR3 182T) then deletes the putative CTD mimic entirely. A final truncation that cuts into the zinc finger domain at amino acid 178 (CR3 178T) was constructed as a negative control. Although these mutants were created by previous students, I cloned them into the appropriate vectors for the purpose of these experiments. For the initial work, mutants of CR3 are fused to a GAL4 DBD (pM) to directly test them as activators in the luciferase assay (Figure 3.1).

HT1080 cells, a fibrosarcoma cell line, were used for activation assays as they express high levels of transfected plasmids and are easily transfected. HT1080 cells were co-transfected with GAL4 DBD fusions (Figure 3.1.) at a 1:1 ratio to the luciferase reporter plasmid [pGL2-(Gal4)$_6$-Luc]. 24 hours post-transfection cell lysates were collected and assayed for luciferase activity. Activity was normalized to protein concentration and expressed as fold activation over that of the vector. Significance was determined by Students T-test.

As expected in these experiments, WT full length CR3 fused to the GAL4 DBD strongly activated expression of the luciferase reporter (Figure 3.2). Compared to WT CR3, the phospho-mimic (CR3 S185/188D) had no significant difference in its ability to activate transcription, whereas the non-phosphorylatable mutant (CR3 S185/188A) shows a significant decrease in its ability to activate transcription. These experiments suggest that phosphorylation of S185 and S188 is important for maximal transactivation by E1A CR3.

In these experiments, truncating CR3 at the zinc finger domain (182T), which deletes both AR1 and the putative CTD mimic, still allows for considerable levels of transactivation with no significant differences when compared to that of WT CR3.
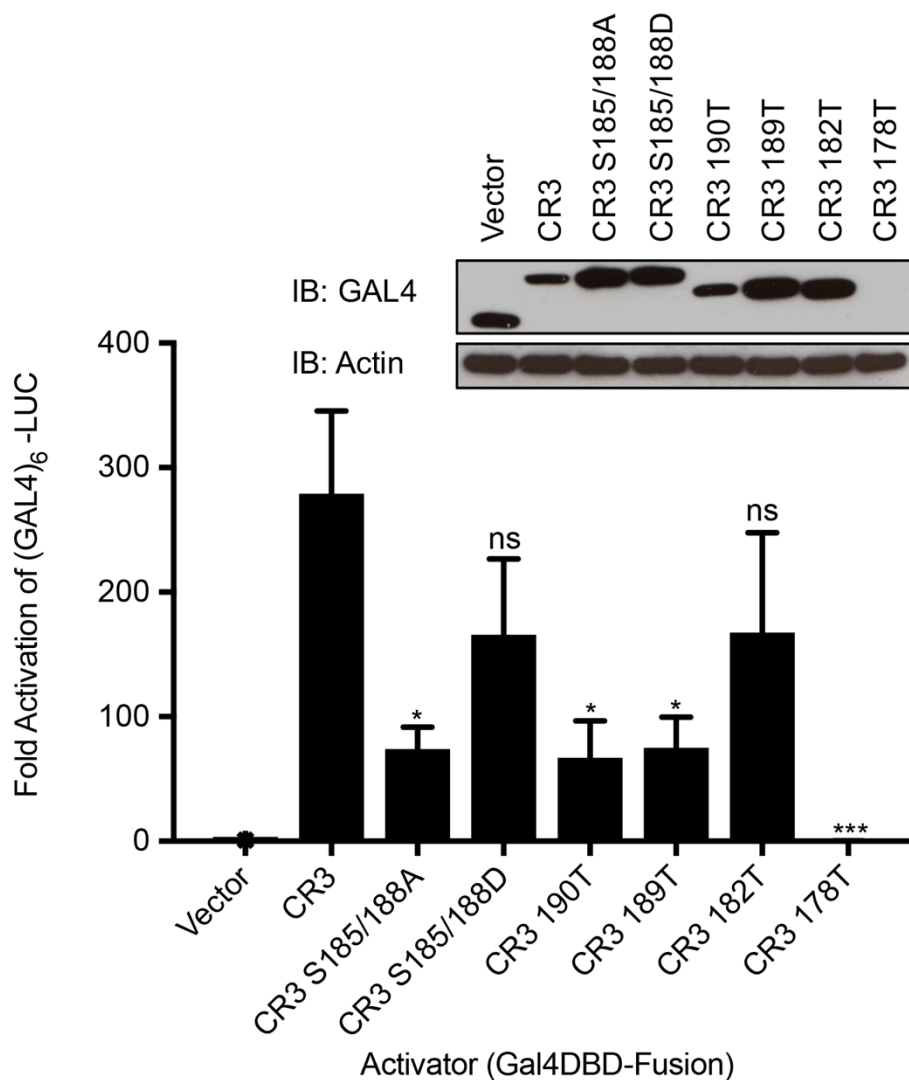
Figure 3.2. Transcriptional activation of E1A-CR3 and selected E1A-CR3 mutants

HT1080 cells were co-transfected with a GAL4-responsive luciferase reporter and vectors expressing the indicated CR3 GAL4 fusions or empty vector. Luciferase activity was normalized to protein concentration and expressed as fold activation over that for the empty vector ± SD (n=4). Activation in E1A-CR3 vs indicated E1A-CR3 mutants were compared by Student's T-Test and significance is indicated. ns=non-significant. * = P<0.05. *** = P< 0.0002.

However, truncations at aa 190 or 189 show decreased transactivation activity when compared to wild type (Figure 3.2). Thus, these residues seem necessary for activation by CR3 when the putative CTD mimic is present but not when it is absent. Lastly, truncating CR3 by cutting into the zinc finger domain (178T) abolishes CR3 transactivation entirely. Unlike the other mutants, this protein may no longer be stable, as shown in the Western blot (Figure 3.2 inset).

Western blot with an antibody for GAL4 was used to determine if differences in protein expression could explain the loss of function by the various mutants (Figure 3.2 inset). I observed consistent amounts of GAL4-E1A CR3 fusion for all constructs with the exception of 178T. Thus, the differences in transactivation by the various mutants, except for the completely defective 178T, are not likely due to differences in protein expression of the GAL4-E1A CR3 fusions. This also provides an explanation for the total ablation of activity when CR3 is truncated at aa 178, as the protein appears to lose stability entirely.

3.1.2   Competition by CR3 and CR3 Point Mutants

As another approach to further understand the role of the putative CTD mimic in transactivation by CR3, we performed competition/ squelching assays (Ablack et al., 2010). In these experiments, a soluble form of CR3 is expressed in conjunction with WT CR3 fused to the GAL4 DBD. If the soluble form of CR3 binds factors required for the promotor bound CR3, the competitive sequestration of these factors can reduce activation of the reporter. In the competition assays that I performed, E1A CR3 and E1A CR3 point mutants were fused to GFP (Figure 3.1) to act as competitors. HT1080 cells were co-transfected with the GAL4 luciferase reporter vector [pGL2-(Gal4)$_6$-Luc] and WT GAL4-CR3 (activator), along with decreasing amounts of GFP fusions (soluble competitor). 100 % activation is that of WT GAL4-E1A CR3 alone with only the empty vector (pGFP) as a competitor. Competition activity is expressed as a percentage of full activation (Figure 3.3). In these assays, if a competitor (pGFP-CR3 fusions) does not target factors required by the activator (GAL4-CR3), the level of transactivation should remain at 100% regardless of the level of competitor present.
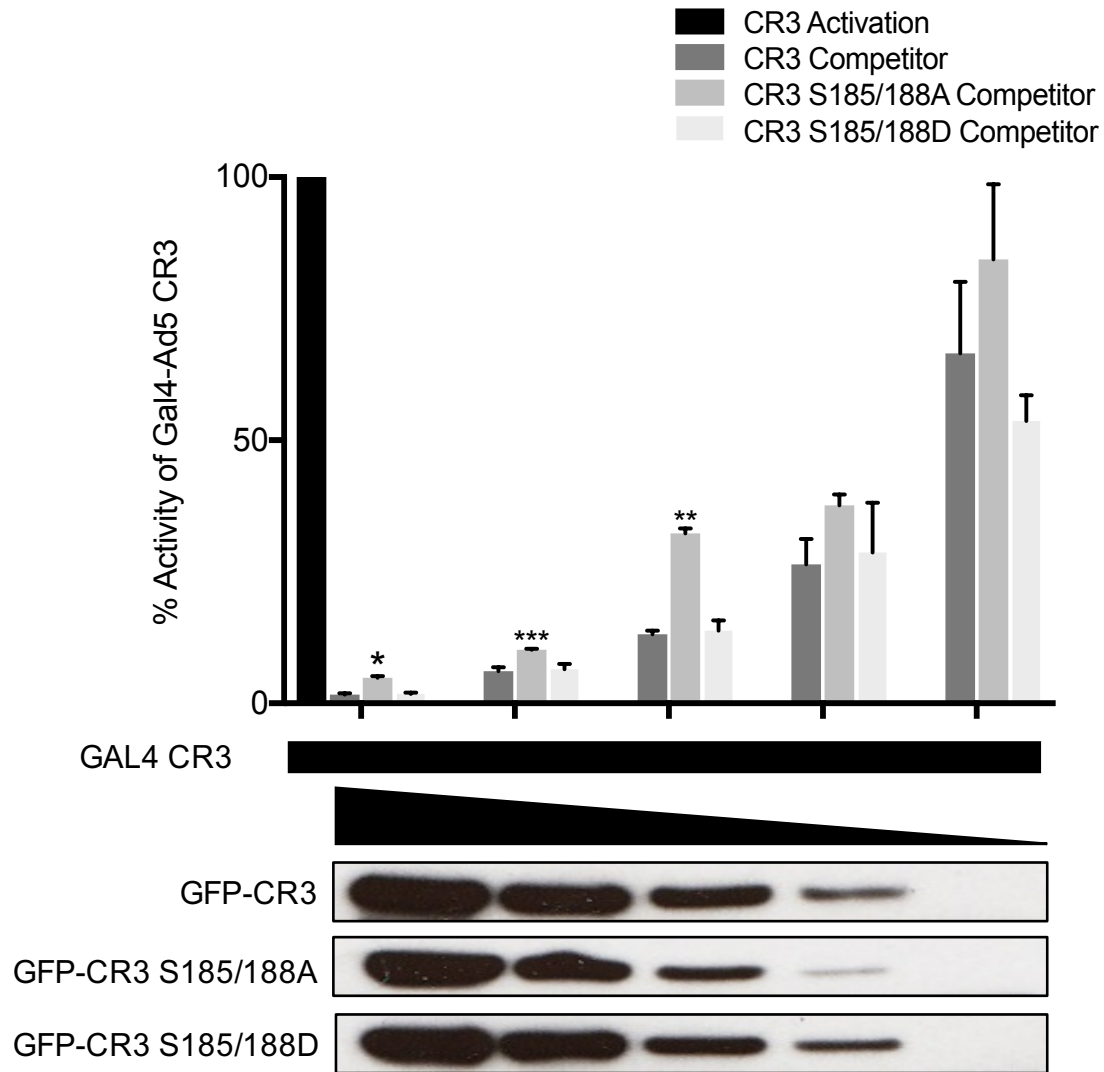
Figure 3.3. Squelching of Ad5 E1A CR3 function is less efficient with non-phosphorylatable CR3 (S185/188A) mutant.

HT1080 cells were co-transfected with a GAL4-responsive luciferase reporter, a GAL4-CR3 (activator) vector and decreasing amounts of GFP-CR3 fusions (soluble competitors). Luciferase activity is expressed as a percentage of the fold activation of GAL4-CR3 (activator) with pGFP (empty vector) as the competitor ± SD. (n=3)

However, if the competitor targets the necessary factors required for function by the activator, a dose dependent restoration of transactivation will be observed as the level of the competitor is decreased.

When WT CR3 or the phospho-mimic of CR3 (CR3 S185/188D) are fused to GFP and used as a competitor, they successfully sequester factors to squelch transactivation in a dose dependent manner (Figure 3.3). Although, the non-phosphorylatable mutant (CR3 S185/188A) also demonstrates an ability to sequester factors and squelch transactivation in a dose dependent manner, it is less efficient in its ability to squelch activation. There is a significant difference, as determined by Student's T-Test, in its ability to compete for factors at high doses of the competitor. The trend continues for lower doses of the competitor. This result suggests that the non-phosphorylatable E1A CR3 mutant is less able to sequester a limiting factor away from promotor bound E1A. This once again highlights the importance of phosphorylated S185 and S188 in CR3 for activation of transcription through binding of an unknown transcriptional regulator.

3.1.3   Activation by the Putative CTD Mimic

Prior experiments studied deletions and mutations in full length CR3, which includes the powerful transactivating capabilities of zinc finger. As the putative CTD mimic is predicted to be unstructured, we next wanted to fuse only this region to the GAL4-DBD and examine its ability to activate transcription on its own. Pairs of self-annealing oligonucleotides (Table 2.1) were designed to express different mutations and truncations of the putative CTD mimic region (aa 183-200) independently from the rest of CR3 (Figure 3.4). As in previous experiments, the serines in the region were substituted with alanine (to create a non-phosphorylatable mutant CR3 S185/188A) and aspartic acid (to create a phospho-mimetic CR3 S185/188D). Truncation mutants cut into the EP repeats of AR1, with plasmids expressing aa 183-196, 183-192 and 183-190 of CR3. An AR1 control, consisting of only the EP repeats, was used ensure that the activity of the other peptides was not simply due to the acidic nature of the peptide but rather to the specific residues
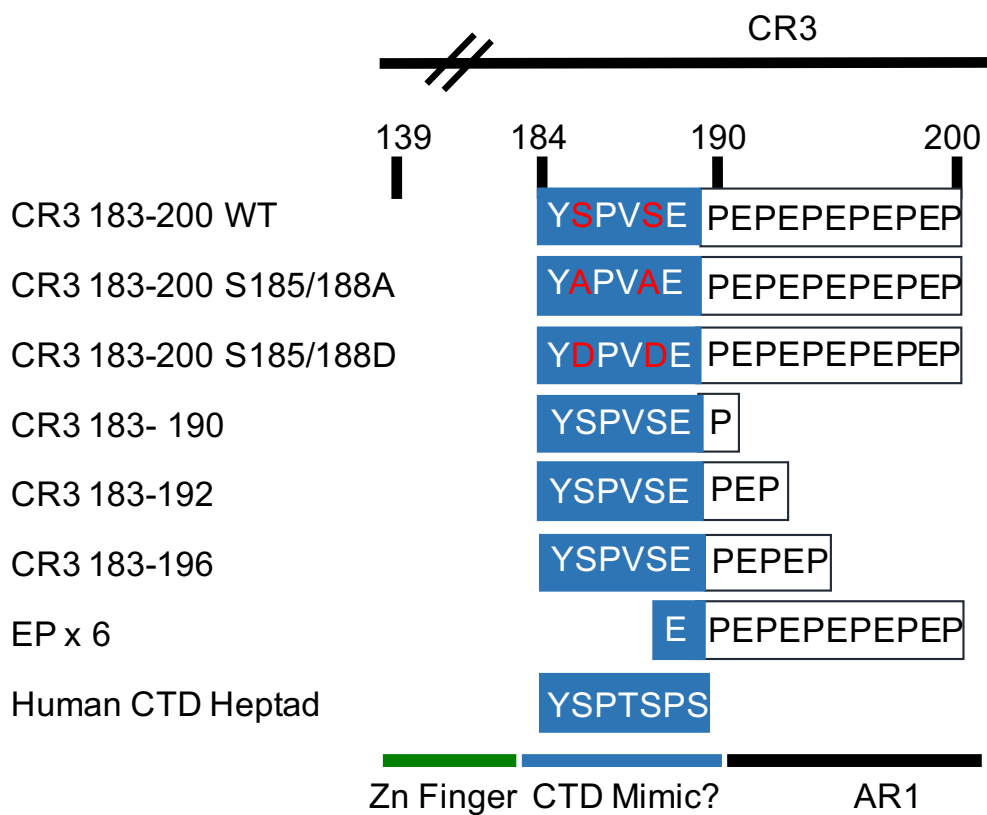
Figure 3.4. Map of CR3 putative CTD mimic constructs.

CR3 WT (aa 183-200). A non-phosphorylatable point mutant (CR3 183-200 S185/188A) and a phospho-mimetic (CR3 183-200 S185/188D). Truncation mutants (CR3 183-190, CR3 183-192, CR3 183-196). The AR1 of CR3 (EP x6). The human RNAPII CTD heptad repeat (YSPTSPS).

that mimic the heptad repeat of the RNAPII CTD. Finally, the human RNAPII CTD heptad consensus sequence was fused to the GAL4-DBD in order to examine its activity compared to the related E1A specific sequence.

HT1080 cells were transfected with GAL4 fusions (Figure 3.4) at a 1:1 ratio to the luciferase reporter plasmid [pGL2-(Gal4)$_6$-Luc]. At 24 hours post-transfection, cell lysates were collected and assayed for luciferase activity. Activity was normalized to protein concentration and expressed as fold activation over that of the vector. Tuckey's multiple comparisons test was used to test for any significant differences between any of GAL4-CR3 peptides. Western blots with an antibody for GAL4 (Figure 3.5 inset) indicate that all GAL4 fusions were expressed at consistent levels. Thus, the differences in transactivation by the various mutants are not likely due to differences in expression of the GAL4 fusions.

The transcriptional activation capabilities of the short peptides of interest appear less than that of full length CR3 (Figure 3.2 and Figure 3.5). This is as expected because the powerful transactivation capabilities of the zinc finger are no longer present. However, it is evident that the putative CTD mimic can activate transcription to some extent on its own. The GAL4-CR3 peptides activate transcription about five times over that of the vector alone, however I did not observe any significant differences between the various mutations and truncations. It is possible that the assay is not sensitive enough to detect small differences in these low activation values due to the wide variation between replicates. Like the CTD mimic (CR3 183-190), the AR1 (EP X6) construct shows a low level of activation. This allows us to conclude that both subregions of CR3 can function independently to activate transcription at a low level. The RNAPII CTD heptad repeat, when fused to a GAL4-DBD shows comparably measurable but weak activity to that of the hAdV5 CTD putative CTD mimic sequence (CR3 183-190). Thus, in addition to the sequence similarity between E1A and the CTD, they function equivalently as transactivators in this assay.
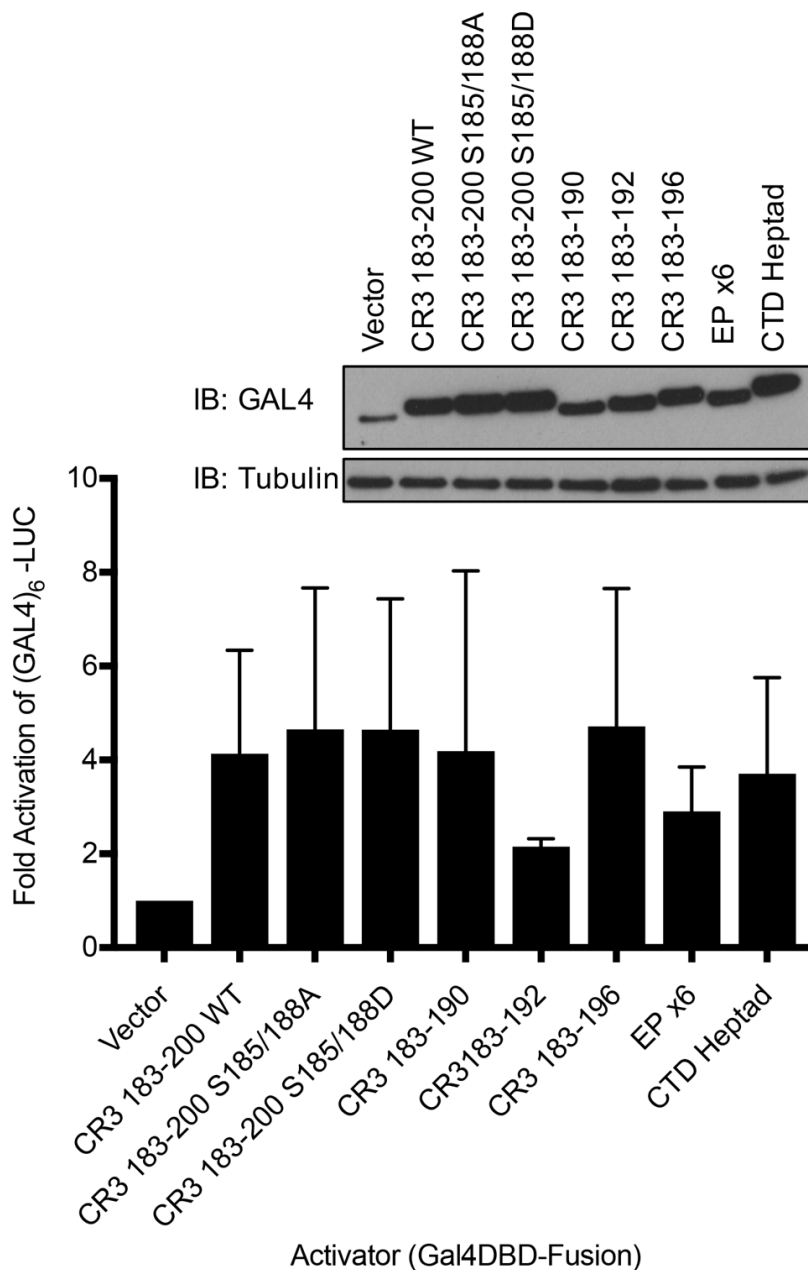
Figure 3.5. Transcriptional activation by putative CTD Mimic.

HT1080 cells were co-transfected with a GAL4-responsive luciferase reporter and vectors expressing the indicated CR3 GAL4-DBD fusions or empty vector. Luciferase activity was normalized to protein concentrations and expressed as fold activation over that for the empty vector ± SD. (n=3)

3.1.4 Competition by the Putative CTD Mimic

In a corresponding competition assay, HT1080 cells were transfected with indicated GFP fusions of the constructs used in the direct transactivation assays presented above (Figure 3.4). GFP-CR3 fusions (soluble competitors) were transfected at a 1:1:1 ratio to GAL4 luciferase reporter vector [pGL2-(Gal4)$_6$-Luc] and GAL4-CR3 (activator). 100 % activation is that of GAL4-CR3 alone with only the empty vector (pGFP) as a competitor. Competition activity is expressed as a percentage of full activation. Tuckey's multiple comparisons test was used to test for any significant differences in squelching ability by the CR3 peptides. Western blots with an antibody for GFP (Figure 3.6 inset) indicate that each construct is consistently expressed as a GFP fusion. Thus, differences in squelching are not due to differences in expression of the GFP-CR3 fusion. GFP-CR3 peptides, that express various mutations and truncations of the putative CTD mimic, are able to squelch activation by approximately 50% (Figure 3.6). While this is not as potent as the squelching by the full length CR3 (Figure 3.3), it does show that the putative CTD mimic is able to bind certain factors away from the promoter and squelch activiation of the full length CR3. Differences between the squelching ability of the various GFP-CR3 fusions are not significant (Tukey's multiple comparisons test). Due to the variance between replicates the assay may not be sensitive enough to look at differences between peptides that act only as weak competitors. The AR1 (EP x6) control peptide and the minimum sequence corresponding to the putative CTD mimic (CR3 183-190) can both function independently as competitors. However, CR3 183-200 WT, which is made of both these subregions, appears to function slightly better as a competitor. Finally, when using the consensus sequence for the RNAPII heptad repeat of the CTD as a competitor (CTD Heptad), it is able to squelch the activity of CR3 comparable to that of the hAdV5 specific sequence believed to act as the CTD mimic (CR3 183-190). Taken together, the putative CTD mimic can function, in a manner comparable to the RNAPII CTD, to bind certain cellular factors in isolation of the zinc finger and squelch activation. These interactions do not necessarily rely on the acidic nature of AR1.
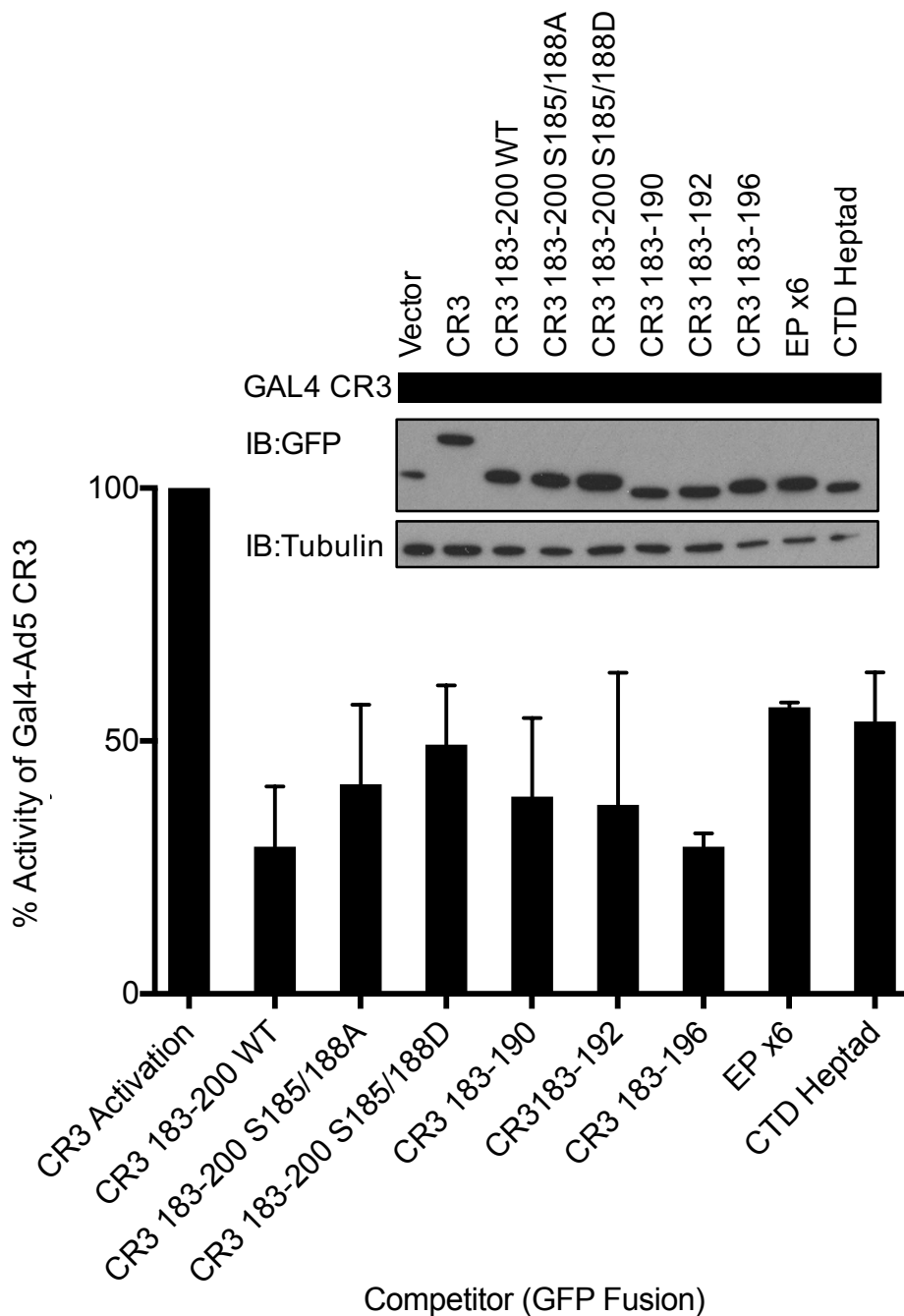
Figure 3.6. Squelching of GAL4 Ad5-CR3 by the putative CTD mimic.

HT1080 cells were co-transfected with a 1:1:1 ratio of GAL4-responsive luciferase reporter : GAL4-Ad5 CR3 (activator) : empty vector (pGFP) or pGFP-CR3 183-200 fusions (competitors). Luciferase activity is expressed as a percentage of the fold activation of GAL4-Ad5 CR3 (activator) with pGFP (empty vector) as the competitor ± SD. (n=4)

3.2   Characterizing the Interaction between CDK9 and E1A CR3

Given the sequence similarity between RNAPII CTD and E1A-CR3, we believe that E1A would functionally mimic RNAPII at a molecular level and would therefore interact with RNAPII interacting proteins such as CDK9, CDK7, CA150, or RNGTT (Eick and Geyer, 2013).

CDK9 was an ideal first candidate by which to test the functional mimicry of the RNAPII CTD by E1A CR3.   CDK9 is a CTD kinase which binds the RNAPII CTD phosphorylated at S2 and S5 and controls the initiation of transcription elongation. (Eick and Geyer, 2013). In a 2013 paper, Vijayalingam and Chinnadurai demonstrated an interaction between CDK9 and 13S E1A (L-E1A) but not 12S E1A (S-E1A). As 12S E1A lacks CR3, but is otherwise identical to 13S E1A, this indicates that CR3 of E1A is responsible for the interaction between CDK9 and E1A. The group further demonstrated that CDK9 played a role in early adenoviral gene transcription and for viral replication (Vijayalingam and Chinnadurai, 2013). We therefore sought to identify whether the putative CTD mimic is involved in the interaction between CDK9 and 13S E1A, specifically through the phosphorylated residues S185 and S188.

3.2.1   Assessment of the Interaction between E1A CR3 and Endogenous CDK9

To test this directly, HT1080 cells were transfected with either GFP (empty vector) or the indicated GFP-CR3 fusions (Figure 3.7). Lysates from transfected cells were immunoprecipitated using a GFP specific antibody and the interaction with CDK9 was assayed by immunoblotting using antibodies specific to GFP and CDK9. It was expected that E1A CR3 alone would co-immunoprecipitate with endogenous CDK9. If the phosphorylation of these two residues played a role in the interaction with CDK9, it would be expected that the non-phosphorylatable mutant E1A CR3 S185/188A would not interact with CDK9.
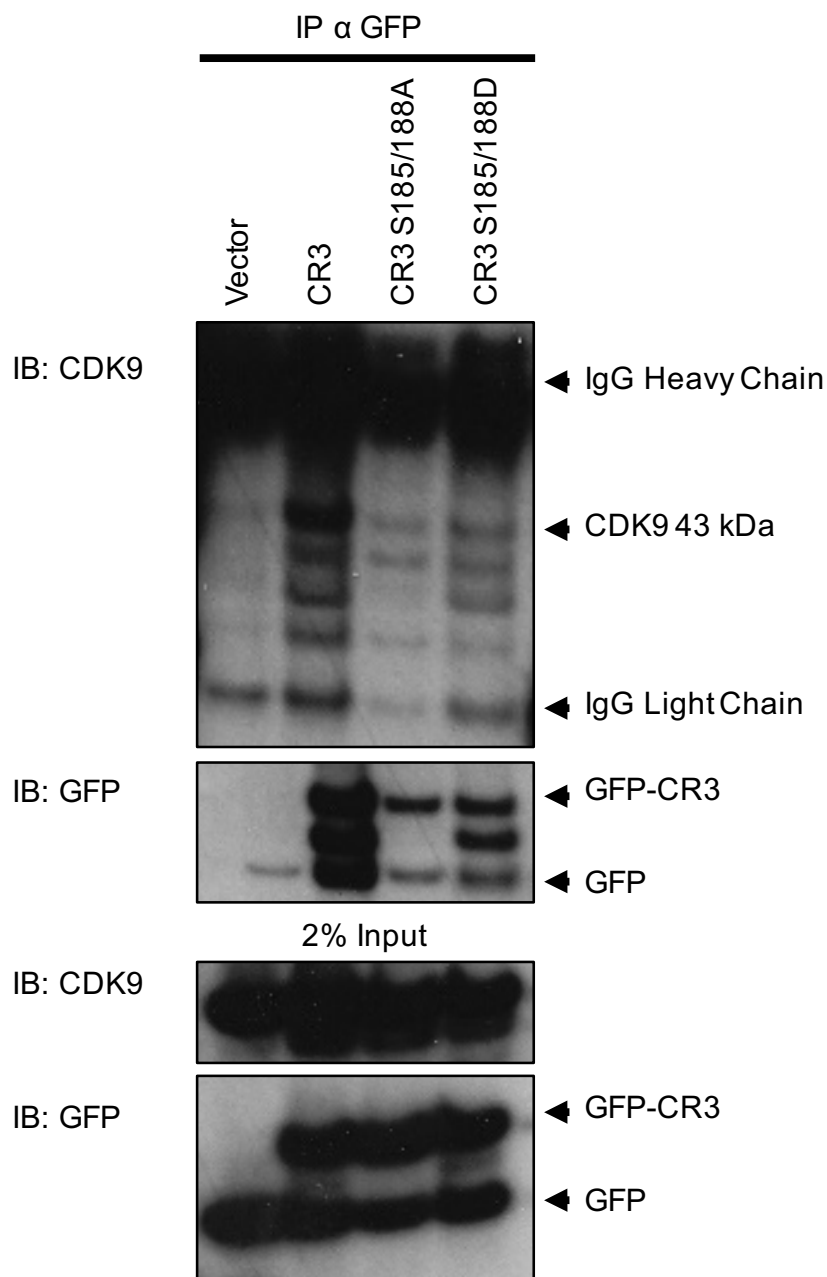
Figure 3.7. Assessment of the Interaction between E1A CR3 and Endogenous CDK9.

HT1080 cells were transfected with GFP (empty vector) or GFP-CR3, GFP-CR3 S185/188A or GFP-CR3 S185/188D. Co-immunoprecipitation was performed by IP with an antibody specific for GFP. Western Blot (IB) analysis was performed with an antibody specific to CDK9 or GFP. Input corresponds to 2% of the total lysate prior to IP.

Then, the phospho-mimetic E1A CR3 S185/188D would co-immunoprecipitate with CDK9, as it would act like WT E1A CR3. However, due to high background from the CDK9 antibody, it cross-reacts with the protein ladder and other proteins non-specifically, it was difficult to conclude the interaction exists between CDK9 and E1A CR3 and that the serine residues play any role in this interaction. Additionally, both the GFP antibodies and the CDK9 antibodies are of the same species (rabbit) which further creates higher levels of background. Attempts to reduce background included pre-blocking the ProteinA Sepharose beads with 0.5% BSA/PBS and pre-binding the antibody by nutating for 1 hour at room temperature (RT). These efforts were met with limited success. While CR3 has been shown to be required for the interaction of E1A with CDK9, it may not be sufficient.

3.2.2 Assessment of the Interaction between Full Length E1A and Endogenous CDK9

Given the limitations using E1A CR3 GFP fusions, we next thought to use plasmids expressing full length E1A and E1A S185/188A (pXC1). This allows us to use mouse monoclonal antibodies for the IP of E1A and rabbit CDK9 antibodies for immunoblotting in an attempt to decrease background levels from species cross-reactivity. Additionally, if CR3 is necessary but not sufficient for CDK9 interaction, we may be able to investigate the role S185 and S188 residues in this interaction, but in the context of full length E1A. Cells were transfected with WT E1A or E1A S185/188A plasmids. Lysates from cells were immunoprecipitated with an antibody cocktail for E1A (M73+M58) (Figure 3.8). If my hypothesis was correct, I anticipated that WT E1A and CDK9 would co-immunoprecipitate but E1A S185/188A would not. However, I did not observe co-immunoprecipitation of either full length WT E1A or E1A S185/188A with endogenous CDK9. I still experienced high levels of background, in particular, the antibody continued to interact with the protein ladder and other unknown proteins.
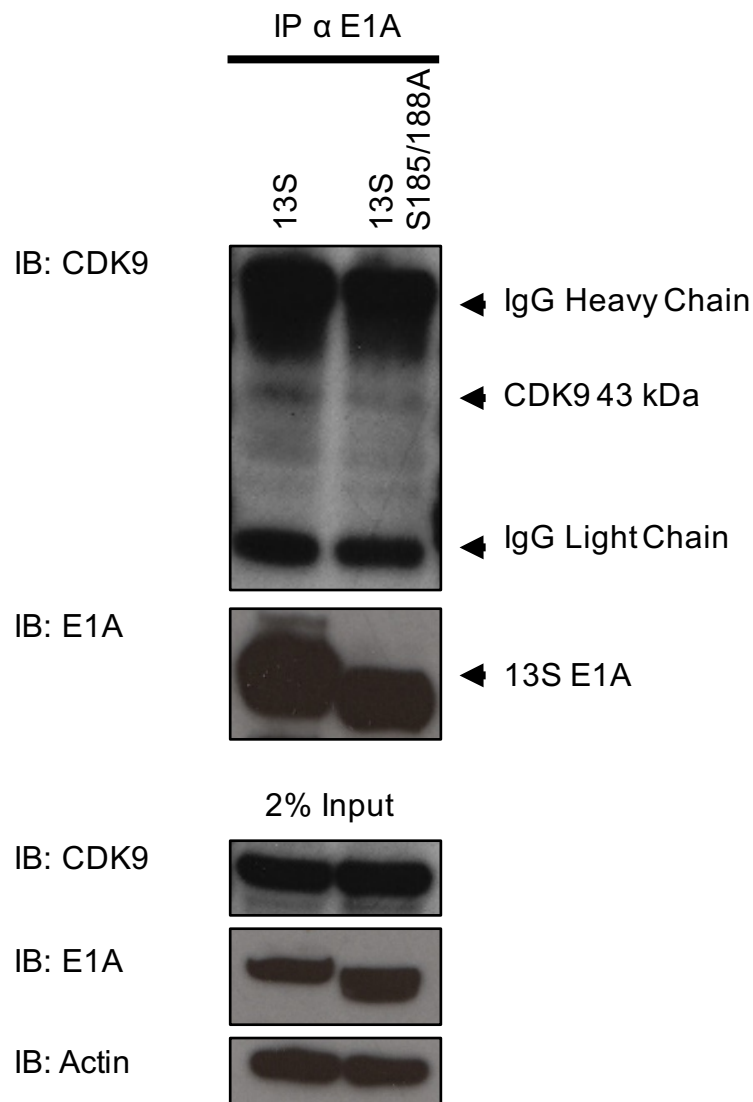
Figure 3.8. Assessment of the Interaction between Full Length E1A and Endogenous CDK9 in HT1080 cells.

HT1080 cells were transfected with pXC1-E1A or pXC1-E1A S185/188A. Co-immunoprecipitation was performed by IP with an antibody specific to E1A (M73+M58). Western Blot analysis was performed with antibodies specific to CDK9, E1A (M73+M58) and actin. Input corresponds to 2% of the total lysate prior to IP.
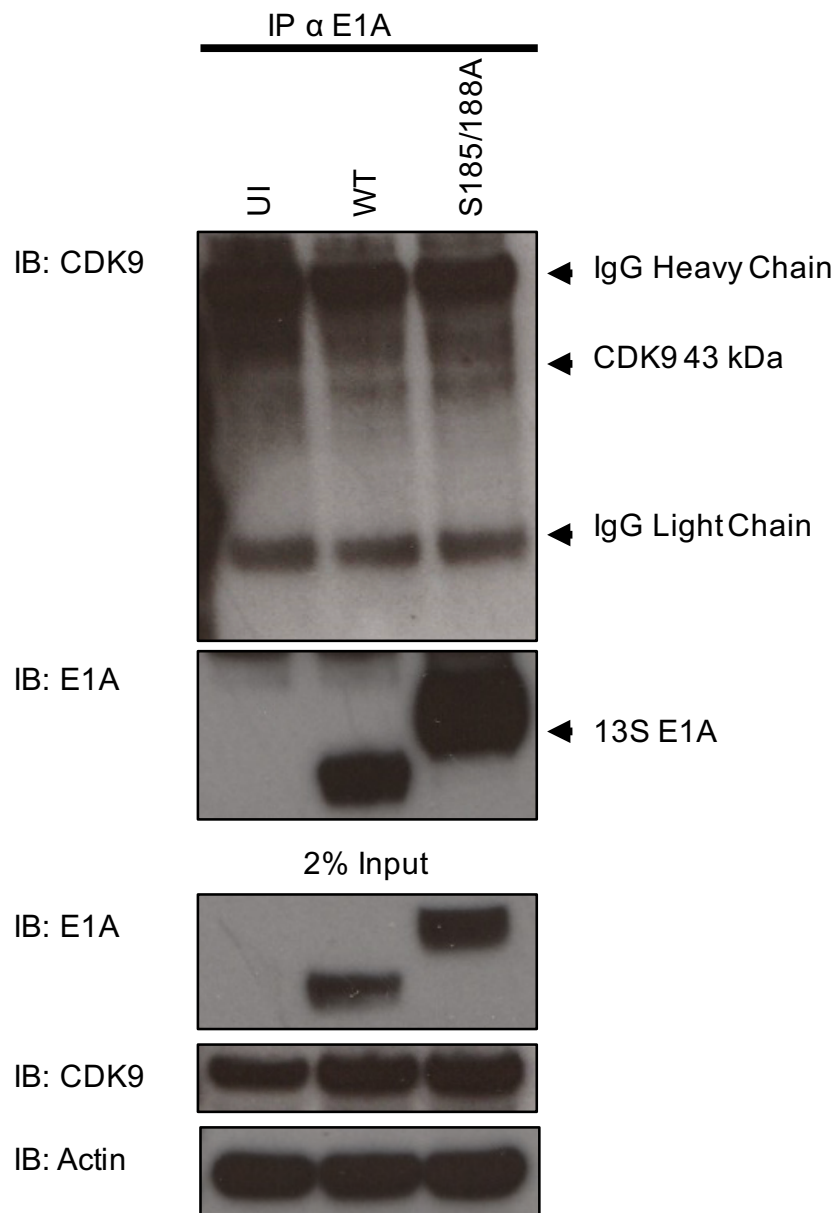
Figure 3.9. Assessment of the Interaction between E1A and Endogenous CDK9 in virally infected A549 cells.

A549 cells were either mock infected (UI) or infected with WT hAdV5 (MOI 3) or JM17-E1A S185/188A virus (MOI 30). Co-immunoprecipitation was performed by IP with an antibody specific to E1A (M73+M58). Western Blot analysis was performed with antibodies specific to CDK9, E1A (M73+M58) and actin. Input corresponds to 2% of the total lysate prior to IP.

As a next step, I thought that transiently transfected full length E1A may not be sufficient for an interaction with CDK9. Since Vijayalingam and Chinnadurai paper shows interaction between E1A and CDK9 in cells infected with a virus expressing WT E1A (Vijayalingam and Chinnadurai, 2013), I thought that the interaction between CDK9 and E1A might require other factors that are present during infection.

Cells were infected with WT virus at an MOI of 3 or with JM17-E1A S185/188A at an MOI of 30 (See results section 3.4). I aimed to express equal amounts of E1A in order to determine the ability of E1A to interact with CDK9 based only on the presence or absence of phosphorylated S185 and S188 and not based on the levels of E1A protein expressed. Lysates from infected cells were immunoprecipitated using an E1A specific antibody cocktail (M73+M58) and the presence of CDK9 was assayed by immunoblotting for endogenous CDK9 (Figure 3.9). However, I was still unable to observe an interaction between E1A and CDK9, whether it be WT E1A or E1A S185/188A. I was also unable to observe any differences between the WT E1A and E1A S185/188A, likely due to continued high levels of background from the CDK9 antibody.

3.2.3   Characterizing the Interaction between E1A CR3 and CDK9-HA

In an attempt to distance ourselves from the CDK9 antibody with it's high background, I instead thought to transiently express CDK9 tagged with the hemagglutinin (HA) epitope tag in order to clean up the immunoprecipitation process. Expressing CDK9-HA though transient transfection also allows CDK9 to be expressed at higher levels than endogenous CDK9. The high levels of CDK9-HA expression following transfection had no observed phenotypic effect on the cells. E.g. I did not observe any differences in cell morphology or an increase in cell death. I ordered a custom gene synthesis of CDK9 from IDT and I subsequently cloned it into a pCDNA4-HA expression plasmid to create the HA tagged CDK9. Thus, future experiments only require the use of the HA antibody to assay for CDK9 expression in immunoblotting. Additionally, the HA antibody is a rat antibody, while GFP is rabbit, so species cross-reactivity will be reduced.
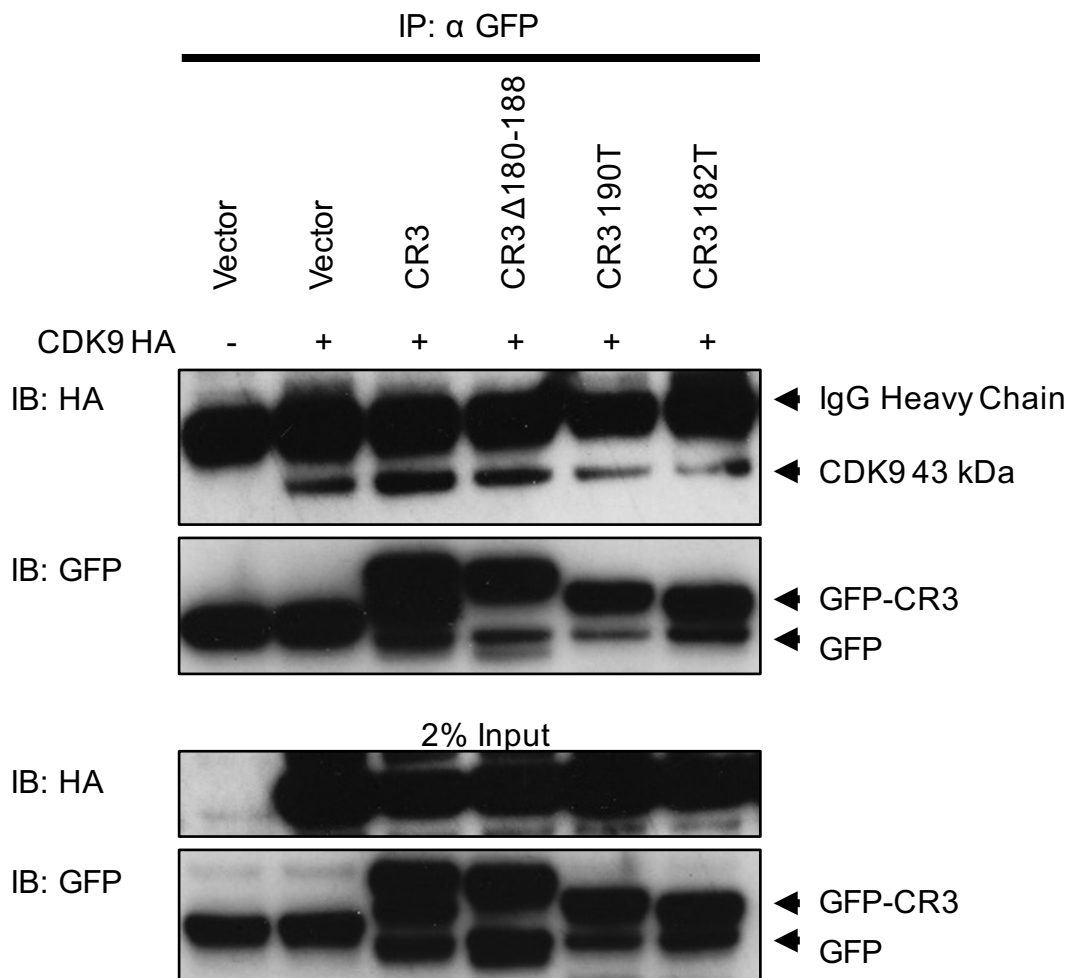
Figure 3.10. Assessment of the Interaction between E1A CR3 and CDK9-HA

HT1080 cells were transfected with GFP (empty vector) or indicated GFP-CR3 fusions along with equal amounts of CDK9-HA plasmid where indicated (+). Co-immunoprecipitation was performed by IP with an antibody specific for GFP. Western blot analysis was performed with antibodies specific to HA or GFP. Input corresponds to 2% of the total lysate prior to IP.
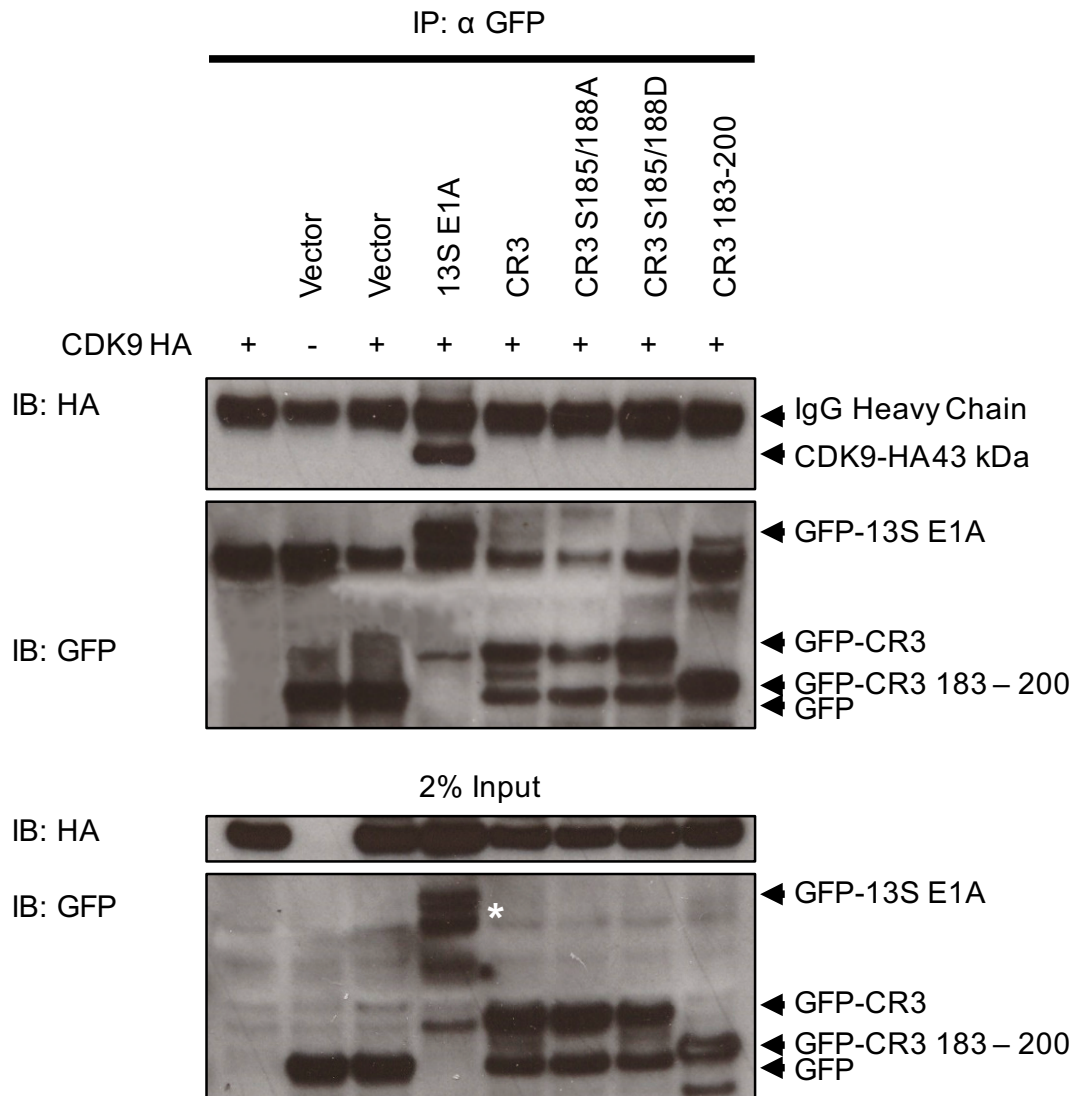
Figure 3.11. CDK9-HA interacts with full Length 13S E1A.

HT1080 cells were transfected with 2μg GFP (empty vector) or 2μg of the indicated GFP-CR3 fusions along with 4μg of CDK9-HA plasmid where indicated (+). Co-immunoprecipitation was performed by IP with an antibody specific for GFP. Western blot analysis was performed with antibodies specific to HA or GFP. Input corresponds to 2% of the total lysate prior to IP. (*) Denotes gel motility shift due to phosphorylation of S89 of E1A.

HT1080 cells were transfected with GFP (empty vector) or indicated GFP-CR3 fusions along with equal amounts of CDK9-HA (Figure 3.10). E1A CR3 mutants were chosen to determine if the putative CTD mimic is necessary for an interaction between E1A CR3 and CDK9. Lysates from transfected cells were immunoprecipitated using an antibody specific to GFP and the interaction with CDK9 was assayed by immunoblotting with an antibody against HA. At first it appeared that CDK9 and E1A CR3 may interact, however we observed GFP (empty vector) our negative control, also interacts with CDK9. Thus, I cannot conclude that E1A CR3 is sufficient for an interaction with CDK9-HA. Any differences observed between CR3 and the CR3 mutants are therefore inconclusive.

Both myself and other students in the lab were plagued with a sticky GFP vector where our empty vector control sticks to our protein of interest, which in my case was CDK9. It was therefore difficult to conclusively demonstrate a clean interaction between E1A CR3 and CDK9. A number of different techniques were employed to minimize the binding of GFP to CDK9 and to abolish the high levels of background in our negative control. Cell lysates were pre-cleared with ProteinA Sepharose beads at RT for 1 hour, or at 4° C for 6 hour or overnight incubations. In some cases, the antibody was blocked with 0.5% BSA/PBS and pre-bound to the beads for 1 hour at RT. IP's were washed up to ten times and samples were vortexed during washes rather than washing by inverting. Finally, antibody incubation time with the lysate was decreased to 4 hours at 4° C rather than overnight at 4°C. However, these variations had little to no effect on the level of background in the negative control lane.

Based on a previous student's report, we last thought to decrease the amount of pGFP plasmids being expressed. Transfections with the pGFP fusions were decreased to 2μg of DNA while CDK9-HA remained at 4μg. HT1080 cells were transfected as described previously and cell lysates were immunoprecipitated using an antibody specific to GFP (Figure 3.11). At last, the pGFP (empty vector) control no longer appears to interact with CDK9. Full length E1A (GFP-13S) interacts with CDK9 as shown previously (Vijayalingam and Chinnadurai, 2013b). E1A 13S GFP appears as two bands on the gel, at 48.5 kDa and 52 kDa. The phosphorylation of serine 89 has been described in the literature as being responsible for this gel-motility shift. The phosphorylation at this site is

not essential for E1A function; de-phosphorylation at this site does not affect the ability of E1A to transform cells or to activate transcription (Dumont et al., 1989; Smith et al., 1989; Tremblay et al., 1989).

Although E1A CR3 is thought to be necessary for interaction of CDK9 in the context of full length E1A, it was not found to be sufficient. Neither E1A CR3 nor any of the CR3 mutants interact with CDK9 under the new transfection conditions. It was expected that if WT E1A CR3 interacts with CDK9, S185 and S188 would prove to be responsible for this interaction. Thus, it was expected that the alanine substitutions in CR3 would disrupt this interaction. However, as I didn't observe an interaction between E1A CR3 alone and CDK9, I could not conclude anything about the involvement of the S185 and S188 residues in this interaction.

Furthermore, this experiment clarifies results from previous experiments (Figure 3.7 and Figure 3.10) where the potential interaction could not be distinguished from background levels with GFP. Figure 3.7 uses 8μg of the GFP plasmid DNA which brings into question the validity of those results, in addition to already high background levels from the antibody. 2μg of transfected GFP was later proved to be sufficient to observe an interaction with CDK9 and that greater than 2μg of transfected GFP led to an interaction in the negative control lane.

3.2.4   Characterizing the Interaction between Full Length 13S E1A and CDK9-HA

While CDK9 did not interact with E1A CR3 alone under the conditions that I tried, it does interact with full length 13S E1A (Vijayalingam and Chinnadurai, 2013 and Figure 3.11). In order to determine if S185 and S188 play a role in this interaction, I cloned full length E1A S185/188A and E1A S185/188D from their respective pXC1 plasmids into pGFP. Once again, only 2μg of pGFP (empty vector) and the indicated pGFP-E1A plasmids were transfected along with 4μg of CDK9-HA plasmid. WT 13S E1A co-precipitated with CDK9-HA and the interaction between full length 13S E1A and CDK9 is once again confirmed (Figure 3.12). Again, 13S E1A appears as two bands on the gel
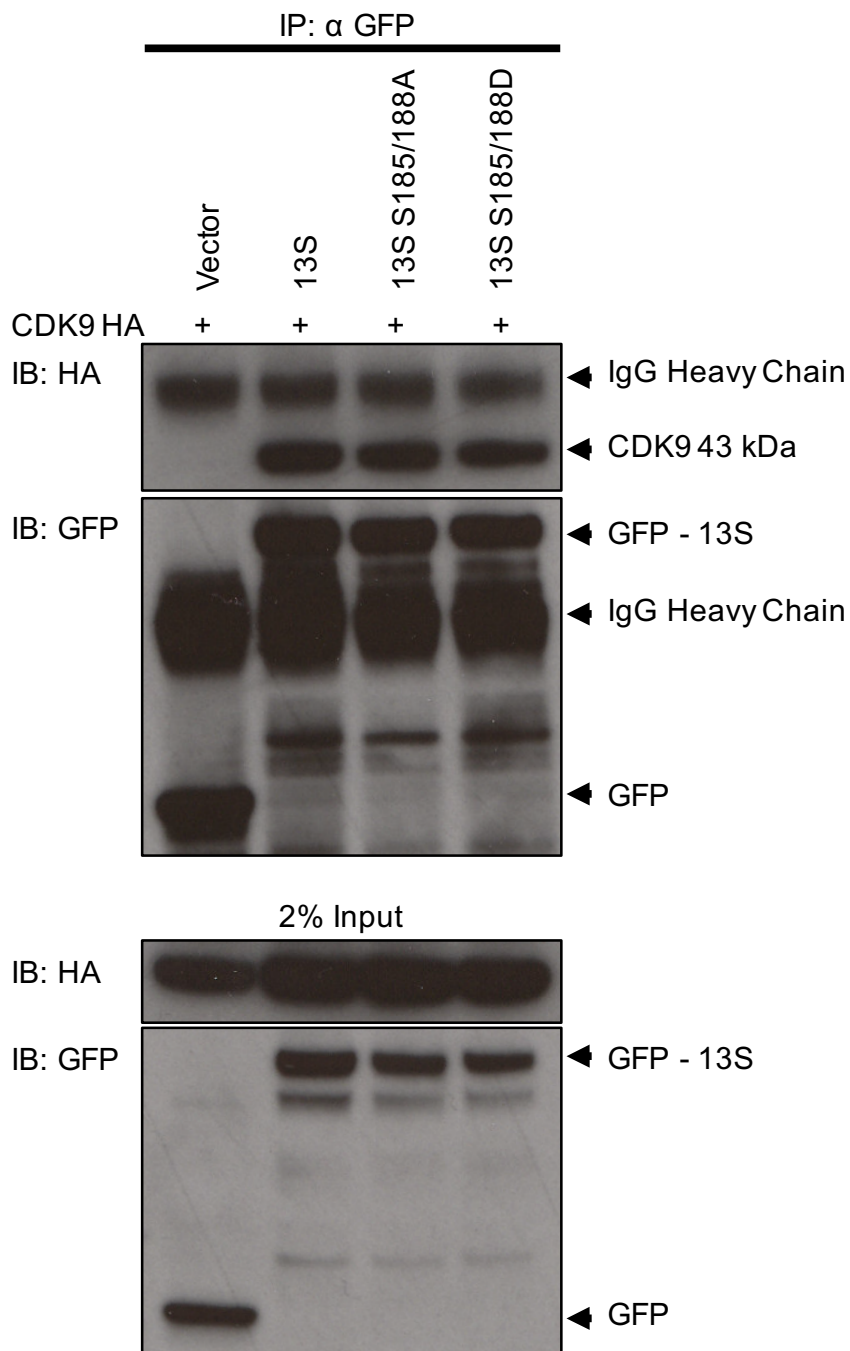
Figure 3.12. Interaction between E1A CR3 and CDK9-HA does not depend on S185/ S188.

HT1080 cells were transfected with 2μg pGFP (empty vector) or 2μg of the indicated GFP-CR3 fusions along with 4μg of CDK9-HA plasmid where indicated (+). Co-immunoprecipitation was performed by IP with an antibody specific for GFP. Western blot analysis was performed with antibodies specific to HA or GFP. Input corresponds to 2% of the total lysate prior to IP.

due to the phosphorylation of S89 (Dumont et al., 1989; Smith et al., 1989; Tremblay et al., 1989). However, while this confirms the interaction of full length E1A with CDK9, both E1A S185/188A and E1A S185/188D bind similarly to WT E1A. The two mutants may both show a slight decrease in the interaction with CDK9-HA compared to WT E1A, but this may also be explained by a slightly lower level of expression from these two plasmids, as seen by the input. If the phosphorylation of these two residues played a role in the interaction with CDK9-HA, it would be expected that the unphosphorylated mutant E1A S185/188A would not interact with CDK9, while the phospho-mimetic E1A S185/188D would retain this interaction. Based on this result, it is therefore not likely that the phosphorylation of both S185 and S188 plays a role in the interaction between E1A and CDK9.

3.3   Investigating Potential Structural Mimicry by E1A CR3

In a previous study in our lab, the N-terminus of E1A was shown to both functionally and structurally mimic a cellular AKAP (King et al., 2016b). In this thesis, I investigated whether E1A functionally mimics the RNAPII CTD by binding to CDK9. Demonstrating that CDK9, or another known target of the RNAPII CTD, could be bound by the putative CTD mimic in E1A, it would suggest that E1A CR3 functionally mimics the RNAPII CTD and would therefore imply that E1A CR3 would also structurally mimic the CTD. We first based our hypothesis on the high degree of sequence similarity between these two motifs (Figure 1.3). Secondly, both the RNAPII CTD and the putative CTD mimic are phosphorylated at serines in position 2 and 5 of the peptide, corresponding to S185 and S188 in E1A (Eick and Geyer, 2013; Whalen et al., 1997). Additionally, both the RNAPII CTD and the region in E1A CR3 are thought to be unstructured (Eick and Geyer, 2013; Pelka et al., 2008). We hypothesized that, based on functional similarities and primary sequence similarities, there would be a high probability of structural homology between the two peptides.

To test for structural mimicry, we would use an antibody specific to the doubly phosphorylated RNAPII CTD to see if it similarly recognizes the phosphorylated E1A-CR3 peptide. Original reports supporting this hypothesis from Dr. Greg Fonseca were promising (Unpublished results, 2013). However, I attempted to reproduce this data several times with varying results, and no clear conclusion.

3.3.1   E1A CR3 Cross-Recognition by an RNAPII Antibody

HT1080 cells were transfected with GFP (empty vector), GFP-CR3, GFP-CR3 S185/188A or GFP-CR3 S185/188D. 24 hours post transfection, cells were harvested and lysates were immunoprecipitated with an antibody for the doubly phosphorylated RNAPII CTD and immunoblotted with an antibody for GFP-E1A CR3. We expected that lysates would demonstrate that E1A CR3 has been immunoprecipitated by the RNAPII antibody with a band at 42 kDa indicating GFP-E1A CR3. We further expected the non-phosphorylatable mutant (CR3 S185/188A) would not be immunoprecipitated by the phosphorylation specific antibody but that the phospho-mimetic (CR3 S185/188D) would also be recognized. Lysates immunoprecipitated with the RNAPII antibody occasionally appear to demonstrate this cross-recognition (Figure 3.13 A-C), with a band at 42 kDa for GFP-E1A CR3. In contrast, RNAPII was also immunoprecipitated by the RNAPII antibody, as the band appears at 260 kDa. In figure 3.13 A, E1A CR3 appeared to have been immunoprecipitated by the RNAPII antibody. However, subsequent attempts show greatly varying results. In figure 3.13 B, E1A CR3 S185/188A, rather than WT E1A CR3, appeared to immunoprecipitated with the RNAPII antibody. In figure 3.13 C, it appears that E1A CR3 was immunoprecipitated by RNAPII irrespective of phosphorylation state and it appears that the negative control is immunoprecipitated in a similar fashion. On many occasions, represented by figure 3.13 D, I observed no cross recognition at all. I could not conclude that that E1A-CR3 was recognized by the RNAPII antibody and I could conclude that this phenomenon is phosphorylation specific. Evidence of structural mimicry was not conclusive.

Figure 3.13. Assessment of the cross-recognition between RNAPII and E1A CR3

HT1080 cells were transfected with GFP (empty vector) or indicated GFP-CR3 fusions. Co-immunoprecipitation was performed by IP with an antibody specific for RNAPII. Western blot analysis was performed with antibodies specific to GFP or RNAPII. Input corresponds to 2% of the total lysate prior to IP.
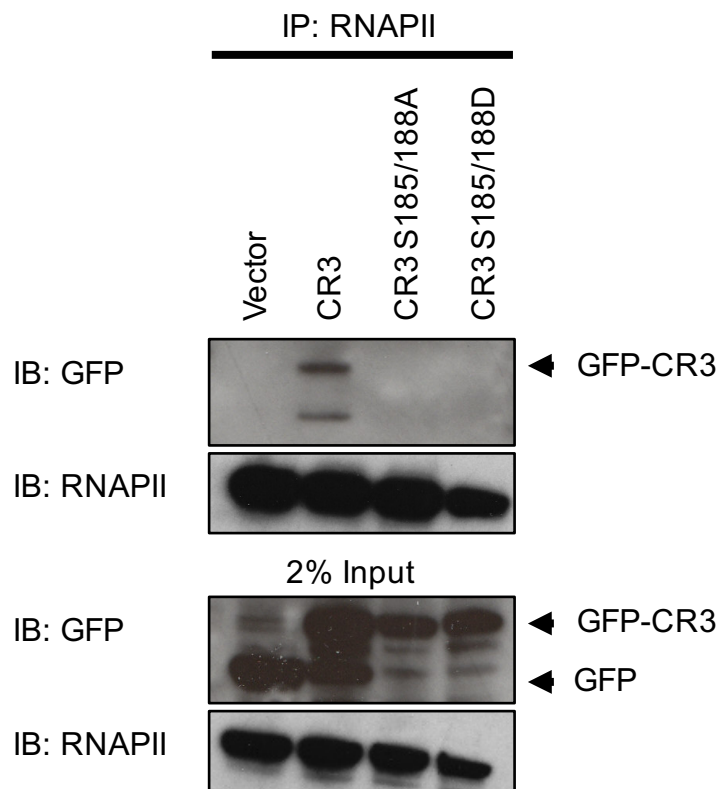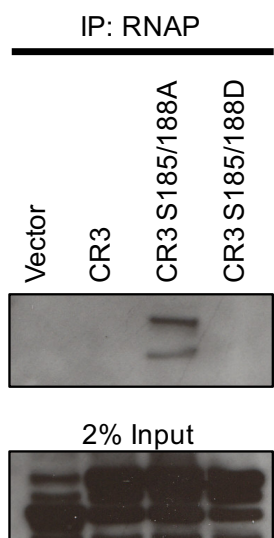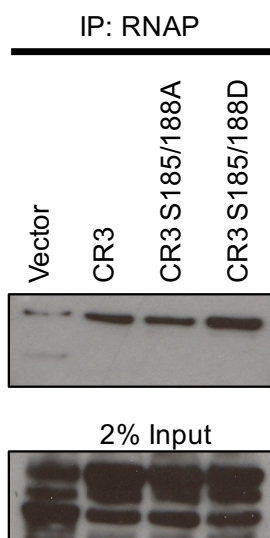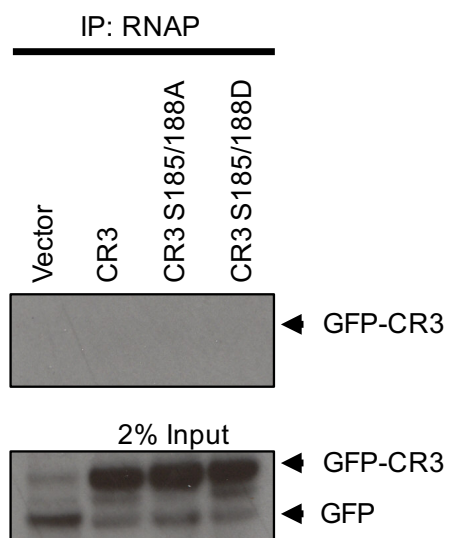
3.3.2   E1A CR3 Interaction with RNAPII

HT1080 cells were transfected and harvested as above. Lysates were immunoprecipitated with an antibody for GFP and immunoblotted with an antibody for the doubly phosphorylated RNAPII. We expected that lysates immunoprecipitated with GFP and immunoblotted with RNAPII would show cross-recognition by RNAPII for GFP-CR3 at approximately 42 kDa. However, lysates instead appeared to show an interaction between E1A CR3 and RNAPII, with a band for phosphorylated RNAPII at 260 kD, rather than cross-recognition by the antibodies. Occasionally it appeared that E1A CR3 may interact with RNAPII in a phosphorylation specific manner. It appeared that WT E1A CR3 and the phospho-mimetic (CR3 S185/188D) interacts with RNAPII but not the phospho-mutant (CR3 S185/188A) (Figure 3.14 A and B). While this observation does not support the hypothesis that E1A CR3 structurally mimics the RNAPII CTD, E1A interacting with RNAPII in a phosphorylation specific manner may have been an interesting result in itself. However, results varied greatly, and subsequent attempts to repeat this finding yielded widely different results (Figure 3.14 C-F). In some cases, RNAPII appeared to interact with each E1A CR3, CR3 mutants, as well as the empty vector with no specificity at all (Figure 3.14 C and F). In other cases it appeared that only the empty vector interacted with RNAPII (Figure 3.14 D). In summary, we could not conclude with confidence that E1A CR3 interacts with RNAPII and it remains unclear if this potential interaction is phosphorylation specific.

Figure 3.14. Assessment of the co-immunoprecipitation between E1A CR3 and RNAPII.

HT1080 cells were transfected with GFP (empty vector) or indicated GFP-CR3 fusions. Co-immunoprecipitation was performed by IP with an antibody specific for GFP. Western blot analysis was performed with antibodies specific to RNAPII or GFP. Input corresponds to 2% of the total lysate prior to IP.
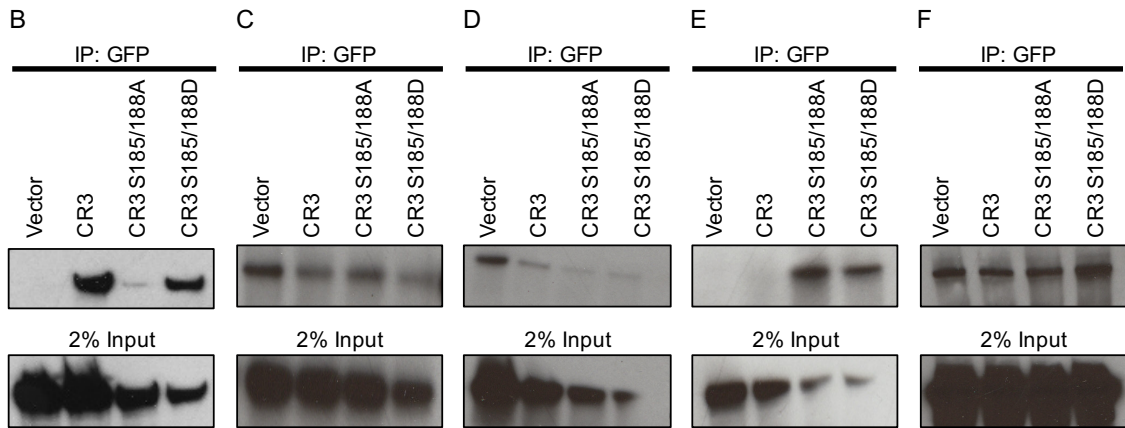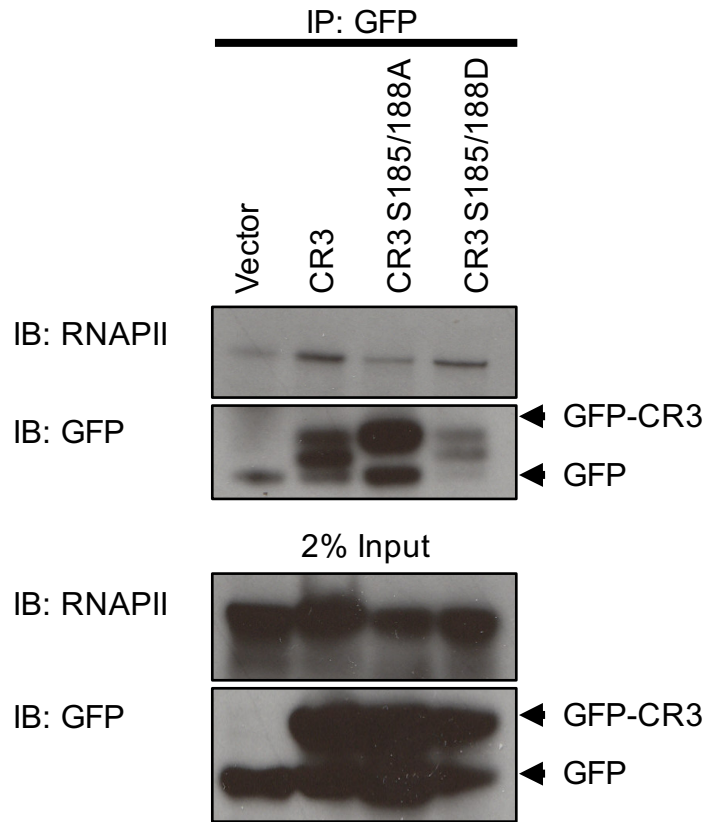
3.4 Characterizing a Novel hAdV Point Mutant

The original mutation that identified the role of the promotor targeting region of CR3 used host range mutant 5 (*hr5*), which corresponds to S185N. These studies demonstrated that the *hr5* mutant could not activate transcription as well as its' WT counterpart, but it could bind to certain cellular transcription factors and squelch them away from WT E1A during a competition assay (Glenn and Ricciardi, 1985, 1987). The same *hr5* mutant virus was used in studies to demonstrate the requirement for phosphorylation of S185 in the transcription of the viral E4 gene (Whalen et al., 1997). Other previous studies used viruses containing various deletion mutants that span aa 178-184 (dl1114) and aa 188-204 (dl115) and identified these regions as part of the transactivating region of E1A (Jelsma et al., 1988). However, researchers have yet to create an infectious virus that could be used to study the role of phosphorylated S185 and S188 within the putative CTD mimic. For this reason, I have created a novel virus with two amino acid substitutions – replacing the S185 and S188 of E1A CR3 with alanine (Figure 2.1). This creates the novel hAdV JM17-E1A S185/188A. This virus expresses a non-phosphorylatable mutant of E1A CR3, allowing me to fully investigate, in an infection model, the role of these amino acids in transactivation on viral genes (specifically E4) and any effect these point mutants may have on replication. Characterizing the kinetics of viral protein and mRNA during infection with the novel JM17-E1A S185/188A virus allows us to assess the effects of the mutations on the virus. After a clear understanding of the properties of this novel virus is obtained, it can then be used as a powerful tool in future experiments.

3.4.1 Infection Time Course WT vs. JM17-E1A S185/188A (MOI 10)

The A549 human alveolar basal epithelial cell line was chosen for my studies, as they are commonly used as a diagnostic cell line for clinical hAdV infection (Smith et al., 1986; Woods and Young, 1988). Approximately 2 x 10^5 A549 cells/well were seeded on a 6 well plate 24 hours prior to infection. Cells were either mock infected (UI) or infected

with either WT virus (MOI 10) or the JM17-E1A S185/188A virus (MOI 10). Cells were harvested at 24 and 48 hours post infection (hpi) from which both RNA and protein samples were collected. Representative Western blots and RT-qPCR data were collected to assess the impact of these mutations on E1A function.

At both 24 and 48 hpi, I observed higher amounts of E1A mRNA transcripts produced by the WT hAdV5 virus compared to that of the mutant S185/188 virus (Figure 3.15 A). This corresponds to an increase in protein expression, as detected via Western blotting with the indicated antibodies for E1A (Figure 3.15 C). E1A, the earliest viral protein expressed during infection, is expressed at high levels by the WT virus at 24 and 48 hpi. In cells infected with the JM17-E1A S185/188A virus, E1A expression is greater at 48 hpi. Whereas the WT virus shows two bands on the Western blot, corresponding to the 13S and the 12S isoforms of E1A being expressed (Harlow et al., 1985, 1986), the S185/188A mutant virus does not show any expression of the 12S isoform of E1A.

To assess the effect of mutating the putative CTD mimic on early viral gene expression, E4 was chosen as a candidate gene because the *hr5* mutant showed a decrease in E4 transactivation (Whalen et al., 1997). I observed an increase in E4 RNA transcripts in the mutant S185/188A virus when compared to that of WT hAdV5 (Figure 3.15 B). There was a corresponding slight increase in the protein expression of other viral genes such as the DBP and viral capsid proteins (Figure 3.15 C). DBP is expressed at both 24 and 48 hours by both the WT virus and the S185/188A virus. The capsid proteins are expressed by both viruses at 48 hours. A Western blot for the actin control shows equal loading of protein.

Previous studies have shown that only a small amount of E1A is required to turn on the other viral genes and allow for virus production. WT hAdV5 virus produces E1A in excess of what is required (Hitt and Graham, 1990). The S185/188A point mutations have an effect on the amount of E1A expressed during infection but these point mutations do not affect the expression of other viral genes such as E4, DBP, and viral capsid proteins (Hexon, Penton, Protein V, Protein VI, Protein VII.)

A
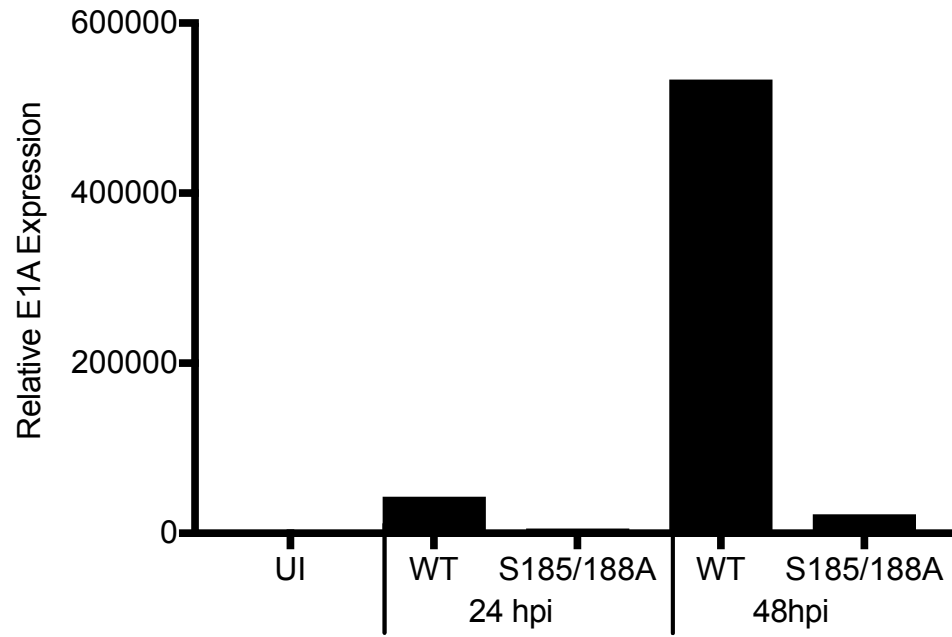
B
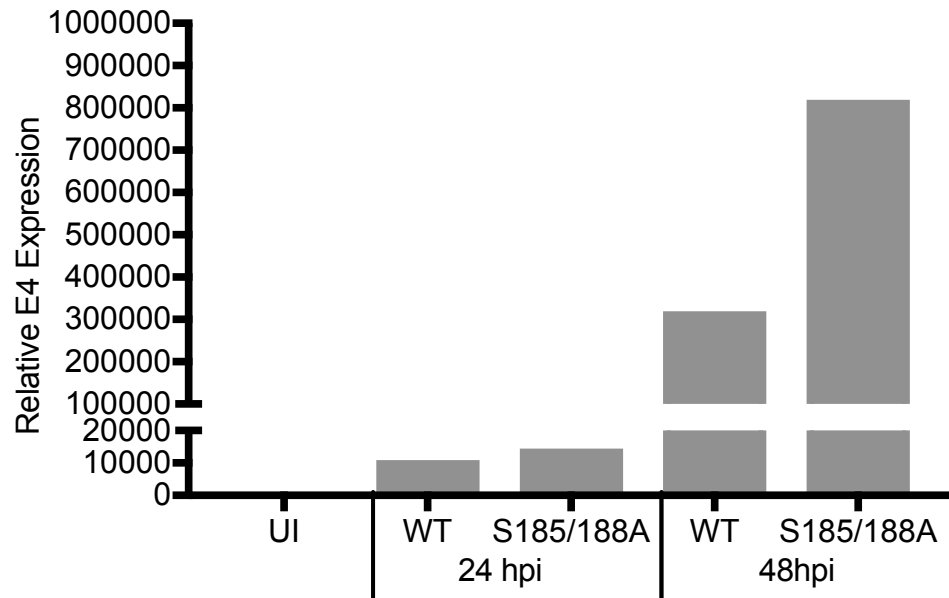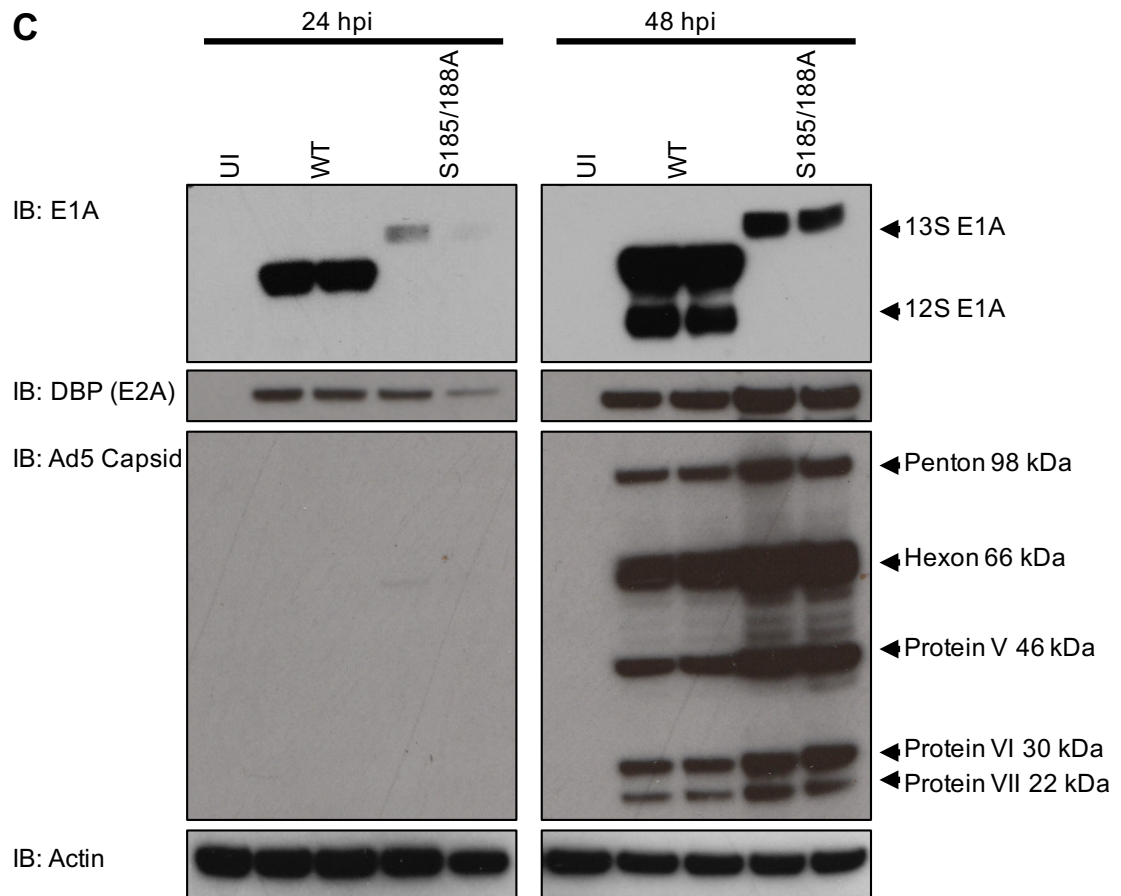
Figure 3.15. Kinetics of virus infection WT Virus vs. JM17-E1A S185/188A Virus (MOI 10).

A549 cells were mock infected (UI) or infected with an MOI of 10 with WT (dl309) and JM17-E1A S185/188A Mutant hAdV. Cells were collected at indicated time points and RNA and protein was collected **A) Relative E1A Expression is higher in WT Virus.** RT-qPCR was performed for early transcripts E1A, normalized to Beta-actin, and plotted as increase over uninfected (UI) samples. **B) Relative E4 Expression is higher in the JM17-E1A S185/188A Mutant Virus.** RT-qPCR was performed for early transcript E4, normalized to Beta-actin, and plotted as increase over UI samples. **C) hAdV5 protein expression.** Protein was detected via Western blotting with the indicated antibodies. E1A represents immediate early gene expression, DBD represents early gene expression, and capsid proteins represent late gene expression.

3.4.2 Virus Time Course WT vs. JM17-E1A S185/188A (MOI 3 vs MOI 30)

My observation that the WT and the JM17-E1A S185/188A mutant virus produce different amounts of E1A when infecting cells with an equal MOI (10) suggested that this differential expression of E1A protein could be masking functional differences. To address this, I next set out to determine the appropriate MOIs at which the WT and S185/188A mutant virus might express comparable amounts of E1A. Approximately 2 x 10^5 A549 cells/well were seeded onto 6 well plates 24 hours prior to infection. Cells were either mock infected (UI) or infected with WT virus (MOI of 1, 3, or 5) and JM17-E1A S185/188A virus (MOI 10 or 30). Cell were harvested at 24, 48 and 72 hpi where both RNA and protein samples were collected. Representative Western blots and RT-qPCR experiments were performed to determine E1A expression at both the protein and mRNA levels across this range of MOIs.

At all three time points (24, 48 and 72 hpi), I observed higher amounts of E1A mRNA transcripts produced by the WT hAdV5 virus compared to that of the mutant S185/188A virus (Figure 3.16 A). This was the case even when the mutant virus was used at an MOI that was 10X that of WT virus. This observation corresponded well with E1A protein expression, detected by Western blotting (Figure 3.16 C). E1A was highly expressed by the WT virus at all three time points, and cells infected at higher MOIs exhibited dose dependent increased levels of E1A expression. However, cells infected with the S185/188A virus do not appear to express comparable amounts of E1A as WT virus. WT virus shows two bands on the Western blot, corresponding to the 13S and the 12S isoforms of E1A being expressed (Harlow et al., 1985, 1986), but the 12S form was not observed in infection with the S185/188A mutant virus.

From these experiments, WT virus at an MOI of 3 and S185/188A virus at an MOI of 30 appear to show comparable amounts of E1A expression. These conditions were therefore used to study the expression of E4 via RT-qPCR. I again observed an increase in E4 RNA transcripts in the mutant S185/188A virus when compared to that of WT hAdV5 (Figure 3.16 B). This corresponds to the increase in protein expression of other viral genes such as DBP and viral capsid proteins (Figure 3.16 C). DBP expression is not affected by the

difference of E1A expression between the two viruses. The S185/188A mutant virus shows a slight increase in DBP protein expression. Capsid proteins are expressed by both viruses from 48 hours post-infection, where the S185/188A virus shows far greater amount of protein expression than the WT virus. A second panel with a shorter exposure time is shown for the 48 and 72 hour time points to more clearly show that the individual capsid proteins are being expressed in both viruses. Expression of capsid proteins did not appear to be affected by the difference in E1A expression between the two viruses. A Western blot for the actin control shows equal loading of protein. These experiments demonstrate that the S185/188A point mutations reduced the amount of E1A expressed during infection. However, these point mutations do not affect the expression of other viral genes such as E4, DBP and viral capsid proteins (Hexon, Penton, Protein V, Protein VI, Protein VII). Although increasing the MOI of the JM17-E1A S185/188A virus compared to WT does not fully rescue E1A expression, it does have the expected dose dependent effect on the expression of other viral proteins.

Interestingly, cells infected with the JM17-E1A S185/188A mutant at an MOI of 30 shows expression of the viral capsid proteins at 24 hpi. It is unusual to see late protein expression earlier in a mutant virus infection than during WT infection. Additionally, cell monolayers show a greater amount of CPE at 72 hours compared to that of WT virus or JM17-E1A S185/188A (MOI 10). It appears that cells infected with an MOI of 30 passes though the replication cycle faster than those infected with a lower MOI.

Figure 3.16. Kinetics of virus infection WT Virus (MOI 1, 3, 5) vs. JM17-E1A S185/188A Virus (MOI 10, 30).

A549 cells were mock infected (UI) or infected with WT (dl309) virus (MOI of 1, 3, or 5) and JM17-E1A S185/188A (MOI 10 or 30). Cells were harvested at indicated time points and RNA and protein was collected **A) Relative E1A Expression is higher in WT Virus.** RT-qPCR was performed for early transcripts E1A, normalized to Beta-actin, and plotted as increase over uninfected (UI) samples. **B) Relative E4 Expression is higher in the JM17-E1A S185/188A Mutant Virus.** RT-qPCR was performed for early transcript E4, normalized to Beta-actin, and plotted as increase over UI samples. **C) hAdV5 protein expression.** Protein was detected via Western blotting with the indicated antibodies. E1A represents immediate early gene expression, DBD represents early gene expression, and capsid proteins represent late gene expression.

A

B
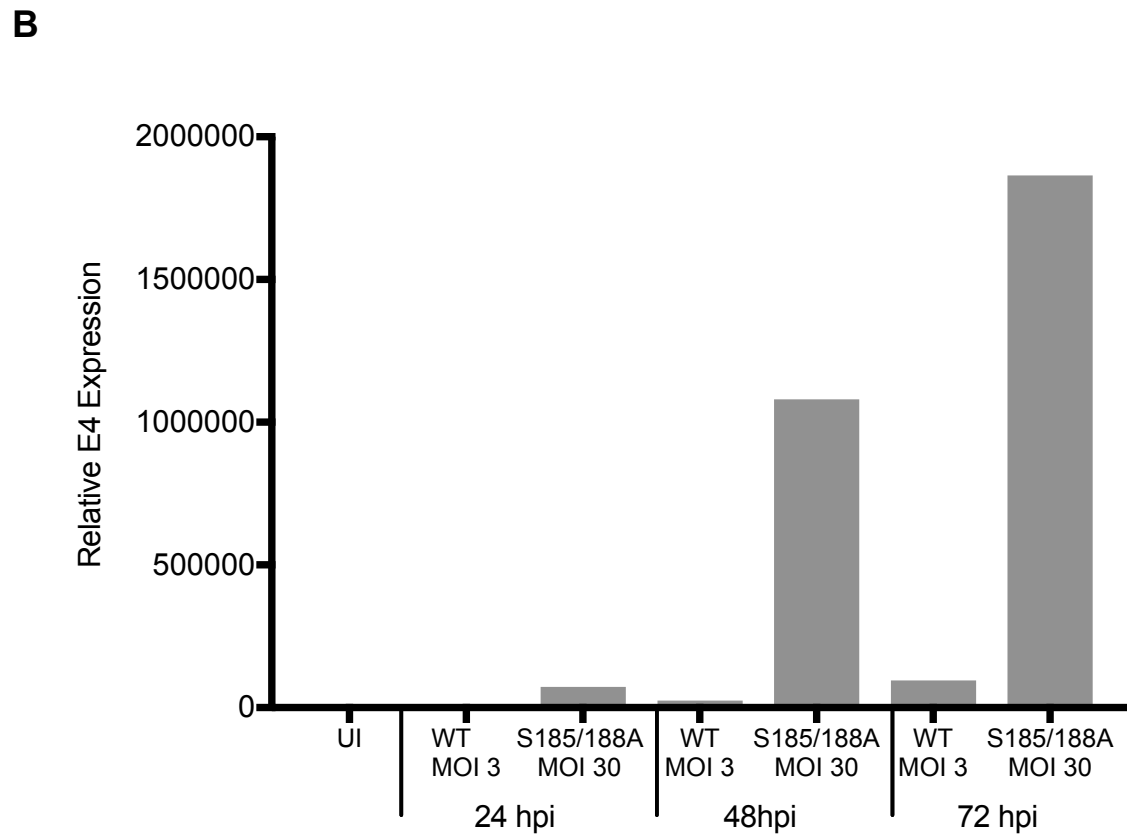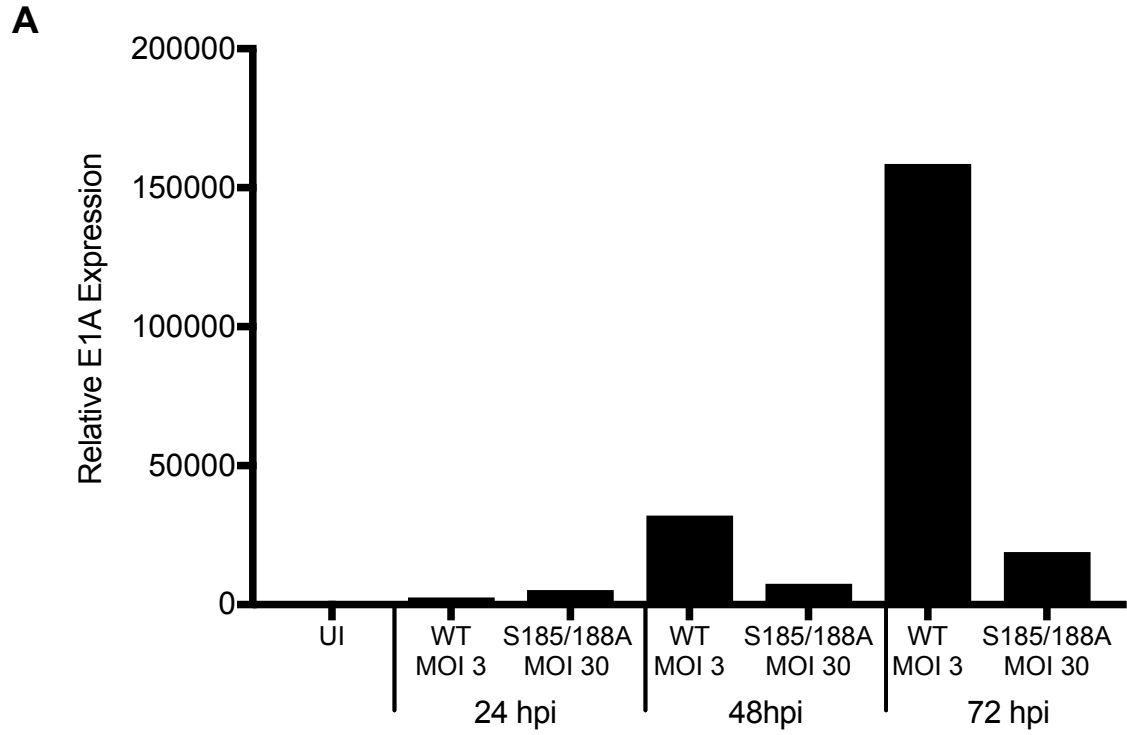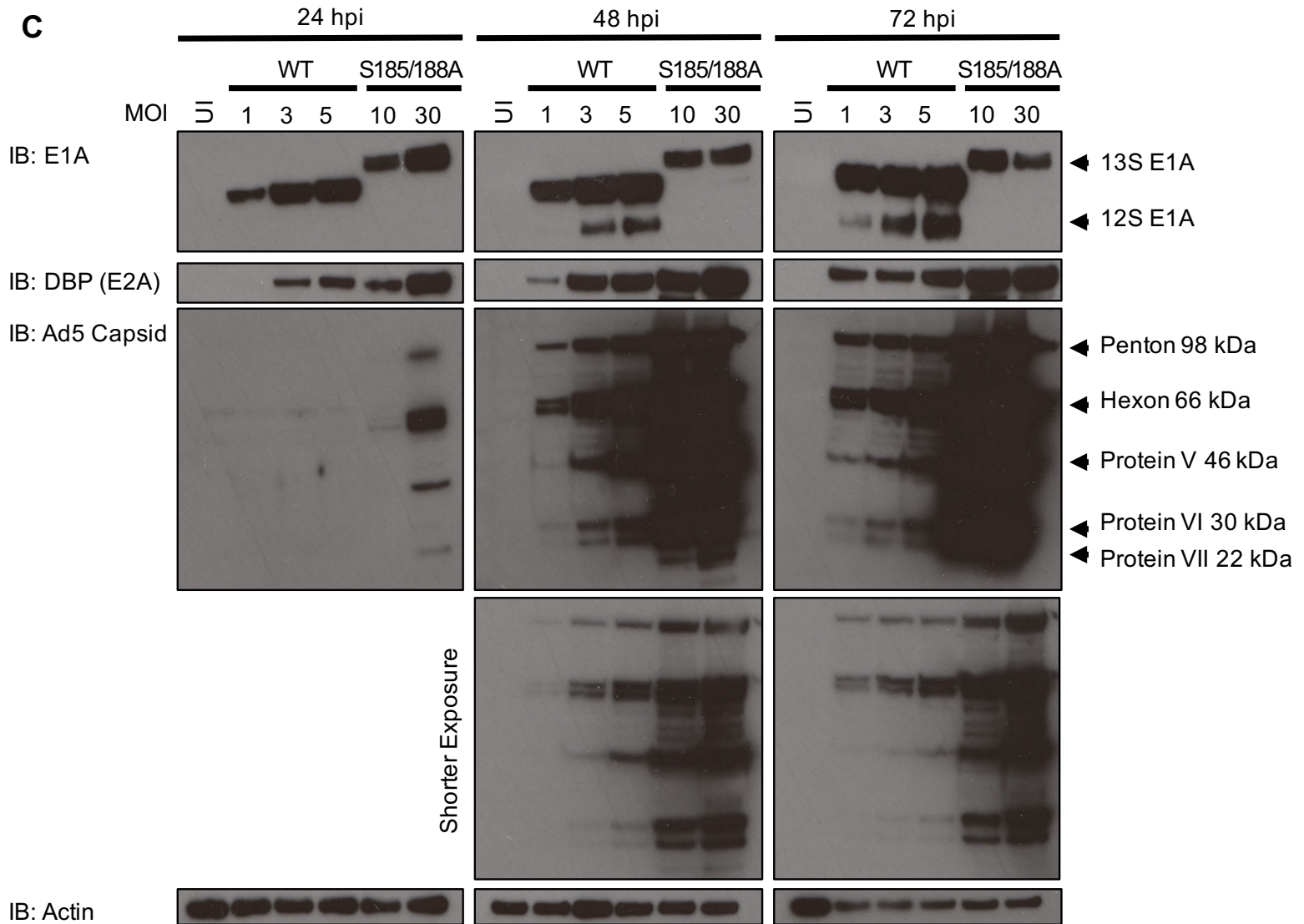
Chapter 4 : Discussion & Future Directions

4   Discussion & Future Directions

The study of molecular and motif mimicry is a common theme in viral infection. Many viruses use ELMs to mimic host cell proteins as a way to get around their limited coding capacity and hijack cellular processes for replication and infection (Davey et al., 2011). A number of different examples of mimicry can be found in Adenovirus E1A, including mimicking cellular AKAP for PKA binding and the binding of cellular pRb via the LxCxE motif (Davey et al., 2011; King et al., 2016b). Of the many examples of mimicry in E1A, none have been reported within CR3, which functions as a strong transactivation domain. Although early mutational studies showed that the promotor targeting region of E1A CR3 is important in the maximum transcriptional activation by the E1 region, the exact determinants, targets and mechanism of action were never fully elucidated (Glenn and Ricciardi, 1987; Webster and Ricciardi, 1991). It was established that this region is specifically required for the transcription of the E4 region, specifically though the phosphorylation of S185 and S188 (Whalen et al., 1997). Interestingly, we observed that this region contains the largest stretch of amino acids that is highly conserved across Adenovirus species, and that this region contains significant sequence homology to the heptad repeat of RNAPII CTD (Figure 1.5). Additionally, the phosphorylated serines, S185 and S188, correspond to the phosphorylated serines S2 and S5 in RNAPII that control the transcription cycle. Based on these similarities, we hypothesized that the promotor targeting region (aa 183-190) of hAdV5 E1A CR3 might act as a mimic of the RNAPII CTD to promote transcription of viral genes and support viral replication. We sought to characterize the roles of the putative CTD mimic in transcriptional activation and to determine the extent of structural and functional mimicry by the putative CTD mimic. Specifically, we examined the interaction between E1A CR3 and CDK9 in order to study the role of this interaction to promote transcriptional elongation. A novel hAdV5 virus containing alanine substitutions in E1A S185 and S188 within the putative CTD mimic was created for future experiments to fully understand the role these two amino acids play in transcription of viral genes and in viral replication.

4.1 The role of the putative CTD mimic in Transactivation

CR3 of E1A hAdV5 is a potent activator of transcription and is commonly used as a model to study the role of cellular and viral factors in the control of gene expression (Ablack et al., 2010; Frisch and Mymryk, 2002; Pelka et al., 2008). A simple system has been used for many years by our lab and others in order to measure the transactivation capabilities of certain proteins, namely E1A, when fused to a heterologous DBD (Ablack et al., 2010; Avvakumov et al., 2003; Jelsma et al., 1988; Pelka et al., 2009a, 2009b; Shuen et al., 2002). We present, for the first time, an in depth analysis of the specific residues in the promotor targeting region of CR3 that are important for transactivation. We show that when CR3 is tethered to a heterologous DBD, that the likely phosphorylation of S185 and S188 are required for maximal transactivation by CR3 in a luciferase activation assay. Our findings support data from early mutation studies that show that any disruption in the promotor targeting region of CR3 impairs transcription activation, specifically the mutation of serine at 185 (Glenn and Ricciardi, 1987). Additionally, we show through a squelching assay, that the phosphorylation of these residues is also important for binding to transcriptional regulators required for CR3 activation. These could potentially include known factors such as members of the ATF family, USF, Sp1, TAFII250, TAFII135 or the S8 component of the 19S regulatory subunit (Pelka et al., 2008). This may also include yet unidentified factors involved in the complex and ever evolving model of transactivation by hAdV E1A (Ablack et al., 2010), such as those we are investigating for their role in interacting with the putative CTD mimic.

Using the DBD fusion system, my experiments show that the putative CTD mimic and AR1 each function as weak activators when fused to the heterologous DBD, activating transcription about 5 times over the vector. The putative CTD mimic can also act to squelch limited cellular factors away from promoter bound E1A CR3. This does not rely on AR1, although AR1 again may be involved in maximal function of the C-terminal portion of CR3. In addition to sequence similarity between E1A and the RNAPII CTD, the putative CTD mimic and the human CTD heptad repeat appear to function similarly to

activate transcription in the transactivation assay. The putative CTD mimic and the human CTD heptad demonstrate comparable ability to sequester cellular factors. Experiments studying full length E1A-CR3 demonstrated the importance of conserved phosphorylated serines for maximum transactivation and squelching abilities. Collectively, these experiments provide some support for the hypothesis that this region of E1A functions as a CTD mimic.

4.2 Functional Mimicry of RNAPII CTD by E1A CR3

To test the functional mimicry of RNAPII CTD by E1A CR3 we wanted to examine the ability of the putative CTD mimic to confer interactions between E1A and proteins that are known to interact with the RNAPII CTD. The first candidate for this type of inquiry was CDK9. CDK9 had been shown previously to interact with E1A specifically though the CR3 region (Vijayalingam and Chinnadurai, 2013). CDK9 typically phosphorylates RNAPII CTD at S2 to initiate elongation of cellular genes. However, in the presence of viral infection from viruses such as EBV and HIV, viral proteins hijack CDK9 to phosphorylate S5 of the RNAPII CTD in order to facilitate elongation of viral genes (Bark-Jones et al., 2006; Eick and Geyer, 2013; Zhou et al., 2000). CDK9 is thus an important target to study for its involvement in the elongation of adenoviral genes. Initially we tested for co-immunoprecipitation between endogenous CDK9 and E1A CR3 or full length E1A. However, the antibody for endogenous CDK9 had high levels of background and I was not able to confirm this interaction. We constructed a plasmid expressing exogenous CDK9 with a HA tag in order to transiently express CDK9 along with E1A CR3. E1A CR3 alone was not found to be sufficient for binding to CDK9 but I was able to confirm that full length 13S E1A was capable of this interaction. I was unable to demonstrate that the phosphorylation S185 and S188 played a role in this interaction in the context of 13S E1A. However, this doesn't rule out the possibility that the putative CTD mimic region as a whole does not play a role in this interaction.

Future co-immunoprecipitation studies should be performed in the context of full length 13S E1A in order to identify the specific residues or regions involved in the interaction

between 13S E1A and CDK9. First, we would need to determine if the putative CTD mimic region, the AR1 region, or perhaps both, are needed for the interaction with CDK9. To do so, we could construct GFP fused 13S E1A, with either Δ183-200 (deletes the putative CTD mimic and AR1), Δ183-190 (deletes only the putative CTD mimic) and Δ189-200 (deletes only AR1). Failure for these proteins to interact with CDK9-HA in co-immunoprecipitation experiments would highlight the role of the putative CTD mimic and AR1 in the interaction between CDK9 and 13S E1A. If the deletion of these regions does affect CDK9 interaction, this would lead us to conclude the C-terminal portion of E1A CR3 does not play a role in the interaction between E1A and CDK9, suggesting that CDK9 interacts with E1A through the zinc-finger region of CR3. If the putative CTD region was found necessary for the interaction between CDK9, this would provide exciting evidence that supports the hypothesis set forth in this thesis.

In their 2013 paper, Vijayalingam and Chinnadurai also employ a similar GAL4-luciferase assay in order to highlight the role of the CDK9/CR3 interaction on E1A CR3 mediated transactivation. They measure activation by promotor bound E1A CR3 either with the addition of increasing concentrations of a CDK9 plasmid or in the presence of a dominant negative CDK9 plasmid. Increasing amounts of CDK9 increased maximal transactivation by CR3 while introducing a dnCDK9 severely impaired the ability of CR3 to activate transcription (Vijayalingam and Chinnadurai, 2013). In future experiments, we might employ similar techniques to test the role of CDK9 in increasing maximal transactivation by full length CR3, CR3 mutants, or the putative CTD mimic peptides. This would demonstrate further which residues are involved in the CDK9 and E1A interaction, as well as providing further evidence to support the hypothesis that E1A is acting as an RNAPII CTD mimic.

Although I found that CR3 was not sufficient for interaction with CDK9, it was reported to be necessary for the interaction with full length E1A (Vijayalingam and Chinnadurai, 2013). Future experiments could examine other residues or regions in E1A to determine if they are required for this interaction with CDK9. Many proteins that interact with E1A have two distinct interaction regions. Similar co-immunoprecipitation experiments to those above could be carried out to examine the interaction between CDK9 and E1A

fragments expressing CR3 with either N-Terminus/CR1, CR2 or CR4. Co-immunoprecipitation of CDK9 with these fragments would identify other CRs, in conjunction with CR3, that are necessary and possibly sufficient for the interaction with CDK9. Additionally, we could use an established panel of deletion mutants, to narrow down the regions of interest, and identify specific residues required for the interaction between full length 13S E1A and CDK9 (Jelsma et al., 1988).

In my experiments, I discovered that S185 and S188 of the putative CTD mimic do not mediate the interaction between full length E1A and CDK9. However, future experiments may show the putative CTD mimic region as a whole is involved in this interaction. Other experiments may be able to pinpoint other residues and CRs of E1A that are involved in this interaction. Characterizing the interaction between CDK9 and E1A will help define the role of CDK9 in transcriptional activation by E1A. These experiments may suggest E1A and CDK9 cooperate to promote efficient elongation of viral genes as proposed in models developed from studies of viral transactivation by HIV, EBV, HSV and CMV (Reviewed in Zaborowska et al., 2016). Alternatively, this would lead to the discovery an entirely new model instead.

While the putative CTD mimic may not interact with CDK9, it is possible that it interacts with other proteins known to interact with the RNAPII CTD. These proteins include, the CTD kinases CDK7 and CDK8, and transcription factors such as Paf1, RNGTT, RPRD1a, CA150 and Set2 (Eick and Geyer, 2013). All of these targets function at various points of the transcription cycle from initiation, to elongation, termination and RNA processing. Specifically, CDK7, a CTD kinase, binds unphosphorylated RNAPII and phosphorylates Serine-5 of the CTD to trigger transcription initiation. CDK8, in complex with Cyclin C, is a subunit of the mediator complex and plays a role in bridging transcription factors with RNAPII in the preinitiation complex (Eick and Geyer, 2013). Paf1 is the major subunit of the Paf1 complex, which binds the phosphorylated S2 CTD, and is involved in histone modification and transcription elongation (Chu et al., 2013). RNGTT is a capping enzyme, a guanyl-transferase, recruited to RNAPII phosphorylated at Serine-5 of the CTD (Dunn and Cowling, 2015). Set2 is a Histone3 Lysine36 (H3K36) methyltransferase that plays a role in transcription elongation though interaction with

doubly phosphorylated RNAPII CTD (Schaft et al., 2003). CA150 is a transcription factor, that regulates RNAPII though the recruitment of other transcription associated proteins. CA150 interacts via its FF domains with the negative charges on the doubly phosphorylated RNAPII CTD. The acidic EP repeats of AR1 may mimic the negative charges in this interaction, expanding the functional domain that mimics the CTD in CR3, and aid in binding to CA150 and other transcription associated factors (Smith et al., 2004). RPRD1a binds the CTD phosphorylated on S2 with S7 and acts as a scaffold for S5 dephosphorylation (Ni et al., 2014). Future work could focus on determining which, if any, of these factors interacts with the putative CTD mimic. This would lead us to identify at which stage of transcription the putative CTD mimic functions: mRNA capping, initiation, elongation, termination. To investigate the interaction between full length 13S E1A and any other proteins that might bind to the putative CTD mimic, I would use similar approaches to those that I propose above with CDK9. Collectively, the results from past and future experiments would allow us to form a working model for the region's involvement in transcription and viral replication.

4.3   Structural Mimicry of RNAPII CTD by E1A CR3

We first based our hypothesis that E1A CR3 structurally mimics the RNAPII CTD based on the high degree of sequence similarity (Figure 1.5). Second, both the RNAPII CTD and the putative CTD mimic are phosphorylated at serines in position 2 and 5 of the peptide, corresponding to S185 and S188 in E1A (Eick and Geyer, 2013; Whalen et al., 1997). Finally, both the RNAPII CTD and the region in E1A CR3 are both thought to be intrinsically disordered (Eick and Geyer, 2013; Pelka et al., 2008). Previous studies in our lab and others suggest a link between functional and structural mimicry (King et al., 2016b; Tsai et al., 2012). By identifying a factor (or factors) that interact with the putative CTD mimic, it would suggest that E1A CR3 functionally mimics the RNAPII CTD and would imply that E1A-CR3 also structurally mimics the RNAPII CTD.

Based on original reports supporting this hypothesis from Dr. Greg Fonseca (Unpublished results, 2013), I attempted to demonstrate this structural mimicry by using an antibody for

the doubly phosphorylated RNAPII CTD to see if it recognizes E1A CR3. However, I was unable to reproduce results from the original reports and subsequent attempts produced a wide variation in results. Lysates immunoprecipitated with RNAPII and immunoblotted with GFP occasionally demonstrated that E1A CR3 has been immunoprecipitated by the RNAPII antibody. However, results were not consistent and often resulted in no evidence of cross recognition at all (Figure 3.13). On the other hand, occasionally lysates immunoprecipitated with GFP and immunoblotted for RNAPII appeared to show an interaction between E1A CR3 and RNAPII. Furthermore, it appeared that E1A CR3 may interact with RNAPII in a phosphorylation specific manner (Figure 3.14 A and B). However, attempts to reproduce this experiment once again resulted in a wide range of different results (Figure 3.14 C-F). Overall, I could not conclude that that E1A CR3 was recognized by the RNAPII antibody nor could I conclude that E1A CR3 interacted with RNAPII. Furthermore, I could not conclude that these results are phosphorylation specific. Thus, evidence of structural mimicry is not conclusive.

Additionally, I discovered during functional mimicry experiments that overexpression (4µg) of transfected GFP leads to positive co-immunoprecipitation results in our negative control conditions. The above structural mimicry experiments were carried out with transfection of 8µg of GFP plasmid DNA per 10cm dish and 2x10cm dishes were used per IP reaction. This further puts into question the validity of these experiments. This likely explains the presence of a band in my negative control lanes, as seen in figure 3.14 A, C, D, and F as well as figure 3.13 C. Any future experiments using GFP should pay special attention to whether the empty vector negative control interacts with the protein of interest, in this case RNAPII. The amount of GFP should be optimized and titrated to minimize this effect.

It would prove very interesting if this cross-recognition is in fact true, that E1A structurally mimics RNAPII CTD. However, to clear up the conflicting results, we should move away from using GFP tagged E1A CR3 and use another protein tag entirely. E1A CR3 peptides can be fused to a FLAG epitope tag (DYKDDDDK) and then use FLAG-specific agarose (ANTI-FLAG® M2 Affinity Gel, Sigma) in order to immunoprecipitate

E1A CR3 (Gerace and Moazed, 2015). This would minimize background and create a more stable platform by which to carry out a co-immunoprecipitation reaction. This would provide clear indications whether CR3 interacts with RNAPII in a phosphorylation specific manner and may be able to confirm whether there are any structural similarities between E1A CR3 and the RNAPII CTD.

4.4   Characterizing JM17-E1A S185/188A

Previous studies with hAdV5 infection used transactivation impaired viruses with deletions from aa 178-184 (dl114) and aa 188-204 (dl115), or the point mutant *hr5* which replaces S185 with asparagine. However, there has never before been a virus created that replaces both S185 and S188 with alanine, designed to study the effects of both conserved phosphorylated serines on transactivation. I constructed the JM17- E1A S185/188A virus by rescuing the desired point substitutions into the viral genome, propagating the virus and ultimately purifying it by a CsCl density gradient for use in current and future experiments (Figure 2.1). The E1A protein produced by this mutant can't be phosphorylated at the two conserved serine residues in the putative CTD mimic. RNA and protein samples were collected over 48 and 72 hour time courses from A549 cells infected with various MOIs in order to characterize this virus. When infecting cells with equal MOIs (10) of both the WT and JM17-E1A S185/188A virus, the mutant virus showed markedly less E1A production in terms of both protein and RNA levels (Figure 3.15 A, C). These results indicate that the mutation affects the ability of E1A to be expressed. Given the corresponding reduction in mRNA levels, this is not simply due to decreased stability of the protein. In contrast to E1A expression, the expression of other viral genes, E4, DBP, and capsid proteins express comparable levels of both protein and RNA (Figure 3.15 B, C). These results indicate that the phosphorylation of the putative CTD mimic is not necessary for efficient viral early gene expression. This differs with the reduction in E4 expression described previously (Whalen et al., 1997). While these residues may be important for transactivation in a transfection model, these residues might not play a significant biological role in transactivation of viral genes during

infection with hAdV, likely due to the presence of other viral factors and a dysregulated cellular environment.

E1A levels of the JM17-E1A S185/188A mutant still did not meet the level of WT when I attempted to obtain comparable levels of E1A expression by infecting cells with 10X the mutant virus (MOI 30) compared to WT virus (MOI 3) (Figure 3.16 A, C). The expression of other viral genes such as E4, DBP and capsid proteins show a dose dependent increase in the mutant when compared to WT (Figure 3.16 B, C). These results further suggest that this mutant does not have a defect in activating early gene expression, other than for expression of E1A itself.

As a consequence of these experiments, this raised the question of whether future experiments should use cells infected with equal MOIs or should use cells infected with different MOIs but with equal E1A expression. For the sake of our immunoprecipitation experiments, we used different MOIs but equal E1A expression in order to test the role of specific residues (S185 and S188) in the interaction between E1A and CDK9, rather than based on amount of E1A present. In other experiments, the alternative approach to normalize the infection could be used, such that the equal number of viral genome templates are available for transcription and the levels of all other viral proteins are produced in equal amounts.

My observation that the JM17-E1A S185/188A mutant virus expresses less E1A was not anticipated. It is known that E1A has separate activation and repression activities including activation and repression of E1A itself via autoregulation (Smith et al., 1985; Tibbetts et al., 1986). E1A also has been shown to represses heterologous SV40 and polyoma promotors, Ad2 E2 late expression, as well as promotors of cellular genes (Borrelli et al., 1984; Hen et al., 1985; Sogawa et al., 1989; Velcich and Ziff, 1985; Webster et al., 1988). These activities are thought to be temporally regulated, early in infection E1A gene products return to the nucleus for auto-amplification. Then later in infection, E1A might repress activation in order to allow for a shift from early gene products to late gene products (Tibbetts et al., 1986). These functions are also spatially separated, where repression takes place at enhancers upstream of the E1A gene and activation takes place at the promotor and initiation start sites (Borrelli et al., 1984; Cogan

et al., 1992; Hearing and Shenk, 1983; Jones and Tibbetts, 1989; Smith et al., 1985). Autoregulation by E1A may explain the differences in E1A expression in the JM17- E1A S185/188A mutant virus at both the RNA and protein level. We thought perhaps there was an issue with the enhancer sequence upstream of E1A, which leads to auto-repression of E1A. Sequencing of the pXC1 S185/188A plasmid that was used to construct the novel virus does not reveal any defects in the promotor/enhancer region. 13S E1A but not 12S E1A can mediate autoregulation suggesting that CR3 plays a role in autoregulation (Hearing and Shenk, 1985). However, sequencing of the coding region of the JM17-E1A S185/188 mutant virus itself did not reveal any unexpected abnormalities in CR3. Although unlikely, this region may have acquired a defect during the initial recombination event and further efforts should be taken to sequence various regions within and surrounding E1A before we may attribute defects in expression specifically to S185/188A.

Early and late gene expression, including E4, DBP (E2E), and capsid proteins depend on activation by E1A for their transcription (Berk, 1986; Jones and Shenk, 1979). But while E1A is expressed to lower levels in the JM17-E1A S185/188A mutant virus (MOI 30) we still observe higher amounts of E4, DBP, and capsid proteins in cells infected with the mutant virus versus WT (MOI 3). The increased expression may be explained due to the fact that there is a higher number of DNA templates available prior to DNA replication in cells infected with the mutant virus at 10X the MOI of WT (Tibbetts et al., 1986). Although E1A is limited, low levels of E1A are sufficient for virus production and infection still results in in expected dose dependent expression of other viral genes (Hitt and Graham, 1990).

4.5 Future Directions into understanding elongation of hAdV genes

Transcription activation and regulation is a complex process, one that E1A intersects with at many points from initiation to termination. Researchers are increasingly keen on investigating the role of E1A in elongation. Some recent work shows that E1A recruits

mediator complex and CDK9 to promote transcription of viral genes, possibly through elongation (Vijayalingam and Chinnadurai, 2013). Additionally, our lab found that that the N-terminus of E1A would make use of the hBre1 protein to recruit the Paf1 complex and promote elongation of viral transcripts (Fonseca et al., 2014). Future experiments could be designed to fully elucidate the mechanism by which E1A is involved in elongation of viral genes. Specifically, to determine if 1) S185 and S188 play a role in elongation, 2) if the putative CTD mimic plays a role in elongation, and 3) what role does the interaction between CDK9 and E1A play in transcription.

To determine the role of phosphorylated S185 and S188 in elongation, experiments will be carried out in a similar fashion to previous elongation studies in our lab. Cells could be infected with either WT of JM17 E1A S185/188A virus after which chromatin immunoprecipitation (ChIP) followed by RT-qPCR that will examine occupancy of RNAPll on viral genes. Primers are designed to amplify amplicons located at the C-terminal (5') and N-terminal (5') of viral genes, including E1A E1B, E2, E3 and E4 (Fonseca et al., 2014). Greater RNAPII occupancy in the 3' end of viral genes, in cells infected with WT versus mutant S185188A virus, indicates that phosphorylated S185 and S188 play a role elongation. Greater RNAPII occupancy at the 5' of viral genes in cells infected with WT virus indicates phosphorylated S185 and S188 play a role in initiation.

We may discover that the phosphorylation of S185 and S188 play a role in elongation or in initiation of viral genes. While S185 and S188 do not appear to contribute to the interaction with CDK9, these residues may be required for interaction with other RNAPII CTD interacting proteins, and these proteins may be involved in the process of initiation and elongation. For example, in previous studies in our lab, siRNA knockdown of hPaf1 in the context of hBre and E1A leads to decreased elongation, which is indicated by decreased occupancy of RNAPII on the 3' region of viral genes (Fonseca et al., 2014). Future experiments could follow this design to highlight the role of E1A interactions in transcription regulation. Thus, it is possible to study if any of the above cellular factors that may have been identified to interact with E1A, are also involved in transcription of viral genes. To do so, siRNA could be used to knock down any of the identified cellular factors. Alternatively, those with enzymatic activity could be targeted with inhibitors,

provided they are available. Studies would compare the effects on transcription in WT versus the JM17-E1A S185/188A mutant. If any of these factors are involved in transcription, knocking down these factors would lead to a decrease in RANPII occupancy in the 5' (initiation) or 3' region (elongation) of viral genes in WT virus. JM17-E1A S185/188A may prove resistant to these changes, and this would highlight the role of phosphorylated serines in the interaction with cellular factors and provide evidence of their ability to function as a CTD mimic during transcription.

While the phosphorylation of S185 and S188A does not seem to play a role in an interaction with CDK9, the putative CTD mimic may still be involved in this interaction. Co-immunoprecipitation experiments may outline which residues of 13S E1A are required for interaction with CDK9, whether it be through the putative CTD mimic or by other regions of E1A. The above ChIP experiments might then be used to study WT virus versus a mutant virus (unable to bind CDK9) and the occupancy of RNAPII on viral genes. Furthermore, experiments could be designed to study, through the use of siRNA and CDK inhibitors, how the presence or absence of CDK9 might affect elongation or initiation. It was expected that the putative E1A CTD mimic will be involved in promoting elongation of viral genes via an interaction with CDK9. HIV and EBV proteins act though the cellular CDK9 to release promotor pausing and promote elongation, and it was expected that Adenovirus E1A would act in a similar fashion (Bark-Jones et al., 2006; Zhou et al., 2000). This may place Adenovirus in the same model as HIV and EBV, highlighting a fascinating mechanism conserved in multiple viruses to hijack host cell machinery to carry out efficient elongation.

Other studies use immunofluorescence microscopy to visualize viral transcription centers during hCMV and HSV infections and to identify the various components that are recruited to these centers. These studies demonstrate the co-localization between CDK9 (and in some cases CDK7) and RNAPII. Additionally, these studies identify other viral proteins required for this interaction, and for active transcription. These groups often use CDK inhibitors or siRNA to knock down CDKs in order to elucidate the mechanism by which this occurs. Researchers also identify temporal differences, at early versus late times post infection. Lastly, during viral infection, and in the presence or absence of

various cellular factors, researchers can examine the total levels of unphosphorylated RNAPII versus S2, S5, or S2/S5 phosphorylated RNAPII, in order to fully understand the effects of the virus in hijacking host cell machinery (Dai-Ju et al., 2006; Durand and Roizman, 2008; Kapasi and Spector, 2008; Kapasi et al., 2009; Tamrakar et al., 2005). We may use the infection of WT versus a JM17-E1A S185/188A virus, or an E1A Δ180-188 virus, along with similar immunofluorescence techniques outlined above to understand the modifications taken by the virus to usurp host transcription machinery and use it for the transcription of viral genes. These experiments will outline the effect of the putative CTD mimic on transcription or demonstrate if in fact the sequence similarity observed between RANPII and E1A does not actually play a functional role in hAdV5 infection and E1A transactivation.

4.6   Significance

We demonstrated the importance for S185 and S188 in E1A CR3 transactivation and show that the highly conserved putative CTD mimic plays a role in transactivation, presumably by binding of cellular factors. While we discovered that the phosphorylation of S185 and S188 does not play a role in the interaction of 13S E1A and CDK9, it is possible that the putative CTD mimic as a whole may still play a role in this interaction. Alternatively, the phosphorylation of S185 and S188 may be involved in an interaction with other cellular factors. Establishing the promotor targeting region as a putative CTD mimic through binding of RNAPII CTD interacting proteins would demonstrate a novel example of mimicry to add to a growing list of examples for the use of mimicry via ELMs in viral evolution, specifically in Adenoviral evolution. Identifying new targets of E1A that depend on the phosphorylation of S185 and S188 mimic may at last provide novel insights into the C-terminal portion of E1A CR3.   This study demonstrates the characterization of a novel point mutant of hAdV5 JM17-E1A S185/188A, which could prove to be a useful tool in studying the effect of these point mutations on transcription of viral genes as well as study the importance of these serines for interaction with identified cellular factors.

Although I confirmed that 13S E1A interacts with CDK9, future work will be required to determine the specific residues involved in this interaction. ChIP experiments may highlight the role of CDK9 in elongation of viral genes, thus identifying a new mechanism by which E1A promotes transcription and places adenovirus in the same model as viruses such as EBV and HIV. Based on this model, there is a potential application of CDK inhibitors as anti-viral therapeutics. These CDK inhibitors, including Flavopiridol (binds to the ATP site of CDK9 though hydrogen like interaction), DRB (an adenosine analogue that is a specific inhibitor of CDK9) and Roscovitine (a purine derivative), have been shown to inhibit HIV replication and transcription by targeting CDK9. Broad spectrum CDK inhibitors tend to have negative effects on cell cycle progression, cellular proliferation and other adverse or cytotoxic effects, thus there is a search for alternatives with less negative effects (Chao et al., 2000; Sadaie et al., 2004). A recent study using the small molecule CDK inhibitor FIT-039 showed an inhibition of replication of HSV-1 and HSV-2, hAdV and hCMV without detrimental effects to mammalian cells (Yamamoto et al., 2014). Thus, drugs targeting such pathways may have utility as novel antiviral agents. Indeed, researchers show that treatment of hAdV2, 5, 8 and 37 infected cells with Flavopiridol, or otherwise inhibiting CDK9, led to a reduction of viral replication, abrogated the production of E1A and altered levels of phosphorylated RNAPII (Prasad et al., 2017).

5   References

Ablack, J.N.G., Pelka, P., Yousef, A.F., Turnell, A.S., Grand, R.J.A., and Mymryk, J.S. (2010). Comparison of E1A CR3-dependent transcriptional activation across six different human adenovirus subgroups. J. Virol. *84*, 12771–12781.

Ablack, J.N.G., Cohen, M., Thillainadesan, G., Fonseca, G.J., Pelka, P., Torchia, J., and Mymryk, J.S. (2012). Cellular GCN5 is a novel regulator of human adenovirus E1A-conserved region 3 transactivation. J. Virol. *86*, 8198–8209.

Albinsson, B., and Kidd, A.H. (1999). Adenovirus type 41 lacks an RGD alpha(v)-integrin binding motif on the penton base and undergoes delayed uptake in A549 cells. Virus Res. *64*, 125–136.

Alcami, A. (2003). Viral mimicry of cytokines, chemokines and their receptors. Nat. Rev. Immunol. *3*, 36–50.

Amalfitano, A., Begy, C.R., and Chamberlain, J.S. (1996). Improved adenovirus packaging cell lines to support the growth of replication-defective gene-delivery vectors. Proc. Natl. Acad. Sci. U. S. A. *93*, 3352–3356.

Andersson, M., Pääbo, S., Nilsson, T., and Peterson, P.A. (1985). Impaired intracellular transport of class I MHC antigens as a possible means for adenoviruses to evade immune surveillance. Cell *43*, 215–222.

Ansieau, S., and Leutz, A. (2002). The conserved Mynd domain of BS69 binds cellular and oncoviral proteins through a common PXLXP motif. J. Biol. Chem. *277*, 4906–4910.

Aoki, K., Benkö, M., Davison, A.J., Echavarria, M., Erdman, D.D., Harrach, B., Kajon, A.E., Schnurr, D., Wadell, G., and Members of the Adenovirus Research Community (2011). Toward an integrated human adenovirus designation system that utilizes molecular and serological data and serves both clinical and fundamental virology. J. Virol. *85*, 5703–5704.

Avgousti, D.C., Herrmann, C., Kulej, K., Pancholi, N.J., Sekulic, N., Petrescu, J., Molden, R.C., Blumenthal, D., Paris, A.J., Reyes, E.D., et al. (2016). A core viral protein binds host nucleosomes to sequester immune danger signals. Nature *535*, 173–177.

Avvakumov, N., Wheeler, R., D'Halluin, J.C., and Mymryk, J.S. (2002). Comparative sequence analysis of the largest E1A proteins of human and simian adenoviruses. J. Virol. *76*, 7968–7975.

Avvakumov, N., Torchia, J., and Mymryk, J.S. (2003). Interaction of the HPV E7 proteins with the pCAF acetyltransferase. Oncogene *22*, 3833–3841.

Avvakumov, N., Kajon, A.E., Hoeben, R.C., and Mymryk, J.S. (2004). Comprehensive sequence analysis of the E1A proteins of human and simian adenoviruses. Virology *329*, 477–492.

Baek, M.-C., Krosky, P.M., Pearson, A., and Coen, D.M. (2004). Phosphorylation of the RNA polymerase II carboxyl-terminal domain in human cytomegalovirus-infected cells and in vitro by the viral UL97 protein kinase. Virology *324*, 184–193.

Bai, M., Harfe, B., and Freimuth, P. (1993). Mutations that alter an Arg-Gly-Asp (RGD) sequence in the adenovirus type 2 penton base protein abolish its cell-rounding activity and delay virus reproduction in flat cells. J. Virol. *67*, 5198–5205.

Bark-Jones, S.J., Webb, H.M., and West, M.J. (2006). EBV EBNA 2 stimulates CDK9-dependent transcription and RNA polymerase II phosphorylation on serine 5. Oncogene *25*, 1775–1785.

Barrasa, M.I., Harel, N.Y., and Alwine, J.C. (2005). The phosphorylation status of the serine-rich region of the human cytomegalovirus 86-kilodalton major immediate-early protein IE2/IEP86 affects temporal viral gene expression. J. Virol. *79*, 1428–1437.

Bastian, T.W., and Rice, S.A. (2009). Identification of sequences in herpes simplex virus type 1 ICP22 that influence RNA polymerase II modification and viral late gene expression. J. Virol. *83*, 128–139.

Benedict, C.A., Norris, P.S., Prigozy, T.I., Bodmer, J.L., Mahr, J.A., Garnett, C.T., Martinon, F., Tschopp, J., Gooding, L.R., and Ware, C.F. (2001). Three adenovirus E3 proteins cooperate to evade apoptosis by tumor necrosis factor-related apoptosis-inducing ligand receptor-1 and -2. J. Biol. Chem. *276*, 3270–3278.

Berk, A.J. (1986). Adenovirus promoters and E1A transactivation. Annu. Rev. Genet. *20*, 45–79.

Berk, A.J. (2005). Recent lessons in gene expression, cell cycle control, and cell biology from adenovirus. Oncogene *24*, 7673–7685.

Berk, A.J. (2007). Adenoviridae: The Viruses and Their Replication (Philadelphia: Wolters Kluwer Health/Lippincott Williams & Wilkins).

Berk, A.J., and Sharp, P.A. (1978). Structure of the adenovirus 2 early mRNAs. Cell *14*, 695–711.

Berk, A.J., Lee, F., Harrison, T., Williams, J., and Sharp, P.A. (1979). Pre-early adenovirus 5 gene product regulates synthesis of early viral messenger RNAs. Cell *17*, 935–944.

Bethesda Research Laboratories (1986). BRL pUC host: E. coli DH5α competent cells. Focus *8*, 9.

Bhowmick, P., Guharoy, M., and Tompa, P. (2015). Bioinformatics Approaches for Predicting Disordered Protein Motifs. Adv. Exp. Med. Biol. *870*, 291–318.

Borrelli, E., Hen, R., and Chambon, P. (1984). Adenovirus-2 E1A products repress enhancer-induced stimulation of transcription. Nature *312*, 608–612.

Bowles, N.E., Ni, J., Kearney, D.L., Pauschinger, M., Schultheiss, H.-P., McCarthy, R., Hare, J., Bricker, J.T., Bowles, K.R., and Towbin, J.A. (2003). Detection of viruses in myocardial tissues by polymerase chain reaction: evidence of adenovirus as a common cause of myocarditis in children and adults. J. Am. Coll. Cardiol. *42*, 466–472.

Boyer, T.G., Martin, M.E., Lees, E., Ricciardi, R.P., and Berk, A.J. (1999). Mammalian Srb/Mediator complex is targeted by adenovirus E1A protein. Nature *399*, 276–279.

Bradshaw, C.S., Denham, I.M., and Fairley, C.K. (2002). Characteristics of adenovirus associated urethritis. Sex. Transm. Infect. *78*, 445–447.

Brehm, A., Ohbo, K., Zwerschke, W., Botquin, V., Jansen-Dürr, P., and Schöler, H.R. (1999). Synergism with germ line transcription factor Oct-4: viral oncoproteins share the ability to mimic a stem cell-specific activity. Mol. Cell. Biol. *19*, 2635–2643.

Brusca, J.S., Jannun, R., and Chinnadurai, G. (1984). Efficient transformation of rat 3Y1 cells by human adenovirus type 9. Virology *136*, 328–337.

Bruton, R.K., Pelka, P., Mapp, K.L., Fonseca, G.J., Torchia, J., Turnell, A.S., Mymryk, J.S., and Grand, R.J.A. (2008). Identification of a Second CtBP Binding Site in Adenovirus Type 5 E1A Conserved Region 3. J. Virol. *82*, 8476–8486.

Burgert, H.G., and Kvist, S. (1985). An adenovirus type 2 glycoprotein blocks cell surface expression of human histocompatibility class I antigens. Cell *41*, 987–997.

Carvalho, T., Seeler, J.S., Ohman, K., Jordan, P., Pettersson, U., Akusjärvi, G., Carmo-Fonseca, M., and Dejean, A. (1995). Targeting of adenovirus E1A and E4-ORF3 proteins to nuclear matrix-associated PML bodies. J. Cell Biol. *131*, 45–56.

Challberg, M.D., and Kelly, T.J. (1979). Adenovirus DNA replication in vitro. Proc. Natl. Acad. Sci. U. S. A. *76*, 655–659.

Chao, S.H., Fujinaga, K., Marion, J.E., Taube, R., Sausville, E.A., Senderowicz, A.M., Peterlin, B.M., and Price, D.H. (2000). Flavopiridol inhibits P-TEFb and blocks HIV-1 replication. J. Biol. Chem. *275*, 28345–28348.

Chemes, L.B., de Prat-Gay, G., and Sánchez, I.E. (2015). Convergent evolution and mimicry of protein linear motifs in host-pathogen interactions. Curr. Opin. Struct. Biol. *32*, 91–101.

Chinnadurai, G. (2002). CtBP, an Unconventional Transcriptional Corepressor in Development and Oncogenesis. Mol. Cell *9*, 213–224.

Chiou, S.K., Tseng, C.C., Rao, L., and White, E. (1994). Functional complementation of the adenovirus E1B 19-kilodalton protein with Bcl-2 in the inhibition of apoptosis in infected cells. J. Virol. *68*, 6553–6566.

Chiu, C.Y., Mathias, P., Nemerow, G.R., and Stewart, P.L. (1999). Structure of adenovirus complexed with its internalization receptor, alphavbeta5 integrin. J. Virol. *73*, 6759–6768.

Cho, W.-K., Jang, M.K., Huang, K., Pise-Masison, C.A., and Brady, J.N. (2010). Human T-lymphotropic virus type 1 Tax protein complexes with P-TEFb and competes for Brd4 and 7SK snRNP/HEXIM1 binding. J. Virol. *84*, 12801–12809.

Chu, X., Qin, X., Xu, H., Li, L., Wang, Z., Li, F., Xie, X., Zhou, H., Shen, Y., and Long, J. (2013). Structural insights into Paf1 complex assembly and histone binding. Nucleic Acids Res. *41*, 10619–10629.

Cogan, J.D., Jones, S.N., Hall, R.K., and Tibbetts, C. (1992). Functional diversity of E1A gene autoregulation among human adenoviruses. J. Virol. *66*, 3833–3845.

Cohen, M.J., Yousef, A.F., Massimi, P., Fonseca, G.J., Todorovic, B., Pelka, P., Turnell, A.S., Banks, L., and Mymryk, J.S. (2013). Dissection of the C-Terminal Region of E1A Redefines the Roles of CtBP and Other Cellular Targets in Oncogenic Transformation. J. Virol. *87*, 10348–10355.

Cramer, P., Armache, K.-J., Baumli, S., Benkert, S., Brueckner, F., Buchen, C., Damsma, G.E., Dengl, S., Geiger, S.R., Jasiak, A.J., et al. (2008). Structure of eukaryotic RNA polymerases. Annu. Rev. Biophys. *37*, 337–352.

Culp, J.S., Webster, L.C., Friedman, D.J., Smith, C.L., Huang, W.J., Wu, F.Y., Rosenberg, M., and Ricciardi, R.P. (1988). The 289-amino acid E1A protein of adenovirus binds zinc in a region that is important for trans-activation. Proc. Natl. Acad. Sci. U. S. A. *85*, 6450–6454.

Cuzange, A., Chroboczek, J., and Jacrot, B. (1994). The penton base of human adenovirus type 3 has the RGD motif. Gene *146*, 257–259.

Dai-Ju, J.Q., Li, L., Johnson, L.A., and Sandri-Goldin, R.M. (2006). ICP27 interacts with the C-terminal domain of RNA polymerase II and facilitates its recruitment to herpes simplex virus 1 transcription sites, where it undergoes proteasomal degradation during infection. J. Virol. *80*, 3567–3581.

Dales, S., and Chardonnet, Y. (1973). Early events in the interaction of adenoviruses with HeLa cells. IV. Association with microtubules and the nuclear pore complex during vectorial movement of the inoculum. Virology *56*, 465–483.

Davey, N.E., Travé, G., and Gibson, T.J. (2011). How viruses hijack cell regulation. Trends Biochem. Sci. *36*, 159–169.

Davey, N.E., Van Roey, K., Weatheritt, R.J., Toedt, G., Uyar, B., Altenberg, B., Budd, A., Diella, F., Dinkel, H., and Gibson, T.J. (2012). Attributes of short linear motifs. Mol. Biosyst. *8*, 268–281.

Dekker, J., Kanellopoulos, P.N., Loonstra, A.K., van Oosterhout, J.A., Leonard, K., Tucker, P.A., and van der Vliet, P.C. (1997). Multimerization of the adenovirus DNA-binding protein is the driving force for ATP-independent DNA unwinding during strand displacement synthesis. EMBO J. *16*, 1455–1463.

Dhurandhar, N.V., Whigham, L.D., Abbott, D.H., Schultz-Darken, N.J., Israel, B.A., Bradley, S.M., Kemnitz, J.W., Allison, D.B., and Atkinson, R.L. (2002). Human adenovirus Ad-36 promotes weight gain in male rhesus and marmoset monkeys. J. Nutr. *132*, 3155–3160.

Dinkel, H., Michael, S., Weatheritt, R.J., Davey, N.E., Van Roey, K., Altenberg, B., Toedt, G., Uyar, B., Seiler, M., Budd, A., et al. (2012). ELM--the database of eukaryotic linear motifs. Nucleic Acids Res. *40*, D242-251.

Dix, I., and Leppard, K.N. (1995). Expression of adenovirus type 5 E4 Orf2 protein during lytic infection. J. Gen. Virol. *76 (Pt 4)*, 1051–1055.

Dobner, T., Horikoshi, N., Rubenwolf, S., and Shenk, T. (1996). Blockage by adenovirus E4orf6 of transcriptional activation by the p53 tumor suppressor. Science *272*, 1470–1473.

Douglas, J.L., and Quinlan, M.P. (1995). Efficient nuclear localization and immortalizing ability, two functions dependent on the adenovirus type 5 (Ad5) E1A second exon, are necessary for cotransformation with Ad5 E1B but not with T24ras. J. Virol. *69*, 8061–8065.

Dumont, D.J., Tremblay, M.L., and Branton, P.E. (1989). Phosphorylation at serine 89 induces a shift in gel mobility but has little effect on the function of adenovirus type 5 E1A proteins. J. Virol. *63*, 987–991.

Dunn, S., and Cowling, V.H. (2015). Myc and mRNA capping. Biochim. Biophys. Acta *1849*, 501–505.

Durand, L.O., and Roizman, B. (2008). Role of cdk9 in the optimization of expression of the genes regulated by ICP22 of herpes simplex virus 1. J. Virol. *82*, 10591–10599.

Durand, L.O., Advani, S.J., Poon, A.P.W., and Roizman, B. (2005). The carboxyl-terminal domain of RNA polymerase II is phosphorylated by a complex containing cdk9 and infected-cell protein 22 of herpes simplex virus 1. J. Virol. *79*, 6757–6762.

Dyer, M.D., Murali, T.M., and Sobral, B.W. (2008). The landscape of human proteins interacting with viruses and other pathogens. PLoS Pathog. *4*, e32.

Dyson, N., Guida, P., McCall, C., and Harlow, E. (1992). Adenovirus E1A makes two distinct contacts with the retinoblastoma protein. J. Virol. *66*, 4606–4611.

Edwards, R.J., and Palopoli, N. (2015). Computational prediction of short linear motifs from protein sequences. Methods Mol. Biol. Clifton NJ *1268*, 89–141.

Eick, D., and Geyer, M. (2013). The RNA polymerase II carboxy-terminal domain (CTD) code. Chem. Rev. *113*, 8456–8490.

Elde, N.C., and Malik, H.S. (2009). The evolutionary conundrum of pathogen mimicry. Nat. Rev. Microbiol. *7*, 787–797.

Elsing, A., and Burgert, H.G. (1998). The adenovirus E3/10.4K-14.5K proteins down-modulate the apoptosis receptor Fas/Apo-1 by inducing its internalization. Proc. Natl. Acad. Sci. U. S. A. *95*, 10072–10077.

Felsani, A., Mileo, A.M., and Paggi, M.G. (2006). Retinoblastoma family proteins as key targets of the small DNA virus oncoproteins. Oncogene *25*, 5277–5285.

Ferguson, B., Krippl, B., Andrisani, O., Jones, N., Westphal, H., and Rosenberg, M. (1985). E1A 13S and 12S mRNA products made in Escherichia coli both function as nucleus-localized transcription activators but do not directly bind DNA. Mol. Cell. Biol. *5*, 2653–2661.

Ferreon, A.C.M., Ferreon, J.C., Wright, P.E., and Deniz, A.A. (2013). Modulation of allostery by protein intrinsic disorder. Nature *498*, 390–394.

Flint, J.S., Racaniello, V.R., Rall, G.F., Skalka, A.-M., and Enquist, L.W. (2015). Appendix: Adenoviruses. In Principles of Virology Volume 1: Molecular Biology, (Washington, DC: ASM Press), pp. 502–503.

Fonseca, G.J., Cohen, M.J., and Mymryk, J.S. (2014). Adenovirus E1A recruits the human Paf1 complex to enhance transcriptional elongation. J. Virol. *88*, 5630–5637.

Fontes, M.R.M., Teh, T., Toth, G., John, A., Pavo, I., Jans, D.A., and Kobe, B. (2003). Role of flanking sequences and phosphorylation in the recognition of the simian-virus-40 large T-antigen nuclear localization sequences by importin-alpha. Biochem. J. *375*, 339–349.

Fraser, K.A., and Rice, S.A. (2005). Herpes simplex virus type 1 infection leads to loss of serine-2 phosphorylation on the carboxyl-terminal domain of RNA polymerase II. J. Virol. *79*, 11323–11334.

Fraser, K.A., and Rice, S.A. (2007). Herpes simplex virus immediate-early protein ICP22 triggers loss of serine 2-phosphorylated RNA polymerase II. J. Virol. *81*, 5091–5101.

Freeman, A.E., Black, P.H., Wolford, R., and Huebner, R.J. (1967). Adenovirus type 12-rat embryo transformation system. J. Virol. *1*, 362–367.

Friedman, J.M., and Horwitz, M.S. (2002). Inhibition of tumor necrosis factor alpha-induced NF-kappa B activation by the adenovirus E3-10.4/14.5K complex. J. Virol. *76*, 5515–5521.

Frisch, S.M., and Mymryk, J.S. (2002). Adenovirus-5 E1A: paradox and paradigm. Nat. Rev. Mol. Cell Biol. *3*, 441–452.

Fuchs, M., Gerber, J., Drapkin, R., Sif, S., Ikura, T., Ogryzko, V., Lane, W.S., Nakatani, Y., and Livingston, D.M. (2001). The p400 complex is an essential E1A transformation target. Cell *106*, 297–307.

Garber, M.E., Mayall, T.P., Suess, E.M., Meisenhelder, J., Thompson, N.E., and Jones, K.A. (2000). CDK9 autophosphorylation regulates high-affinity binding of the human immunodeficiency virus type 1 tat-P-TEFb complex to TAR RNA. Mol. Cell. Biol. *20*, 6958–6969.

Geisberg, J.V., Lee, W.S., Berk, A.J., and Ricciardi, R.P. (1994). The zinc finger region of the adenovirus E1A transactivating domain complexes with the TATA box binding protein. Proc. Natl. Acad. Sci. U. S. A. *91*, 2488–2492.

Geisberg, J.V., Chen, J.L., and Ricciardi, R.P. (1995). Subregions of the adenovirus E1A transactivation domain target multiple components of the TFIID complex. Mol. Cell. Biol. *15*, 6283–6290.

Gerace, E., and Moazed, D. (2015). Affinity Pull-Down of Proteins Using Anti-FLAG M2 Agarose Beads. Methods Enzymol. *559*, 99–110.

Ghosh-Choudhury, G., Haj-Ahmad, Y., and Graham, F.L. (1987). Protein IX, a minor component of the human adenovirus capsid, is essential for the packaging of full length genomes. EMBO J. *6*, 1733–1739.

Gilardi, P., and Perricaudet, M. (1986). The E4 promoter of adenovirus type 2 contains an E1A dependent cis-acting element. Nucleic Acids Res. *14*, 9035–9049.

Gires, O., Kohlhuber, F., Kilger, E., Baumann, M., Kieser, A., Kaiser, C., Zeidler, R., Scheffer, B., Ueffing, M., and Hammerschmidt, W. (1999). Latent membrane protein 1 of Epstein–Barr virus interacts with JAK3 and activates STAT proteins. EMBO J. *18*, 3064–3073.

Glenn, G.M., and Ricciardi, R.P. (1985). Adenovirus 5 early region 1A host range mutants hr3, hr4, and hr5 contain point mutations which generate single amino acid substitutions. J. Virol. *56*, 66–74.

Glenn, G.M., and Ricciardi, R.P. (1987). An adenovirus type 5 E1A protein with a single amino acid substitution blocks wild-type E1A transactivation. Mol. Cell. Biol. *7*, 1004–1011.

Gooding, L.R., Sofola, I.O., Tollefson, A.E., Duerksen-Hughes, P., and Wold, W.S. (1990). The adenovirus E3-14.7K protein is a general inhibitor of tumor necrosis factor-mediated cytolysis. J. Immunol. Baltim. Md 1950 *145*, 3080–3086.

Graf, L., Webel, R., Wagner, S., Hamilton, S.T., Rawlinson, W.D., Sticht, H., and Marschall, M. (2013). The cyclin-dependent kinase ortholog pUL97 of human cytomegalovirus interacts with cyclins. Viruses *5*, 3213–3230.

Graham, F.L., Smiley, J., Russell, W.C., and Nairn, R. (1977). Characteristics of a human cell line transformed by DNA from human adenovirus type 5. J. Gen. Virol. *36*, 59–74.

Greber, U.F., and Way, M. (2006). A superhighway to virus infection. Cell *124*, 741–754.

Guo, L., Wu, W., Liu, L., Wang, L., Zhang, Y., Wu, L., Guan, Y., and Li, Q. (2012). Herpes simplex virus 1 ICP22 inhibits the transcription of viral gene promoters by binding to and blocking the recruitment of P-TEFb. PloS One *7*, e45749.

Hagai, T., Azia, A., Babu, M.M., and Andino, R. (2014). Use of host-like peptide motifs in viral proteins is a prevalent strategy in host-virus interactions. Cell Rep. *7*, 1729–1739.

Halbert, D.N., Cutt, J.R., and Shenk, T. (1985). Adenovirus early region 4 encodes functions required for efficient DNA replication, late gene expression, and host cell shutoff. J. Virol. *56*, 250–257.

Harlow, E., Franza, B.R., and Schley, C. (1985). Monoclonal antibodies specific for adenovirus early region 1A proteins: extensive heterogeneity in early region 1A products. J. Virol. *55*, 533–546.

Harlow, E., Whyte, P., Franza, B.R., and Schley, C. (1986). Association of adenovirus early-region 1A proteins with cellular polypeptides. Mol. Cell. Biol. *6*, 1579–1589.

Hateboer, G., Gennissen, A., Ramos, Y.F., Kerkhoven, R.M., Sonntag-Buck, V., Stunnenberg, H.G., and Bernards, R. (1995). BS69, a novel adenovirus E1A-associated protein that inhibits E1A transactivation. EMBO J. *14*, 3159–3169.

Hawkins, L.K., and Wold, W.S. (1992). A 12,500 MW protein is coded by region E3 of adenovirus. Virology *188*, 486–494.

Hearing, P., and Shenk, T. (1983). The adenovirus type 5 E1A transcriptional control region contains a duplicated enhancer element. Cell *33*, 695–703.

Hearing, P., and Shenk, T. (1985). Sequence-independent autoregulation of the adenovirus type 5 E1A transcription unit. Mol. Cell. Biol. *5*, 3214–3221.

Hen, R., Borrelli, E., and Chambon, P. (1985). Repression of the immunoglobulin heavy chain enhancer by the adenovirus-2 E1A products. Science *230*, 1391–1394.

Hitt, M.M., and Graham, F.L. (1990). Adenovirus E1A under the control of heterologous promoters: wide variation in E1A expression levels has little effect on virus replication. Virology *179*, 667–678.

Hoeben, R.C., and Uil, T.G. (2013). Adenovirus DNA replication. Cold Spring Harb. Perspect. Biol. *5*, a013003.

Hogg, J.C. (2001). Role of Latent Viral Infections in Chronic Obstructive Pulmonary Disease and Asthma. Am. J. Respir. Crit. Care Med. *164*, S71–S75.

Howley, P.M., and Livingston, D.M. (2009). Small DNA tumor viruses: large contributors to biomedical sciences. Virology *384*, 256–259.

Huebner, R.J., Rowe, W.P., Ward, T.G., Parrott, R.H., and Bell, J.A. (1954). Adenoidal-pharyngeal-conjunctival agents: a newly recognized group of common viruses of the respiratory system. N. Engl. J. Med. *251*, 1077–1086.

Huebner, R.J., Rowe, W.P., and Lane, W.T. (1962). ONCOGENIC EFFECTS IN HAMSTERS OF HUMAN ADENOVIRUS TYPES 12 AND 18. Proc. Natl. Acad. Sci. U. S. A. *48*, 2051–2058.

Javier, R.T. (1994). Adenovirus type 9 E4 open reading frame 1 encodes a transforming protein required for the production of mammary tumors in rats. J. Virol. *68*, 3917–3924.

Jelsma, T.N., Howe, J.A., Evelegh, C.M., Cunniff, N.F., Skiadopoulos, M.H., Floroff, M.R., Denman, J.E., and Bayley, S.T. (1988). Use of deletion and point mutants spanning the coding region of the adenovirus 5 E1A gene to define a domain that is essential for transcriptional activation. Virology *163*, 494–502.

Johnson, J.S., Osheim, Y.N., Xue, Y., Emanuel, M.R., Lewis, P.W., Bankovich, A., Beyer, A.L., and Engel, D.A. (2004). Adenovirus Protein VII Condenses DNA, Represses Transcription, and Associates with Transcriptional Activator E1A. J. Virol. *78*, 6459–6468.

Jones, N., and Shenk, T. (1979). An adenovirus type 5 early gene function regulates expression of other early viral genes. Proc. Natl. Acad. Sci. U. S. A. *76*, 3665–3669.

Jones, S.N., and Tibbetts, C. (1989). Upstream DNA sequences determine different autoregulatory responses of the adenovirus types 5 and 3 E1A promoters. J. Virol. *63*, 1833–1838.

Jones, M.S., Harrach, B., Ganac, R.D., Gozum, M.M.A., Dela Cruz, W.P., Riedel, B., Pan, C., Delwart, E.L., and Schnurr, D.P. (2007). New adenovirus species found in a patient presenting with gastroenteritis. J. Virol. *81*, 5978–5984.

Kapasi, A.J., and Spector, D.H. (2008). Inhibition of the cyclin-dependent kinases at the beginning of human cytomegalovirus infection specifically alters the levels and

localization of the RNA polymerase II carboxyl-terminal domain kinases cdk9 and cdk7 at the viral transcriptosome. J. Virol. *82*, 394–407.

Kapasi, A.J., Clark, C.L., Tran, K., and Spector, D.H. (2009). Recruitment of cdk9 to the immediate-early viral transcriptosomes during human cytomegalovirus infection requires efficient binding to cyclin T1, a threshold level of IE2 86, and active transcription. J. Virol. *83*, 5904–5917.

Kapila, M., Khosla, P., and Dhurandhar, N.V. (2004). Novel short-term effects of adenovirus Ad-36 on hamster lipoproteins. Int. J. Obes. *28*, 1521–1527.

Karen, K.A., Hoey, P.J., Young, C.S.H., and Hearing, P. (2009). Temporal regulation of the Mre11-Rad50-Nbs1 complex during adenovirus infection. J. Virol. *83*, 4565–4573.

Ketner, G., and Boyer, J. (2007). Isolation, growth, and purification of defective adenovirus deletion mutants. Methods Mol. Med. *130*, 19–28.

Kim, Y.K., Bourgeois, C.F., Isel, C., Churcher, M.J., and Karn, J. (2002). Phosphorylation of the RNA polymerase II carboxyl-terminal domain by CDK9 is directly responsible for human immunodeficiency virus type 1 Tat-activated transcriptional elongation. Mol. Cell. Biol. *22*, 4622–4637.

King, A.M.Q., Adams, M.J., Carstens, E.B., and Lefkowitz, E.J. (2012). Family - Adenoviridae. In Virus Taxonomy - Ninth Report of the International Committee on Taxonomy of Viruses., (San Diego: Elsevier), pp. 125–141.

King, C.R., Zhang, A., and Mymryk, J.S. (2016a). The Persistent Mystery of Adenovirus Persistence. Trends Microbiol. *24*, 323–324.

King, C.R., Cohen, M.J., Fonseca, G.J., Dirk, B.S., Dikeakos, J.D., and Mymryk, J.S. (2016b). Functional and Structural Mimicry of Cellular Protein Kinase A Anchoring Proteins by a Viral Oncoprotein. PLoS Pathog. *12*, e1005621.

King, C.R., Tessier, T.M., and Mymryk, J.S. (2016c). Color Me Infected: Painting Cellular Chromatin with a Viral Histone Mimic. Trends Microbiol. *24*, 774–776.

Kleinberger, T., and Shenk, T. (1993). Adenovirus E4orf4 protein binds to protein phosphatase 2A, and the complex down regulates E1A-enhanced junB transcription. J. Virol. *67*, 7556–7560.

Köhler, M., Görlich, D., Hartmann, E., and Franke, J. (2001). Adenoviral E1A Protein Nuclear Import Is Preferentially Mediated by Importin α3 in Vitro. Virology *289*, 186–191.

Kojaoghlanian, T., Flomenberg, P., and Horwitz, M.S. (2003). The impact of adenovirus infection on the immunocompromised host. Rev. Med. Virol. *13*, 155–171.

Komorek, J., Kuppuswamy, M., Subramanian, T., Vijayalingam, S., Lomonosova, E., Zhao, L., Mymryk, J.S., Schmitt, K., and Chinnadurai, G. (2010). Adenovirus Type 5 E1A and E6 Proteins of Low-Risk Cutaneous Beta-Human Papillomaviruses Suppress Cell Transformation through Interaction with FOXK1/K2 Transcription Factors. J. Virol. *84*, 2719–2731.

Krougliak, V., and Graham, F.L. (1995). Development of cell lines capable of complementing E1, E4, and protein IX defective adenovirus type 5 mutants. Hum. Gene Ther. *6*, 1575–1586.

Kühl, U., Pauschinger, M., Seeberg, B., Lassner, D., Noutsias, M., Poller, W., and Schultheiss, H.-P. (2005). Viral persistence in the myocardium is associated with progressive cardiac dysfunction. Circulation *112*, 1965–1970.

Lau, L., Gray, E.E., Brunette, R.L., and Stetson, D.B. (2015). DNA tumor virus oncogenes antagonize the cGAS-STING DNA-sensing pathway. Science *350*, 568–571.

Leopold, P.L., Kreitzer, G., Miyazawa, N., Rempel, S., Pfister, K.K., Rodriguez-Boulan, E., and Crystal, R.G. (2000). Dynein- and microtubule-mediated translocation of adenovirus serotype 5 occurs after endosomal lysis. Hum. Gene Ther. *11*, 151–165.

Lewis, B.A., Tullis, G., Seto, E., Horikoshi, N., Weinmann, R., and Shenk, T. (1995). Adenovirus E1A proteins interact with the cellular YY1 transcription factor. J. Virol. *69*, 1628–1636.

Lichtenstein, D.L., Toth, K., Doronin, K., Tollefson, A.E., and Wold, W.S.M. (2004). Functions and mechanisms of action of the adenovirus E3 proteins. Int. Rev. Immunol. *23*, 75–111.

Liddle, O.L., Samuel, M.I., Sudhanva, M., Ellis, J., and Taylor, C. (2015). Adenovirus urethritis and concurrent conjunctivitis: a case series and review of the literature. Sex. Transm. Infect. *91*, 87–90.

Lillie, J.W., and Green, M.R. (1989). Transcription activation by the adenovirus E1a protein. Nature *338*, 39–44.

Lion, T. (2014). Adenovirus Infections in Immunocompetent and Immunocompromised Patients. Clin. Microbiol. Rev. *27*, 441–462.

Liu, F., and Green, M.R. (1990). A specific member of the ATF transcription factor family can mediate transcription activation by the adenovirus E1a protein. Cell *61*, 1217–1224.

Liu, F., and Green, M.R. (1994). Promoter targeting by adenovirus E1a through interaction with different cellular DNA-binding domains. Nature *368*, 520–525.

Liu, P., Kenney, J.M., Stiller, J.W., and Greenleaf, A.L. (2010). Genetic organization, length conservation, and evolution of RNA polymerase II carboxyl-terminal domain. Mol. Biol. Evol. *27*, 2628–2641.

Lonberg-Holm, K., and Philipson, L. (1969). Early events of virus-cell interaction in an adenovirus system. J. Virol. *4*, 323–338.

Lu, S., and Cullen, B.R. (2004). Adenovirus VA1 Noncoding RNA Can Inhibit Small Interfering RNA and MicroRNA Biogenesis. J. Virol. *78*, 12868–12876.

Lyons, R.H., Ferguson, B.Q., and Rosenberg, M. (1987). Pentapeptide nuclear localization signal in adenovirus E1a. Mol. Cell. Biol. *7*, 2451–2456.

Ma, Y., and Mathews, M.B. (1996). Structure, function, and evolution of adenovirus-associated RNA: a phylogenetic approach. J. Virol. *70*, 5083–5099.

Marcellus, R.C., Lavoie, J.N., Boivin, D., Shore, G.C., Ketner, G., and Branton, P.E. (1998). The early region 4 orf4 protein of human adenovirus type 5 induces p53-independent cell death by apoptosis. J. Virol. *72*, 7144–7153.

Marthaler, A.G., Adachi, K., Tiemann, U., Wu, G., Sabour, D., Velychko, S., Kleiter, I., Schöler, H.R., and Tapia, N. (2016). Enhanced OCT4 transcriptional activity substitutes for exogenous SOX2 in cellular reprogramming. Sci. Rep. *6*, 19415.

Mathews, M.B., and Shenk, T. (1991). Adenovirus virus-associated RNA and translation control. J. Virol. *65*, 5657–5662.

McCarthy, M.K., Procario, M.C., Twisselmann, N., Wilkinson, J.E., Archambeau, A.J., Michele, D.E., Day, S.M., and Weinberg, J.B. (2015). Proinflammatory effects of interferon gamma in mouse adenovirus 1 myocarditis. J. Virol. *89*, 468–479.

McGrory, W.J., Bautista, D.S., and Graham, F.L. (1988). A simple technique for the rescue of early region I mutations into infectious human adenovirus type 5. Virology *163*, 614–617.

McKinnon, R.D., Bacchetti, S., and Graham, F.L. (1982). Tn5 mutagenesis of the transforming genes of human adenovirus type 5. Gene *19*, 33–42.

McKinnon, R.D., Waye, J.S., Bautista, D.S., and Graham, F.L. (1985). Nonrandom insertion of Tn5 into cloned human adenovirus DNA. Gene *40*, 31–38.

Meinhart, A., Kamenski, T., Hoeppner, S., Baumli, S., and Cramer, P. (2005). A structural perspective of CTD function. Genes Dev. *19*, 1401–1415.

Miller, M.S., Pelka, P., Fonseca, G.J., Cohen, M.J., Kelly, J.N., Barr, S.D., Grand, R.J.A., Turnell, A.S., Whyte, P., and Mymryk, J.S. (2012). Characterization of the 55-residue protein encoded by the 9S E1A mRNA of species C adenovirus. J. Virol. *86*, 4222–4233.

Mitchell, T., and Sugden, B. (1995). Stimulation of NF-kappa B-mediated transcription by mutant derivatives of the latent membrane protein of Epstein-Barr virus. J. Virol. *69*, 2968–2976.

Mitra, A.K., and Clarke, K. (2010). Viral obesity: fact or fiction? Obes. Rev. Off. J. Int. Assoc. Study Obes. *11*, 289–296.

Moarefi, I., LaFevre-Bernt, M., Sicheri, F., Huse, M., Lee, C.H., Kuriyan, J., and Miller, W.T. (1997). Activation of the Src-family tyrosine kinase Hck by SH3 domain displacement. Nature *385*, 650–653.

Moise, A.R., Grant, J.R., Vitalis, T.Z., and Jefferies, W.A. (2002). Adenovirus E3-6.7K maintains calcium homeostasis and prevents apoptosis and arachidonic acid release. J. Virol. *76*, 1578–1587.

Moroco, J.A., Baumgartner, M.P., Rust, H.L., Choi, H.G., Hur, W., Gray, N.S., Camacho, C.J., and Smithgall, T.E. (2015). A Discovery Strategy for Selective Inhibitors of c-Src in Complex with the Focal Adhesion Kinase SH3/SH2-binding Region. Chem. Biol. Drug Des. *86*, 144–155.

Morris, E.J., and Dyson, N.J. (2001). Retinoblastoma protein partners. Adv. Cancer Res. *82*, 1–54.

Mukaigawa, J., and Nayak, D.P. (1991). Two signals mediate nuclear localization of influenza virus (A/WSN/33) polymerase basic protein 2. J. Virol. *65*, 245–253.

Mul, Y.M., and van der Vliet, P.C. (1993). The adenovirus DNA binding protein effects the kinetics of DNA replication by a mechanism distinct from NFI or Oct-1. Nucleic Acids Res. *21*, 641–647.

Neill, S.D., Hemstrom, C., Virtanen, A., and Nevins, J.R. (1990). An adenovirus E4 gene product trans-activates E2 transcription and stimulates stable E2F binding through a direct association with E2F. Proc. Natl. Acad. Sci. U. S. A. *87*, 2008–2012.

Nemerow, G.R., and Stewart, P.L. (2016). Insights into Adenovirus Uncoating from Interactions with Integrins and Mediators of Host Immunity. Viruses *8*, 337.

Nevels, M., Täuber, B., Kremmer, E., Spruss, T., Wolf, H., and Dobner, T. (1999). Transforming potential of the adenovirus type 5 E4orf3 protein. J. Virol. *73*, 1591–1600.

Ni, Z., Xu, C., Guo, X., Hunter, G.O., Kuznetsova, O.V., Tempel, W., Marcon, E., Zhong, G., Guo, H., Kuo, W.-H.W., et al. (2014). RPRD1A and RPRD1B are human RNA polymerase II C-terminal domain scaffolds for Ser5 dephosphorylation. Nat. Struct. Mol. Biol. *21*, 686–695.

O'Connor, M.J., Zimmermann, H., Nielsen, S., Bernard, H.U., and Kouzarides, T. (1999). Characterization of an E1A-CBP interaction defines a novel transcriptional adapter motif (TRAM) in CBP/p300. J. Virol. *73*, 3574–3581.

Ott, M., Geyer, M., and Zhou, Q. (2011). The control of HIV transcription: keeping RNA polymerase II on track. Cell Host Microbe *10*, 426–435.

Ou, M., and Sandri-Goldin, R.M. (2013). Inhibition of cdk9 during herpes simplex virus 1 infection impedes viral transcription. PloS One *8*, e79007.

Pankuweit, S., and Klingel, K. (2013). Viral myocarditis: from experimental models to molecular diagnosis in patients. Heart Fail. Rev. *18*, 683–702.

Pasarica, M., Shin, A.C., Yu, M., Yang, H.-M.O., Rathod, M., Jen, K.-L.C., Kumar, S.M., MohanKumar, P.S., Markward, N., and Dhurandhar, N.V. (2006). Human Adenovirus 36 Induces Adiposity, Increases Insulin Sensitivity, and Alters Hypothalamic Monoamines in Rats. Obesity *14*, 1905–1913.

Pelka, P., Scimè, A., Mandalfino, C., Joch, M., Abdulla, P., and Whyte, P. (2007). Adenovirus E1A proteins direct subcellular redistribution of Nek9, a NimA-related kinase. J. Cell. Physiol. *212*, 13–25.

Pelka, P., Ablack, J.N.G., Fonseca, G.J., Yousef, A.F., and Mymryk, J.S. (2008). Intrinsic structural disorder in adenovirus E1A: a viral molecular hub linking multiple diverse processes. J. Virol. *82*, 7252–7263.

Pelka, P., Ablack, J.N.G., Shuen, M., Yousef, A.F., Rasti, M., Grand, R.J., Turnell, A.S., and Mymryk, J.S. (2009). Identification of a second independent binding site for the pCAF acetyltransferase in adenovirus E1A. Virology *391*, 90–98.

Perng, Y.-C., Campbell, J.A., Lenschow, D.J., and Yu, D. (2014). Human cytomegalovirus pUL79 is an elongation factor of RNA polymerase II for viral gene transcription. PLoS Pathog. *10*, e1004350.

Perricaudet, M., Akusjärvi, G., Virtanen, A., and Pettersson, U. (1979). Structure of two spliced mRNAs from the transforming region of human subgroup C adenoviruses. Nature *281*, 694–696.

Philipson, L., and Lonberg-Holm, K. (1969). Fate of adenovirus during the early phase of infection. J. Gen. Microbiol. *57*, x–xi.

Ponterio, E., and Gnessi, L. (2015). Adenovirus 36 and Obesity: An Overview. Viruses *7*, 3719–3740.

Prasad, V., Suomalainen, M., Hemmi, S., and Greber, U.F. (2017). The cell cycle-dependent kinase Cdk9 is a post-exposure drug target against human adenoviruses. ACS Infect. Dis.

Querido, E., Blanchette, P., Yan, Q., Kamura, T., Morrison, M., Boivin, D., Kaelin, W.G., Conaway, R.C., Conaway, J.W., and Branton, P.E. (2001). Degradation of p53 by adenovirus E4orf6 and E1B55K proteins occurs via a novel mechanism involving a Cullin-containing complex. Genes Dev. *15*, 3104–3117.

Radke, J.R., Grigera, F., Ucker, D.S., and Cook, J.L. (2014). Adenovirus E1B 19-kilodalton protein modulates innate immunity through apoptotic mimicry. J. Virol. *88*, 2658–2669.

Rasti, M., Grand, R.J.A., Mymryk, J.S., Gallimore, P.H., and Turnell, A.S. (2005). Recruitment of CBP/p300, TATA-binding protein, and S8 to distinct regions at the N terminus of adenovirus E1A. J. Virol. *79*, 5594–5605.

Rasti, M., Grand, R.J.A., Yousef, A.F., Shuen, M., Mymryk, J.S., Gallimore, P.H., and Turnell, A.S. (2006). Roles for APIS and the 20S proteasome in adenovirus E1A-dependent transcription. EMBO J. *25*, 2710–2722.

Rechter, S., Scott, G.M., Eickhoff, J., Zielke, K., Auerochs, S., Müller, R., Stamminger, T., Rawlinson, W.D., and Marschall, M. (2009). Cyclin-dependent Kinases Phosphorylate the Cytomegalovirus RNA Export Protein pUL69 and Modulate Its Nuclear Localization and Activity. J. Biol. Chem. *284*, 8605–8613.

Rekosh, D.M., Russell, W.C., Bellet, A.J., and Robinson, A.J. (1977). Identification of a protein linked to the ends of adenovirus DNA. Cell *11*, 283–295.

Rice, S.A., Long, M.C., Lam, V., Schaffer, P.A., and Spencer, C.A. (1995). Herpes simplex virus immediate-early protein ICP22 is required for viral modification of host RNA polymerase II and establishment of the normal viral transcription program. J. Virol. *69*, 5550–5559.

Roberts, B.E., Miller, J.S., Kimelman, D., Cepko, C.L., Lemischka, I.R., and Mulligan, R.C. (1985). Individual adenovirus type 5 early region 1A gene products elicit distinct alterations of cellular morphology and gene expression. J. Virol. *56*, 404–413.

Roelvink, P.W., Lizonova, A., Lee, J.G., Li, Y., Bergelson, J.M., Finberg, R.W., Brough, D.E., Kovesdi, I., and Wickham, T.J. (1998). The coxsackievirus-adenovirus receptor protein can function as a cellular attachment protein for adenovirus serotypes from subgroups A, C, D, E, and F. J. Virol. *72*, 7909–7915.

ROSONINA, E., and BLENCOWE, B.J. (2004). Analysis of the requirement for RNA polymerase II CTD heptapeptide repeats in pre-mRNA splicing and 3′-end cleavage. RNA *10*, 581–589.

Rowe, W.P., Huebner, R.J., Gilmore, L.K., Parrott, R.H., and Ward, T.G. (1953). Isolation of a cytopathogenic agent from human adenoids undergoing spontaneous degeneration in tissue culture. Proc. Soc. Exp. Biol. Med. Soc. Exp. Biol. Med. N. Y. N *84*, 570–573.

Russell, W.C. (2009). Adenoviruses: update on structure and function. J. Gen. Virol. *90*, 1–20.

Russell, K.L., Hawksworth, A.W., Ryan, M.A.K., Strickler, J., Irvine, M., Hansen, C.J., Gray, G.C., and Gaydos, J.C. (2006). Vaccine-preventable adenoviral respiratory illness in US military recruits, 1999-2004. Vaccine *24*, 2835–2842.

Sadaie, M.R., Mayner, R., and Doniger, J. (2004). A novel approach to develop anti-HIV drugs: adapting non-nucleoside anticancer chemotherapeutics. Antiviral Res. *61*, 1–18.

Saksela, K., Cheng, G., and Baltimore, D. (1995). Proline-rich (PxxP) motifs in HIV-1 Nef bind to SH3 domains of a subset of Src kinases and are required for the enhanced growth of Nef+ viruses but not for down-regulation of CD4. EMBO J. *14*, 484.

Schaeper, U., Boyd, J.M., Verma, S., Uhlmann, E., Subramanian, T., and Chinnadurai, G. (1995). Molecular cloning and characterization of a cellular phosphoprotein that interacts with a conserved C-terminal domain of adenovirus E1A involved in negative modulation of oncogenic transformation. Proc. Natl. Acad. Sci. U. S. A. *92*, 10467–10471.

Schaeper, U., Subramanian, T., Lim, L., Boyd, J.M., and Chinnadurai, G. (1998). Interaction between a cellular protein that binds to the C-terminal region of adenovirus E1A (CtBP) and a novel cellular protein is disrupted by E1A through a conserved PLDLS motif. J. Biol. Chem. *273*, 8549–8552.

Schaft, D., Roguev, A., Kotovic, K.M., Shevchenko, A., Sarov, M., Shevchenko, A., Neugebauer, K.M., and Stewart, A.F. (2003). The histone 3 lysine 36 methyltransferase, SET2, is involved in transcriptional elongation. Nucleic Acids Res. *31*, 2475–2482.

Schöler, H.R., Ciesiolka, T., and Gruss, P. (1991). A nexus between Oct-4 and E1 A: Implications for gene regulation in embryonic stem cells. Cell *66*, 291–304.

Seya, T., Nomura, M., Murakami, Y., Begum, N.A., Matsumoto, M., and Nagasawa, S. (1998). CD46 (membrane cofactor protein of complement, measles virus receptor): structural and functional divergence among species (review). Int. J. Mol. Med. *1*, 809–816.

Shuen, M., Avvakumov, N., Walfish, P.G., Brandl, C.J., and Mymryk, J.S. (2002). The adenovirus E1A protein targets the SAGA but not the ADA transcriptional regulatory complex through multiple independent domains. J. Biol. Chem. *277*, 30844–30851.

Smith, C.D., Craft, D.W., Shiromoto, R.S., and Yan, P.O. (1986). Alternative cell line for virus isolation. J. Clin. Microbiol. *24*, 265–268.

Smith, C.L., Debouck, C., Rosenberg, M., and Culp, J.S. (1989). Phosphorylation of serine residue 89 of human adenovirus E1A proteins is responsible for their characteristic electrophoretic mobility shifts, and its mutation affects biological function. J. Virol. *63*, 1569–1577.

Smith, D.H., Kegler, D.M., and Ziff, E.B. (1985). Vector expression of adenovirus type 5 E1a proteins: evidence for E1a autoregulation. Mol. Cell. Biol. *5*, 2684–2696.

Smith, M.J., Kulkarni, S., and Pawson, T. (2004). FF domains of CA150 bind transcription and splicing factors through multiple weak interactions. Mol. Cell. Biol. *24*, 9274–9285.

Sogawa, K., Handa, H., Fujisawa-Sehara, A., Hiromasa, T., Yamane, M., and Fujii-Kuriyama, Y. (1989). Repression of cytochrome P-450c gene expression by cotransfection with adenovirus E1a DNA. Eur. J. Biochem. *181*, 539–544.

Srivastava, R., and Ahn, S.H. (2015). Modifications of RNA polymerase II CTD: Connections to the histone code and cellular function. Biotechnol. Adv. *33*, 856–872.

Stephens, C., and Harlow, E. (1987). Differential splicing yields novel adenovirus 5 E1A mRNAs that encode 30 kd and 35 kd proteins. EMBO J. *6*, 2027–2035.

Stevens, J.L., Cantin, G.T., Wang, G., Shevchenko, A., Shevchenko, A., and Berk, A.J. (2002). Transcription control by E1A and MAP kinase pathway via Sur2 mediator subunit. Science *296*, 755–758.

Stracker, T.H., Carson, C.T., and Weitzman, M.D. (2002). Adenovirus oncoproteins inactivate the Mre11-Rad50-NBS1 DNA repair complex. Nature *418*, 348–352.

Ström, A.C., Ohlsson, P., and Akusjärvi, G. (1998). AR1 is an integral part of the adenovirus type 2 E1A-CR3 transactivation domain. J. Virol. *72*, 5978–5983.

Subramanian, T., Malstrom, S.E., and Chinnadurai, G. (1991). Requirement of the C-terminal region of adenovirus E1a for cell transformation in cooperation with E1b. Oncogene *6*, 1171–1173.

Sundararajan, R., Cuconati, A., Nelson, D., and White, E. (2001). Tumor necrosis factor-alpha induces Bax-Bak interaction and apoptosis, which is inhibited by adenovirus E1B 19K. J. Biol. Chem. *276*, 45120–45127.

Suzuki, M. (1989). SPXX, a frequent sequence motif in gene regulatory proteins. J. Mol. Biol. *207*, 61–84.

Tambo, A., Roshan, M.H.K., and Pace, N.P. (2016). The Microbial Hypothesis: Contributions of Adenovirus Infection and Metabolic Endotoxaemia to the Pathogenesis of Obesity. Int. J. Chronic Dis. *2016*, 7030795.

Tamrakar, S., Kapasi, A.J., and Spector, D.H. (2005). Human cytomegalovirus infection induces specific hyperphosphorylation of the carboxyl-terminal domain of the large subunit of RNA polymerase II that is associated with changes in the abundance, activity, and localization of cdk9 and cdk7. J. Virol. *79*, 15477–15493.

Tarendeau, F., Boudet, J., Guilligay, D., Mas, P.J., Bougault, C.M., Boulo, S., Baudin, F., Ruigrok, R.W.H., Daigle, N., Ellenberg, J., et al. (2007). Structure and nuclear import function of the C-terminal domain of influenza virus polymerase PB2 subunit. Nat. Struct. Mol. Biol. *14*, 229–233.

Tátrai, E., Hartyánszky, I., Lászik, A., Acsády, G., Sótonyi, P., and Hubay, M. (2011). The role of viral infections in the development of dilated cardiomyopathy. Pathol. Oncol. Res. POR *17*, 229–235.

Täuber, B., and Dobner, T. (2001). Adenovirus early E4 genes in viral oncogenesis. Oncogene *20*, 7847–7854.

Tibbetts, C., Larsen, P.L., and Jones, S.N. (1986). Autoregulation of adenovirus E1A gene expression. J. Virol. *57*, 1055–1064.

Tigges, M.A., and Raskas, H.J. (1984). Splice junctions in adenovirus 2 early region 4 mRNAs: multiple splice sites produce 18 to 24 RNAs. J. Virol. *50*, 106–117.

Tollefson, A.E., Scaria, A., Hermiston, T.W., Ryerse, J.S., Wold, L.J., and Wold, W.S. (1996). The adenovirus death protein (E3-11.6K) is required at very late stages of infection for efficient cell lysis and release of adenovirus from infected cells. J. Virol. *70*, 2296–2306.

Tollefson, A.E., Toth, K., Doronin, K., Kuppuswamy, M., Doronina, O.A., Lichtenstein, D.L., Hermiston, T.W., Smith, C.A., and Wold, W.S. (2001). Inhibition of TRAIL-induced apoptosis and forced internalization of TRAIL receptor 1 by adenovirus proteins. J. Virol. *75*, 8875–8887.

Tollefson, A.E., Kuppuswamy, M., Shashkova, E.V., Doronin, K., and Wold, W.S.M. (2007). Preparation and titration of CsCl-banded adenovirus stocks. Methods Mol. Med. *130*, 223–235.

Tremblay, M.L., Dumont, D.J., and Branton, P.E. (1989). Analysis of phosphorylation sites in the exon 1 region of E1A proteins of human adenovirus type 5. Virology *169*, 397–407.

Trentin, J.J., Yabe, Y., and Taylor, G. (1962). The quest for human cancer viruses. Science *137*, 835–841.

Trible, R.P., Emert-Sedlak, L., and Smithgall, T.E. (2006). HIV-1 Nef Selectively Activates Src Family Kinases Hck, Lyn, and c-Src through Direct SH3 Domain Interaction. J. Biol. Chem. *281*, 27029–27038.

Tsai, W.-H., Wang, P.-W., Lin, S.-Y., Wu, I.-L., Ko, Y.-C., Chen, Y.-L., Li, M., and Lin, S.-F. (2012). Ser-634 and Ser-636 of Kaposi's Sarcoma-Associated Herpesvirus RTA are Involved in Transactivation and are Potential Cdk9 Phosphorylation Sites. Front. Microbiol. *3*, 60.

Ulfendahl, P.J., Linder, S., Kreivi, J.P., Nordqvist, K., Sevensson, C., Hultberg, H., and Akusjärvi, G. (1987). A novel adenovirus-2 E1A mRNA encoding a protein with transcription activation properties. EMBO J. *6*, 2037–2044.

Vachon, V.K., and Conn, G.L. (2016). Adenovirus VA RNA: An essential pro-viral non-coding RNA. Virus Res. *212*, 39–52.

Varga, M.J., Weibull, C., and Everitt, E. (1991). Infectious entry pathway of adenovirus type 2. J. Virol. *65*, 6061–6070.

Vayda, M.E., Rogers, A.E., and Flint, S.J. (1983). The structure of nucleoprotein cores released from adenovirions. Nucleic Acids Res. *11*, 441–460.

Vectorbiolabs.com (2016). Vector Biolabs: Recombinant Adenovirus Construction.

Velcich, A., and Ziff, E. (1985). Adenovirus E1a proteins repress transcription from the SV40 early promoter. Cell *40*, 705–716.

Vijayalingam, S., and Chinnadurai, G. (2013). Adenovirus L-E1A activates transcription through mediator complex-dependent recruitment of the super elongation complex. J. Virol. *87*, 3425–3434.

Virtanen, A., and Pettersson, U. (1983). The molecular structure of the 9S mRNA from early region 1A of adenovirus serotype 2. J. Mol. Biol. *165*, 496–499.

Vora, G.J., Lin, B., Gratwick, K., Meador, C., Hansen, C., Tibbetts, C., Stenger, D.A., Irvine, M., Seto, D., Purkayastha, A., et al. (2006). Co-infections of adenovirus species in previously vaccinated patients. Emerg. Infect. Dis. *12*, 921–930.

Wales, T.E., Hochrein, J.M., Morgan, C.R., Emert-Sedlak, L.A., Smithgall, T.E., and Engen, J.R. (2015). Subtle Dynamic Changes Accompany Hck Activation by HIV-1 Nef and are Reversed by an Antiretroviral Kinase Inhibitor. Biochemistry (Mosc.) *54*, 6382–6391.

Wang, S.-L., Chi, C.-Y., Kuo, P.-H., Tsai, H.-P., Wang, S.-M., Liu, C.-C., Su, I.-J., and Wang, J.-R. (2013). High-Incidence of Human Adenoviral Co-Infections in Taiwan. PLOS ONE *8*, e75208.

Webster, L.C., and Ricciardi, R.P. (1991). trans-dominant mutants of E1A provide genetic evidence that the zinc finger of the trans-activating domain binds a transcription factor. Mol. Cell. Biol. *11*, 4287–4296.

Webster, K.A., Muscat, G.E., and Kedes, L. (1988). Adenovirus E1A products suppress myogenic differentiation and inhibit transcription from muscle-specific promoters. Nature *332*, 553–557.

Weinberg, J.B., Stempfle, G.S., Wilkinson, J.E., Younger, J.G., and Spindler, K.R. (2005). Acute respiratory infection with mouse adenovirus type 1. Virology *340*, 245–254.

Weiss, R.S., Lee, S.S., Prasad, B.V., and Javier, R.T. (1997). Human adenovirus early region 4 open reading frame 1 genes encode growth-transforming proteins that may be distantly related to dUTP pyrophosphatase enzymes. J. Virol. *71*, 1857–1870.

Weitzman, M.D. (2005). Functions of the adenovirus E4 proteins and their impact on viral vectors. Front. Biosci. J. Virtual Libr. *10*, 1106–1117.

Whalen, S.G., Marcellus, R.C., Whalen, A., Ahn, N.G., Ricciardi, R.P., and Branton, P.E. (1997). Phosphorylation within the transactivation domain of adenovirus E1A protein by mitogen-activated protein kinase regulates expression of early region 4. J. Virol. *71*, 3545–3553.

White, E., Sabbatini, P., Debbas, M., Wold, W.S., Kusher, D.I., and Gooding, L.R. (1992). The 19-kilodalton adenovirus E1B transforming protein inhibits programmed cell death and prevents cytolysis by tumor necrosis factor alpha. Mol. Cell. Biol. *12*, 2570–2580.

Whittaker, J.L., Byrd, P.J., Grand, R.J., and Gallimore, P.H. (1984). Isolation and characterization of four adenovirus type 12-transformed human embryo kidney cell lines. Mol. Cell. Biol. *4*, 110–116.

Wickham, T.J., Mathias, P., Cheresh, D.A., and Nemerow, G.R. (1993). Integrins alpha v beta 3 and alpha v beta 5 promote adenovirus internalization but not virus attachment. Cell *73*, 309–319.

Woods, G.L., and Young, A. (1988). Use of A-549 cells in a clinical virology laboratory. J. Clin. Microbiol. *26*, 1026–1028.

Wright, P.E., and Dyson, H.J. (2015). Intrinsically disordered proteins in cellular signalling and regulation. Nat. Rev. Mol. Cell Biol. *16*, 18–29.

Xu, N., Segerman, B., Zhou, X., and Akusjärvi, G. (2007). Adenovirus Virus-Associated RNAII-Derived Small RNAs Are Efficiently Incorporated into the RNA-Induced Silencing Complex and Associate with Polyribosomes. J. Virol. *81*, 10540–10549.

Yamamoto, M., Onogi, H., Kii, I., Yoshida, S., Iida, K., Sakai, H., Abe, M., Tsubota, T., Ito, N., Hosoya, T., et al. (2014). CDK9 inhibitor FIT-039 prevents replication of multiple DNA viruses. J. Clin. Invest. *124*, 3479–3488.

Yamamoto, Y., Nagasato, M., Yoshida, T., and Aoki, K. (2017). Recent Advances in Genetic Modification of Adenovirus Vectors for Cancer Treatment. Cancer Sci.

Ye, H., Park, Y.C., Kreishman, M., Kieff, E., and Wu, H. (1999). The structural basis for the recognition of diverse receptor sequences by TRAF2. Mol. Cell *4*, 321–330.

Yew, P.R., and Berk, A.J. (1992). Inhibition of p53 transactivation required for transformation by adenovirus early 1B protein. Nature *357*, 82–85.

Yew, P.R., Liu, X., and Berk, A.J. (1994). Adenovirus E1B oncoprotein tethers a transcriptional repression domain to p53. Genes Dev. *8*, 190–202.

Yoder, S.S., and Berget, S.M. (1986). Role of adenovirus type 2 early region 4 in the early-to-late switch during productive infection. J. Virol. *60*, 779–781.

Yoshitomi, H., Sera, N., Gonzalez, G., Hanaoka, N., and Fujimoto, T. (2016). First isolation of a potentially new type of human adenovirus (genotype 72), species Human mastadenovirus B (B2) from sewage water in Japan. J. Med. Virol.

Yousef, A.F., Fonseca, G.J., Pelka, P., Ablack, J.N.G., Walsh, C., Dick, F.A., Bazett-Jones, D.P., Shaw, G.S., and Mymryk, J.S. (2010). Identification of a molecular recognition feature in the E1A oncoprotein that binds the SUMO conjugase UBC9 and likely interferes with polySUMOylation. Oncogene *29*, 4693–4704.

Zaborowska, J., Isa, N.F., and Murphy, S. (2016). P-TEFb goes viral. Cell *1*, 106–116.

Zhang, Z., Smith, M.M., and Mymryk, J.S. (2001). Interaction of the E1A Oncoprotein with Yak1p, a Novel Regulator of Yeast Pseudohyphal Differentiation, and Related Mammalian Kinases. Mol. Biol. Cell *12*, 699–710.

Zheng, Y., Stamminger, T., and Hearing, P. (2016). E2F/Rb Family Proteins Mediate Interferon Induced Repression of Adenovirus Immediate Early Transcription to Promote Persistent Viral Infection. PLOS Pathog. *12*, e1005415.

Zhou, M., Halanski, M.A., Radonovich, M.F., Kashanchi, F., Peng, J., Price, D.H., and Brady, J.N. (2000). Tat modifies the activity of CDK9 to phosphorylate serine 5 of the RNA polymerase II carboxyl-terminal domain during human immunodeficiency virus type 1 transcription. Mol. Cell. Biol. *20*, 5077–5086.

Zhou, M., Lu, H., Park, H., Wilson-Chiru, J., Linton, R., and Brady, J.N. (2006). Tax interacts with P-TEFb in a novel manner to stimulate human T-lymphotropic virus type 1 transcription. J. Virol. *80*, 4781–4791.

Curriculum Vitae

Name: Kristianne Galpin

Post-secondary Education and Degrees:

First Class Honours BSc. Microbiology and Immunology
Dalhousie University
Halifax, Nova Scotia Canada
2009-2013

MSc. Microbiology and Immunology
The University of Western Ontario
London, Ontario Canada
2014-2017

Honours and Awards:

Dr. FW Luney Graduate Travel Award in Microbiology & Immunology (2016)
Dalhousie In-Course Scholarship (2011 and 2013)
Commodore Bruce S Oland Scholarship (2012)
Dean's List (2010, 2011 and 2012)
James G MacGregor Memorial Prize (2010)
Dalhousie Entrance Scholarship (2009)

Related Work Experience:

January 2016-April 2016 and September 2016-December 2016
Teaching Assistant MICROIMM 2500, The University of Western Ontario

September-April 2011-2012 and September – April 2012-2013
Teaching Assistant Genetics (BIOL2030), laboratory component, Dalhousie University

Conferences:

July 18-22, 2016: DNA Tumour Virus Meeting, International Centre for Genetic Engineering and Biotechnology (ICGEB) Montreal, Quebec Canada
        Oral Presentation: Investigating E1A as a RNA Polymerase II C-Terminal Domain Mimic and its Role in Transcriptional Activation

June 17, 2016: Oncology Research & Education Day London, Ontario Canada
        Poster Presentation: Investigating Adenovirus E1A as a Mimic of the RNA Polymerase II C-Terminal Domain and its Role in Viral Transcription

March 29, 2016: London Health Research Day London, Ontario Canada
　　　　Poster Presentation: Investigating Adenovirus E1A as a Mimic of the RNA Polymerase II C-Terminal Domain and its Role in Viral Transcription

November 6, 2015: Infection & Immunity Research Forum, Department of Microbiology and Immunology at Western University London, Ontario Canada
　　　　Poster Presentation: Investigating Adenovirus E1A as a Mimic of the RNA Polymerase II C-Terminal Domain and its Role in Viral Transcription

July 21-26, 2015: DNA Tumour Virus Meeting, International Centre for Genetic Engineering and Biotechnology (ICGEB) Trieste, Italy
　　　　Poster Presentation: Investigating Adenovirus E1A as a Mimic of the RNA Polymerase II C-Terminal Domain and its Role in Viral Transcription